AIR FORCE INSTITUTE OF TECHNOLOGY

AIR UNIVERSITY
UNITED STATES AIR FORCE

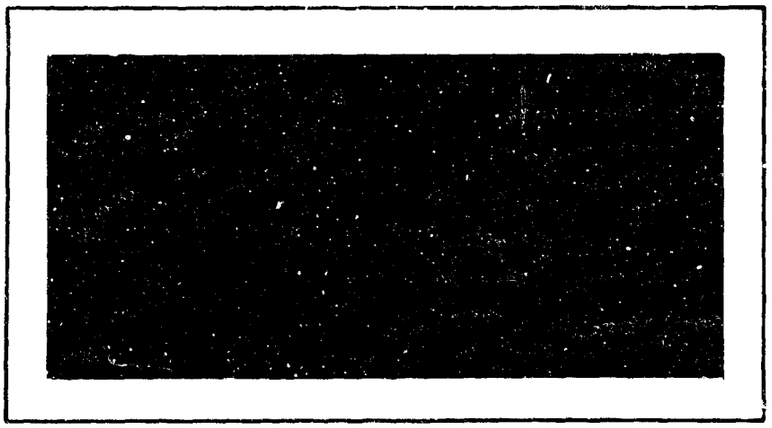

SCHOOL OF ENGINEERING

WRIGHT–PATTERSON AIR FORCE BASE, OHIO

A SELF-ADAPTIVE AIRCRAFT PITCH RATE CONTROL SYSTEM EMPLOYING DIFFERENCE EQUATIONS FOR PARAMETER IDENTIFICATION

THESIS

GA/EE/67-2

Ian Stuart Parry
Flt. Lt. RAF

AFLC-WPAFB-JAN 68 35

A SELF-ADAPTIVE AIRCRAFT PITCH RATE CONTROL SYSTEM EMPLOYING DIFFERENCE EQUATIONS FOR PARAMETER IDENTIFICATION

THESIS

Presented to the Faculty of the School of Engineering of

the Air Force Institute of Technology

Air University

in Partial Fulfillment of the

Requirements for the Degree of

Master of Science

by

Ian Stuart Parry, B.Sc.(Eng.)

Flight Lieutenant RAF

Graduate Astronautics

June 1967

Preface

This investigation was sponsored by the Flight Control Division of the Air Force Flight Dynamics Laboratory, Wright-Patterson AFB. My thanks are expressed to Mr. M. A. Ostgaard of that Division for his helpful discussions on the problems of flight control, and for his assistance in providing me with an introduction to current literature on the subject.

In addition, I want to thank Mr. F. J. Sansom of the Directorate of Computation for his advice on the use of the MIMIC programming system in the IBM 7094 computer, and also my thesis advisor, Professor C. H. Houpis of the Air Force Institute of Technology, for his support and encouragement.

It has been said[1] that,

> A decade of promise and a dearth of actual applications mark the turbulent past of self-adaptive flight control.

Presented in this thesis is an outline of the problem involved in designing a control system for a high performance aircraft or aerospace vehicle, and an indication is made of one possible avenue of approach to its solution which may, perhaps, be worth further development.

For the student of control theory or electrical engineering who is unfamiliar with the particular field of aircraft control systems, the article referenced below is recommended as an introduction to the subject.

---

[1] Andeen, R. E. "Self-Adaptive Autopilots." Space/Aeronautics: pp. 46-52, April 1965.

Contents

List of Figures

Abstract

In a high performance aircraft changes in Mach number, angle of attack and altitude can cause a large variation in the short-period transfer function. To provide the pilot with a constant pitch rate control characteristic an airborne computer, with inputs of elevator deflection angle and pitch rate, is used to identify and track changes in the elevator effectiveness.

Empirical equations are defined to approximate the aircraft time constant, damping factor and natural frequency as functions of elevator effectiveness in three difference equations, which are iterated to model the aircraft. Parameters in the difference equations are perturbed until the equation which uses a value of elevator effectiveness intermediate between the values in the other two equations also has the smallest mean square error from the actual aircraft response. The value of elevator effectiveness in this intermediate equation is then presumed to be the same as that of the aircraft, and is used to set the loop gain to a predetermined suitable value.

Simulation with an aircraft whose elevator effectiveness varied over a range of 240:1 showed that the desired loop gain was maintained within a factor of two for both pilot command inputs and for random wind gust disturbances of root-mean-square magnitude 20 ft./sec. Gain adjustment rates of up to 6 dB/sec. were achieved.

A SELF-ADAPTIVE AIRCRAFT PITCH RATE CONTROL SYSTEM EMPLOYING DIFFERENCE EQUATIONS FOR PARAMETER IDENTIFICATION

I. Introduction

Feedback Design Philosophy

For a plant which has well defined and relatively constant parameters the techniques for designing a closed loop control system which has a fast response and adequate stability have been extensively formulated. These techniques ensure that small amounts of drift in the values of the plant parameters, due to ageing or environmental changes, have an insignificant effect on the overall performance.

However, in the case where the gain of the plant (as distinct from its dynamic terms) has a wide range of variation, the design problem becomes acute: if the loop gain is set to a value which provides satisfactory operation when the plant gain is high, the control response will be slow when the plant gain decreases; but if the loop gain is set to a value suitable for low plant gains, the system may become unstable when the plant gain is high. One way of reconciling these conflicting requirements is to use lead compensation to increase the frequency at which the loop phase shift reaches -180 deg. When such compensation is made, it is theoretically possible to achieve the desired loop gain for low plant gains, with sufficient gain margin to accommodate the maximum plant gain.

In principle, for a truly linear control system, any degree of plant gain variation may be tolerated if enough lead compensation is used. Practical considerations, however, impose restrictions on the effective amount of compensation which can be applied. As the plant gain increases from its minimum value, so also does the control system bandwidth, so that for large plant gains the bandwidth is greater than necessary. The result is that the control system has undue sensitivity to noise arising from spurious inputs to the loop, and from the feedback sensors. Additionally, high order plant

dynamics cause phase shifts at high frequencies which tend to destabilize the loop. Thus, in the event of large variations in the magnitudes of the plant parameters, an alternative approach to control system design is indicated.

Adaptive Control Systems

A high performance aircraft is an example of a plant for which the design of a control system entirely by conventional means is difficult, if not sometimes impossible, without degradation of the handling qualities in some flight regimes. This situation arises largely because of the variation in control surface effectiveness as a result of changes in Mach number, air density and angle of attack, etc. Design of a control system in which gain is scheduled as a function of the output of an air data computer is one solution. A system of this type is called adaptive, since it is continuously altered automatically to suit the surrounding environment. The major limitation is that the relationship between aircraft response characteristics and particular Flight Conditions (F.C.) is indirect, so that a completely satisfactory gain scheduling program can only be arrived at after extensive flight testing.

Self-adaptive systems, in which gain (and possibly other control parameter) adjustment is made after an internal measurement and evaluation of the actual dynamic response, offer a more direct method of achieving a consistent control performance. Among the many self-adaptive aircraft control systems which have been proposed and investigated the Minneapolis-Honeywell and General Electric systems have probably undergone the furthest development. The first of these (Ref. 12) was first flown in the X-15 in December 1961, while a version of the General Electric system (Ref. 6) is now being installed in production F-111 aircraft.

Identification

Inherent in the use of self-adaptive control systems is the need to identify the aircraft parameters. An explicit identification of the aircraft transfer function coefficients involves a

large amount of digital data processing (e.g. Ref. 22) on control input and output signals. The information thereby obtained is more than is required, unless the self-adaptive system is coupled with control system parameter optimization to minimize an integral square error criterion of performance. Optimization in this sense, simply to achieve acceptable handling qualities, has not so far been found necessary, although in thrust or fuel management systems such criteria are of importance in minimizing time to climb to altitude, or maximizing range.

The success of the Honeywell and General Electric systems undoubtedly lies in the fact that they can be mechanized without the need for an airborne digital computer. In neither case is any attempt made to completely identify the aircraft parameters. Instead, the assumption is made in both systems that there are prescribed regions in the complex plane which define possible locations for the aircraft zero and open loop poles. By suitable choice of rate gyro, servo/actuator and compensator, the locus of the pair of complex actuator poles (the first to become unstable) is forced to approach the imaginary axis in the required direction for all flight conditions. The angle of approach towards the imaginary axis is determined by two different considerations:

a. Honeywell System. The actuator poles approach the imaginary axis horizontally, so that the frequency of the actuator mode (w_o) is constant near the axis. A bandpass filter and rectifier circuit measures the amplitude of frequency components at w_o and, in a control loop containing a limiting amplifier and variable gain element, the gain is constantly adjusted to stabilize a small amplitude limit cycle. The action of the gain adjustment process is thus similar to that in a radio super-regenerative detector, and in operation the limit cycle shows a similar squegging tendency (Ref. 1:45).

b. General Electric System. The actuator poles approach the imaginary axis with a positive slope for increasing loop gain, so that the locus passes through a mode frequency w_{ref} with a

damping factor of approximately 0.25. A bandpass filter centered on w_{ref} is used in conjunction with a frequency sensor to detect on which side of w_{ref} the actuator mode occurs whenever it is excited by control inputs, and the loop gain is then adjusted to return the mode to w_{ref}.

Scope of the Thesis

The self-adaptive pitch rate control system which was proposed and investigated in this thesis resembles the Honeywell and General Electric systems in that complete parameter identification is not made; only the magnitude of the control surface effectiveness is determined, and this information is used to adjust the loop gain to provide constant gain and phase margins for all flight conditions. A distinction is that, whereas design of the Honeywell and General Electric systems was carried out by root locus methods, with identification in the frequency domain, in this thesis the reverse procedure was followed; the control loop design was by frequency response analysis, and identification was made in the time domain.

Figure 1 shows a functional block diagram of the control system, which includes an airborne digital computer (the gain computer) and a pre-filter model reference to define the desired aircraft response. The aircraft dynamics were represented by those for the X-15, and the pre-filter was a first order lag with a time constant of 0.5 sec. The way in which the gain computer was used to obtain the required setting for the variable gain element (K_v) is described in the body of the thesis, where results of the system simulation are presented, together with comments, conclusions and recommendations.

Details of a system simulation program for the IBM 7094 computer are contained in Appendix A, and in Appendix B the effects of random wind gusts on the gain computer are shown. Approximations made in deriving the aircraft equations of motion are discussed in Appendix C, while the design of a compensator for the control loop is considered in Appendix D. Finally, difference equation approximations for the aircraft transfer function are given in Appendix E.

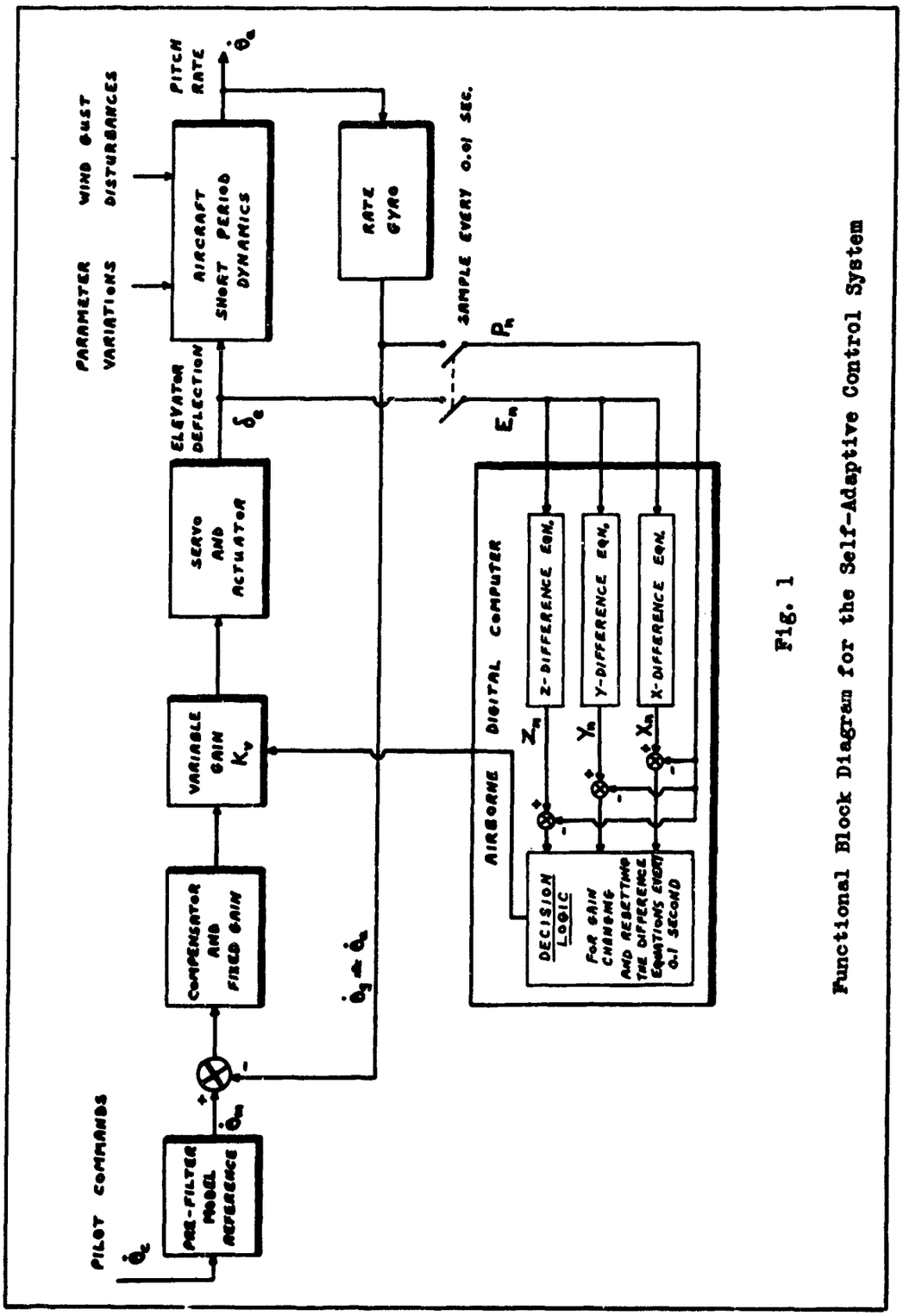

Fig. 1

Functional Block Diagram for the Self-Adaptive Control System

II. Identification by Difference Equations

The Aircraft Transfer Function

The transfer function which relates aircraft pitch rate ($\dot{\theta}_a$) to elevator deflection angle (δ_e) is derived in Appendix C as,

$$\frac{\dot{\theta}_a(s)}{\delta_e(s)} = M_\delta \frac{s + 1/T_a}{s^2 + 2\zeta_a w_a s + w_a^2} \qquad (C.4)$$

where the aircraft parameters T_a, ζ_a and w_a are the short-period time constant, damping factor and natural frequency, respectively. The parameter M_δ is the elevator effectiveness, and from the form of equation (C.4) it is seen to be an aerodynamic gain factor. In Appendix D it is shown that a constant pitch rate response characteristic may be achieved for the control system by adjusting only a variable gain element, to compensate for changes in the loop gain caused by variations in M_δ. Thus, the self-adaptive control problem becomes one of identifying the elevator effectiveness, and tracking changes in it over a range of values of 240:1.

Values for the Aircraft Parameters

Figures 2, 3 and 4 illustrate the wide range of variation of the aircraft parameters for thirty-three Flight Conditions (F.C.) along a typical flight path of the X-15. These parameters are plotted against the decibel value of elevator effectiveness relative to that for F.C. 32, the landing condition. Specifically, for an arbitrary F.C. n,

$$M_\delta \text{ (in dBl)} = 20 \log_{10} \frac{M_\delta \text{ (for F.C. n)}}{M_\delta \text{ (for F.C. 32)}} \qquad (1)$$

The usefulness of presenting the data in this way is that, as an approximation, the parameter values may be considered to have only one degree of freedom (Ref. 10). Therefore, when straight lines are drawn through the centers of the distributions of parameter values in Figs. 2, 3 and 4, the following approximate relations are obtained if M_δ is in dBl:

$$\zeta_a w_a \approx 1/T_a \approx 0.002 \exp(0.152\, M_\delta) \qquad (2)$$

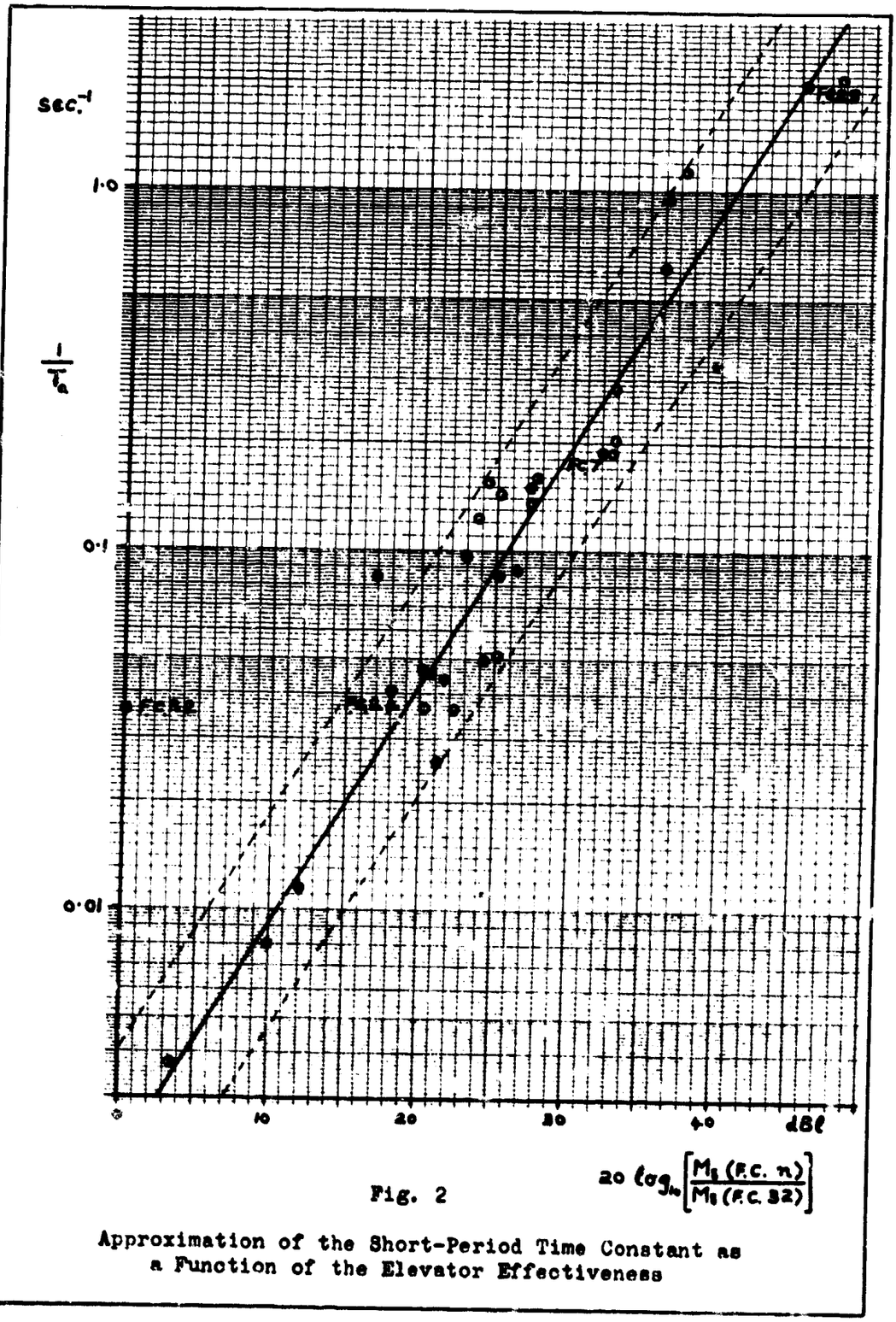

Fig. 2

Approximation of the Short-Period Time Constant as a Function of the Elevator Effectiveness

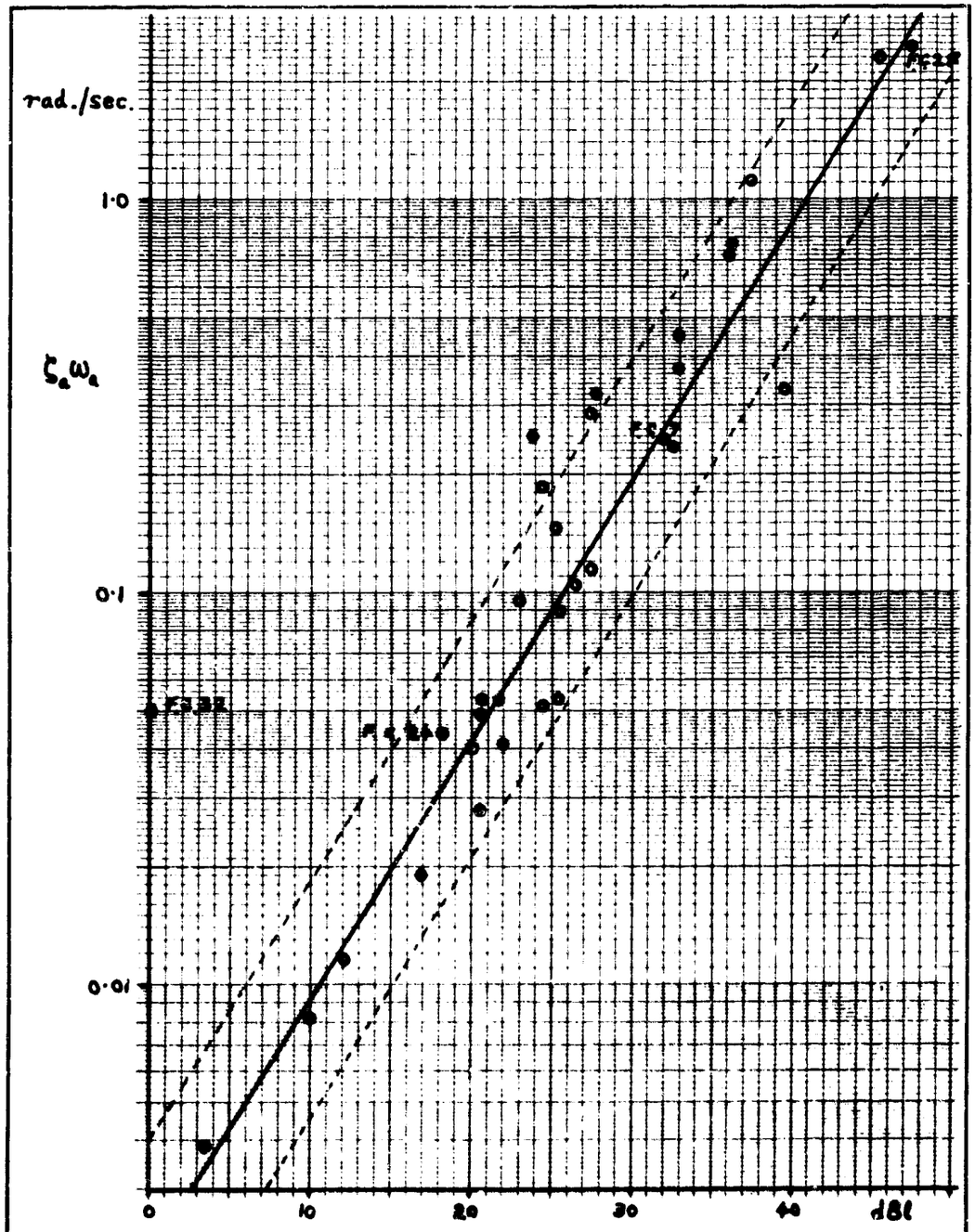

Fig. 3

Approximation of the Short-Period Damping Coefficient (Half-Value) as a Function of the Elevator Effectiveness

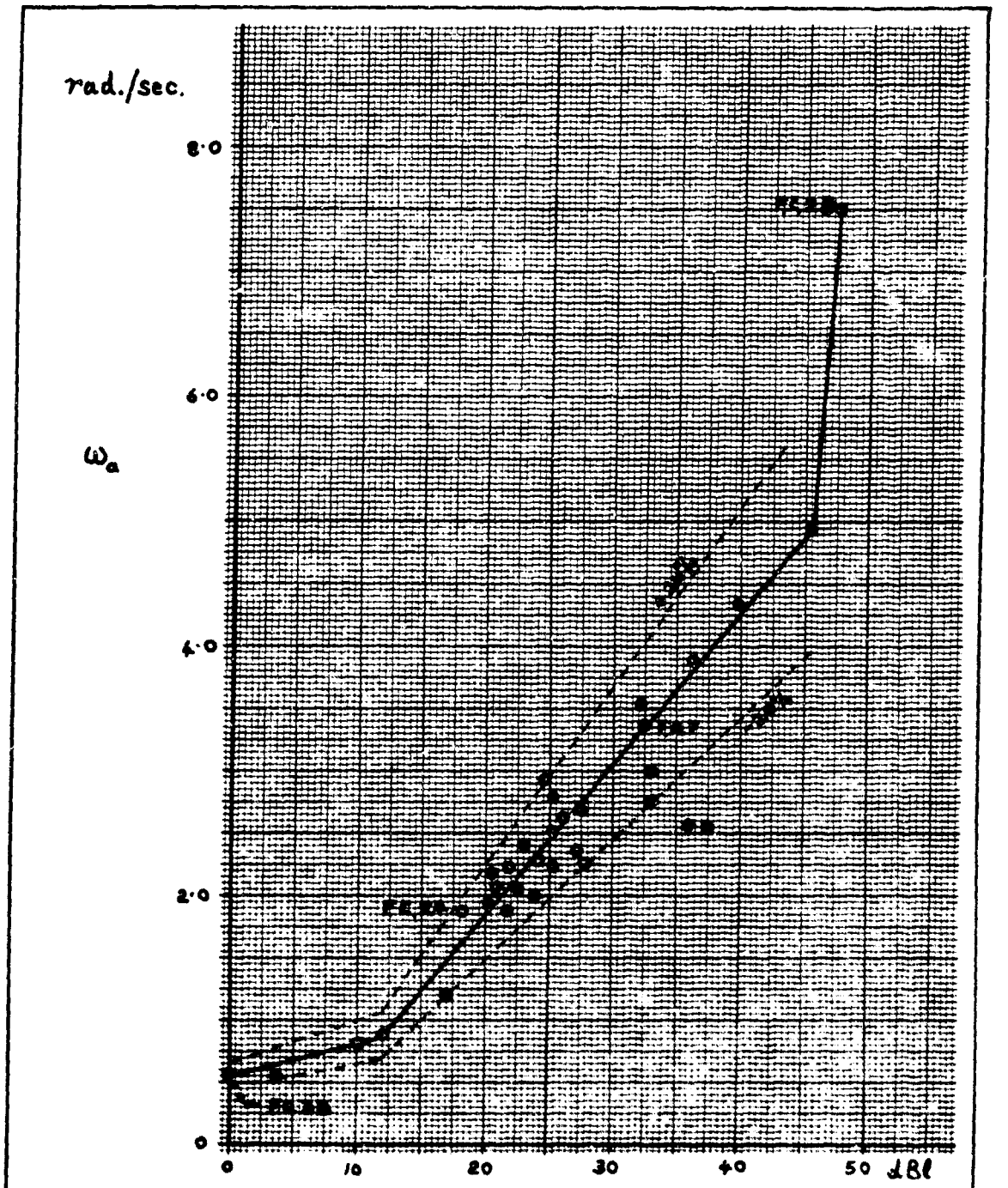

Fig. 4

Approximation of the Short-Period Natural Frequency as a Function of the Elevator Effectiveness

$$w_a = \begin{cases} +0.50 + 0.03\,M_\delta\ ; & 11 > M_\delta \\ -0.57 + 0.121\,M_\delta\ ; & 11 \leq M_\delta \leq 45.5 \\ -40.6 + M_\delta\ ; & M_\delta > 45.5 \end{cases} \qquad (3)$$

Broken lines in Figs. 2 and 3 are drawn for values of $1/T_a$ and $\zeta_a w_a$ twice and one-half those given by equation (2). Similarly, in Fig. 4 the broken lines are for values of w_a at ±20 per cent from the values given by equation (3). In the Figures it is seen that almost all of the distributions of parameter values fall within the pairs of broken lines, so that these lines indicate the order of approximation involved in estimating the other parameter values from M_δ (in dBl). To test if there was any significant bias error in equations (2) and (3), a calculation was made tc find the mean errors involved in estimating $1/T_a$, $\zeta_a w_a$ and w_a from M_δ. This was done by using the known values of the parameters at each of the plotted points. It was found that the mean error in $1/T_a$ was 10.9 per cent, in $\zeta_a w_a$ was -3.65 per cent and in w_a was 4.62 per cent. Because of the comparatively much larger spread in errors no attempt was made to improve the accuracy of equations (2) and (3).

Difference Equations

In Appendix E a method for approximating the aircraft pitch rate transfer function by a number of finite difference equations is presented. Comparative tests with five types of difference equations showed (Ref. Figs. E.3 and E.4) that 1st. order central differences gave root-mean-square (r.m.s.) errors two orders of magnitude less than the other 1st. order derivative approximations, and one order less than that of 2nd. order backward differences. Therefore, the following central difference equation was chosen to represent the aircraft transfer function in the gain computer (Fig.1),

$$Y_{i+1} = \frac{1}{1 + \zeta_a w_a \tau_s} \left[(2 - w_a^2 \tau_s^2)\, Y_i - (1 - \zeta_a w_a \tau_s)\, Y_{i-1} + \frac{\tau_s M_\delta}{2} (E_{i+1} - E_{i-1}) + \frac{\tau_s^2 M_\delta}{T_a} E_i \right] \qquad (E.2)$$

In equation (E.2) τ_s is the iteration interval, and Y_{i+1} is the calculated pitch rate at the instant when the elevator deflection angle is E_{i+1}. Also, the samples Y_i, E_i and Y_{i-1}, E_{i-1} represent the pitch rate and elevator deflection at the previous iteration, and the one before that, respectively.

To find the r.m.s. error inherent in the use of equation (E.2) the iterated values, Y_n ($n = 1, 2, 3, \ldots$), were compared with analytically calculated values of pitch rate (P_n), for an elevator deflection,

$$\delta_e(t) = S\left[1 + A_3 \exp(-B_3 t) \sin(C_3 t - D_3)\right] \qquad (E.7)$$

Thus, equation (E.7) represents the response of a second order transfer function to a step input of amplitude S. The difference equation normalized r.m.s. error as a function of the number of iterations was calculated as,

$$R(n) = \sqrt{\frac{\sum_n (Y_n - P_n)^2}{\sum_n P_n^2}} \times 100\% \qquad (4)$$

When the same typical values of aircraft parameters were used in both the central difference equation (with $\tau_s = 0.01$ sec.) and in the analytical solution for aircraft pitch rate, the difference equation r.m.s. error was only 0.01 per cent after 200 iterations. In practise, the aircraft pitch rate must be measured by a rate gyro, which may be expected to have an error at least this great. It was therefore concluded that the inherent error in the difference equation (E.2), when iterated at a suffiently fast rate, was insignificant compared with the errors that would be introduced by using approximations to the aircraft parameters in the equation.

Identification

Consider the self-adaptive control system shown in Fig. 1. At first, when the identification process is started, the gain computer has no knowledge of the values of the aircraft parameters. It does, however, contain approximate relations between the values of the aircraft parameters, as given by equations (2) and (3). Suppose

that there is only one equation iterated in the gain computer and, since the value of elevator effectiveness is not known, let M_{δ_y} be some arbitrary but reasonable value used in this y-difference equation. From equations (2) and (3), approximate values for $1/T_a$, $\frac{1}{T_a}w_a$ and w_a may then be computed.

When the subscript i is set equal to zero in equation (E.2) an expression for Y_1 is obtained in terms of Y_o, E_o and Y_{-1}, E_{-1}, the initial conditions, as well as E_1, the latest sample of elevator deflection. Numerical values of Y_o and Y_1 are available from the rate gyro samples of aircraft pitch rate, so that $Y_o = P_o$ and $Y_{-1} = P_{-1}$.

To ensure that the four initial conditions (denoted now by P_o, E_o and P_{-1}, E_{-1}) are available in the gain computer for the first iteration, it is necessary to delay this iteration by two sampling intervals. Thereafter, the second and subsequent iterations may be made as soon as soon as each new sample of elevator deflection is taken, without the need for further rate gyro samples.

As each new value Y_n is calculated the quantity $(Y_n - P_n)^2$ is formed, to test the accuracy with which the difference equation response matches the actual aircraft response. Consequently, after m iterations the following sum-square error is produced,

$$S_y(m) = \sum_{n=1}^{m} (Y_n - P_n)^2 \qquad (5)$$

By itself, $S_y(m)$ is clearly not of any use in the identification process, since it only indicates that there was an error between the actual aircraft parameters and those used in the difference equation; it does not indicate, for example, whether M_{δ_y} was too large or too small. Furthermore, even if the correct elevator effectiveness had initially been chosen for M_{δ_y} the magnitude of $S_y(m)$ would still not be zero, because of the very rough approximations contained in equations (2) and (3). Thus, at least one further difference equation (the x-difference equation) must also be iterated in the gain computer.

Suppose that, in the x- and y-difference equations, the ratio $M_{\delta_x} : M_{\delta_y}$ is 0.5 : 1.0, and that after every m iterations of both equations the sum-square errors $S_x(m)$ and $S_y(m)$ are formed. Suppose also, for example, that the initial value arbitrarily chosen for M_{δ_y} is smaller than the true value of aircraft elevator effectiveness (M_δ).

If $S_x > S_y$ after the first m iterations, it may be inferred that the parameters in the y-difference equation were a better match to the true aircraft parameters than those in the x-difference equation, and in particular that $M_{\delta_x} < M_{\delta_y} < M_\delta$. Therefore, to get closer to the true aircraft parameters, both M_{δ_x} and M_{δ_y} are increased by a small fraction of their initial values. The difference equations are initialized again, and iterated another m times, using further samples of elevator deflection as the forcing function.

The process is continually repeated, until it is found that $S_x < S_y$. At this point it is concluded that, in the previous iteration sequence, the parameters in the x-difference equation were a better match to the aircraft parameters than those in the y-difference equation, so that $M_{\delta_x} < M_\delta < M_{\delta_y}$. It is now necessary to decrease the values of M_{δ_x} and M_{δ_y} by a small fraction.

Thus, at this stage the difference equations may be said to be 'locked-on' to the true elevator effectiveness. At the end of every succeeding iteration sequence M_{δ_x} and M_{δ_y} are incrementally increased if $S_x > S_y$ and decreased if $S_x < S_y$ to maintain the relationship $M_{\delta_x} < M_\delta < M_{\delta_y}$. In this way the value of M_δ may be identified as lying approximately mid-way between the values of M_{δ_x} and M_{δ_y}. Also, by the use of this type of decision process, slow changes in the magnitude of the aircraft elevator effectiveness will be 'tracked' by the difference equations.

Error Correction

A disadvantage in the use of only two difference equations for identification is that the precise value of M_δ is not determined. This problem may be circumvented by using an additional equation (the z-difference equation). In addition, the use of three differ-

ence equations provides redundant information that may be used to detect errors in the calculation of the mean-square errors. For example, because of the approximations involved in equations (2) and (3), it is possible that sometimes S_x will be less than S_y even though M_{δ_y} may be closer to M_δ than is M_{δ_x}.

In the system simulation program (Ref. Appendix A) normalized r.m.s. errors were calculated for three difference equations in which $M_{\delta_x} < M_{\delta_y} < M_{\delta_z}$. The following equation shows how the r.m.s. error for the y-difference equation was calculated, and the r.m.s. errors for the x- and z-difference equations were calculated in a similar manner,

$$R_y(m) = \left[\sum_{n=1}^{m}(Y_n - P_n)^2 \Big/ \sum_{n=1}^{m}(P_n - P_o)^2\right]^{1/2} \qquad (6)$$

If the r.m.s. errors and the sum-square errors are each arranged in ascending order after any iteration sequence, it may be seen that both sets will have the subscripts x, y and z in the same relative positions. Thus, either error criterion may be used to test which difference equation response is the best match to the actual aircraft response. In practise, equation (5) is preferred to equation (6), because it involves less computation. However, in the system simulation, equation (6) was used because it enabled an order-of-magnitude comparison to be made between sets of r.m.s. errors, independently of the magnitude of the aircraft response.

With three difference equations iterated in the gain computer, the following decision logic was used to search for and track changes in aircraft elevator effectiveness:

a. $R_x > R_y > R_z$. The values of M_{δ_x}, M_{δ_y} and M_{δ_z} were all incremented by 0.6 dB relative to their previous values (a factor of 1.072).

b. $R_x < R_y < R_z$. The values of M_{δ_x}, M_{δ_y} and M_{δ_z} were all reduced by 0.3 dB relative to their previous values (a factor of 1.035).

c. $(R_y < R_x)$ AND $(R_y < R_z)$. With this result, the difference equations were presumed to be locked-on to the true elevator effectiveness, and so no change was made in the values of M_{δ_x}, M_{δ_y} and M_{δ_z}.

d. Other Combinations. The only other possible combinations of the r.m.s. errors are;

(1) $R_z < R_x < R_y$, and,

(2) $R_x < R_z < R_y$.

When either of these combinations occurred the implication was that both M_{δ_x} and M_{δ_z} were closer to the true M_δ than was the value of M_{δ_y}. Since this is impossible, such results were ignored, and no changes were made in the values of M_{δ_x}, M_{δ_y} and M_{δ_z}. The recognition and rejection of these combinations of r.m.s. errors constituted a partial check against errors introduced in the difference equations by the approximations made in equations (2) and (3).

In summary, the decision logic which was used to change the values of M_{δ_x}, M_{δ_y} and M_{δ_z} was designed with the object of making the r.m.s. error associated with the y-difference equation the smallest of the three. Consequently, the identified value of elevator effectiveness was taken to be equal to the value of M_{δ_y}. The variable gain element (K_v) in the control loop was then changed inversely to changes in M_{δ_y}, as given by equation (D.6). Thus, when M_{δ_y} was increased by 0.6 dB the value of K_v was decreased by 0.6 dB, and when M_{δ_y} was decreased by 0.3 dB the value of K_v was increased by 0.3 dB. The step decreases in K_v were made larger than the increases to ensure stability of the control loop in flight conditions where the aircraft elevator effectiveness was increasing.

Length of Iteration Sequence

A further limitation introduced by the use of equations (2) and (3) is that if the iteration sequences are too long the r.m.s. errors become so large that identification of M_δ is impossible.

Before a simulation program for the complete closed loop control system was written, an investigation was therefore made to find a suitable iteration length. In a similar manner to that previously described (Ref. page 11) for finding the error inherent in the use of difference equations, r.m.s. errors were computed for the x-, y- and z-difference equations as a function of the number of iterations. A value of 0.01 sec. was used for τ_s, and the ratios of $M_{\delta_x} : M_{\delta_y} : M_{\delta_z}$ were 0.5 : 1.0 : 2.0.

Analytical values for the aircraft response to the elevator deflection function given by equation (E.7) were calculated for ten flight conditions. For the same elevator deflection function, r.m.s. errors for the x-, y- and z-difference equations were calculated for values of M_{δ_y} removed from the true value of elevator effectiveness by up to +30 dB and -36 dB. To provide a representative sample of results, twenty-one computer runs were made in which the combinations of flight condition and value of M_{δ_y} relative M_δ were chosen at random.

For values of m equal to 10, 20, 40, 60, 80 and 100 the decision rules for incrementing, reducing or leaving unchanged the values of M_{δ_x}, M_{δ_y} and M_{δ_z} were applied to the r.m.s. errors $R_x(m)$, $R_y(m)$ and $R_z(m)$. A correct decision was assumed to have been made if the r.m.s. errors indicated a need for a change in M_{δ_y} which would have made it more nearly equal to M_δ (or left M_{δ_y} unchanged if it was already equal to M_δ).

The results of this investigation are presented in Fig. 5, where it is shown that the r.m.s. error criterion gave 21 correct decisions out of 21 up to an iteration length of 0.4 sec. (i.e. up to 40 iterations). With longer iteration times the number of correct decisions was reduced, until after one second only 14 correct decisions were made.

In addition to r.m.s. errors, the correlation coefficients were calculated between the difference equation responses and the aircraft response. The following equation defines the correlation coefficient between the y-difference equation response and the

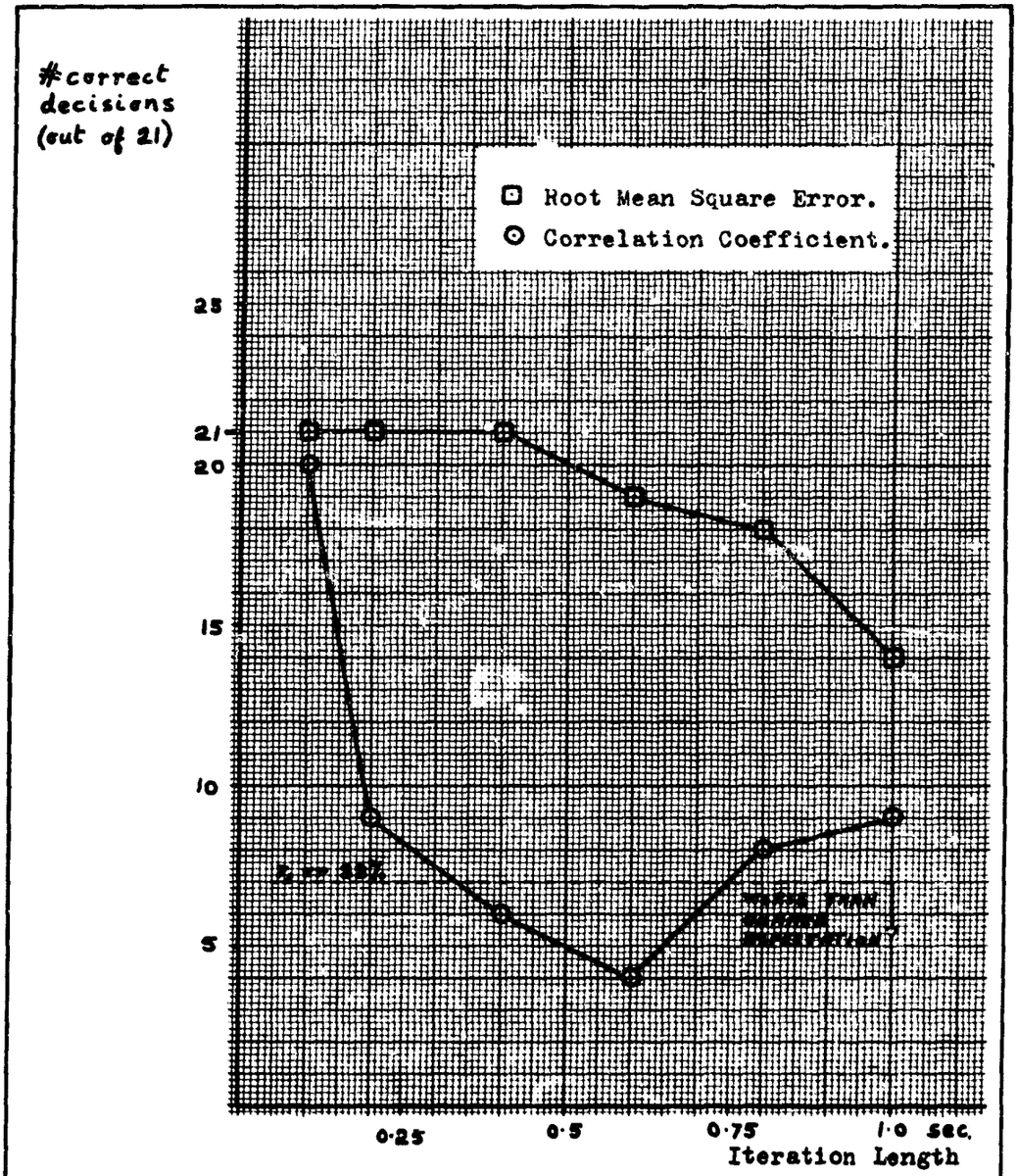

Fig. 5

Performance of the Decision Logic Which was Used to Search for and Track Changes in Elevator Effectiveness

aircraft response, and the correlation coefficients for the x- and z-difference equations were calculated in a similar manner,

$$C_y(m) = \sum_{n=1}^{m} (Y_n P_n) \Big/ \left[\sum_{n=1}^{m} Y_n^2 \sum_{n=1}^{m} P_n^2 \right]^{1/2} \qquad (7)$$

If, in equation (7) all the difference equation samples, Y_n, are multiplied by a constant factor, the value of $C_y(m)$ is unchanged. The values of C_x, C_y and C_z are not, therefore, directly affected by the different values of elevator effectiveness used in the x-, y- and z-difference equations. Consequently, the correlation coefficients depend only on the fidelity with which the wave-shapes of the difference equation responses match the aircraft response. The magnitudes of the correlation coefficients are particularly sensitive to mismatches in the times at which axis crossings occur. It follows from these considerations that the degree of correlation depends only on the accuracy of the approximations to the aircraft parameters $1/T_a$, $\zeta_a w_a$ and w_a used in the difference equations (for a given elevator deflection function).

In Fig. 5, a correct decision is plotted for the cases where the difference equation which best correlated with the aircraft response also used an elevator effectiveness nearest in value to M_δ. Because there were three difference equations, a correct decision had a probability of 1/3rd. of occurring by chance. Up to the first 0.1 sec. iteration of the difference equations, their correlations with the aircraft response were good enough to give 20 correct decisions out of 21. Thereafter, when the difference equation responses started to diverge from the aircraft response, the number of correct decisions was worse than chance expectation. Towards the end of the run, however, the decision by correlation coefficients began to improve slightly, as the values of the coefficients stabilized with the increased sample size.

Based on the results of this investigation, an iteration length of 0.1 sec. was selected for the identification interval. It was also found that when $M_{\delta_y} = M_\delta$ the value of R_z was consistently greater than R_x, so that the ratios $M_{\delta_x} : M_{\delta_y} : M_{\delta_z}$ were changed from

0.5 : 1.0 : 2.0 to the ratios 0.5 : 1.0 : 1.5 for the closed loop system simulation program.

Closed Loop Test of the Identification Process

A simulation program (Ref. Appendix A) was written for the IBM 7094 computer to investigate the usefulness and accuracy of the identification process. This program simulated the complete self-adaptive pitch rate control system shown in Fig. 1. It included the X-15 dynamics for four widely different flight conditions (Ref. Appendix C, Table II), all the control system components, and the airborne digital computer.

Results of the simulation for pilot command inputs are given in Chapter IV; results for random wind gusts are given in Appendix B, together with details of the technique used to generate band-limited noise samples to represent wind gusts. The objectives of the investigation were:

a. To demonstrate that the high-gain control loop was capable of forcing the aircraft pitch rate to accurately follow the output of the pre-filter model reference.

b. To show that by adjusting a variable gain element in the loop to compensate for changes in elevator effectiveness (M_δ) a consistently accurate control performance could be achieved for all flight conditions.

c. To test the speed and accuracy with which the airborne computer (the gain computer) was able to search for and identify the aircraft elevator effectiveness, and set the control loop gain accordingly (Ref. equation (D.6)).

d. To confirm that the identification and self-adaptive process was feasible, without any need for external air data information.

e. To investigate the effect of severe wind gusts on the performance of the self-adaptive system.

III. Simplified Analysis of the Identification Process

The Simplified Control Loop

Pilot pitch rate commands are passed through a pre-filter, which is a first-order lag with a break frequency of 2 rad./sec. For this analysis it is therefore assumed that, for pilot commands, the signal components in the control loop are mainly composed of low frequency terms. Thus, as a first approximation, all transfer functions are replaced by their low frequency gain factors, as shown in Fig. 6.

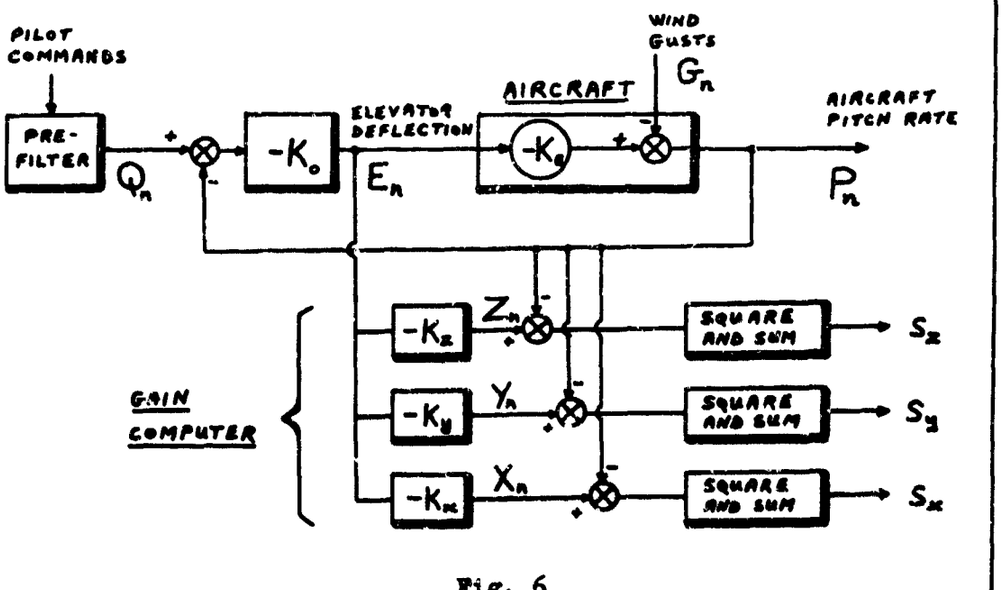

Fig. 6

Low-Frequency Model of the Control System

It is assumed that the ratios of the difference equation gain factors, $K_x : K_y : K_z$ are given by 0.5 : 1.0 : 1.5. Since a positive pilot command input causes a negative elevator deflection, which in turn results in a positive aircraft pitch rate, all the gain factors, K_o, K_a, K_x, K_y and K_z, are positive. Terms with a subscript n are sampled values of signals in the control system at the difference equation iteration times (every τ_s sec.).

From equation (5),

$$S_z = \sum_n (Z_n - P_n)^2 \tag{8a}$$

$$S_y = \sum_n (Y_n - P_n)^2 \tag{8b}$$

$$S_x = \sum_n (X_n - P_n)^2 \tag{8c}$$

But, $Z_n = -K_z E_n$, $Y_n = -K_y E_n$ and $X_n = -K_x E_n$, so that,

$$S_z = \sum_n (K_z E_n + P_n)^2 \tag{9a}$$

$$S_y = \sum_n (K_y E_n + P_n)^2 \tag{9b}$$

$$S_x = \sum_n (K_x E_n + P_n)^2 \tag{9c}$$

Case 1 - Command Inputs Only

In this case, $G_n = 0$ for all n, and $P_n = -K_a E_n$ (10)

Substituting in equations (9) for P_n,

$$S_z = (K_z - K_a)^2 \sum_n E_n^2 \tag{11a}$$

$$S_y = (K_y - K_a)^2 \sum_n E_n^2 \tag{11b}$$

$$S_x = (K_x - K_a)^2 \sum_n E_n^2 \tag{11c}$$

When the difference equations are locked-on to the true value of elevator effectiveness, $K_y = K_a$, and also, $K_x = 0.5K_a$

and $K_z = 1.5K_a$

Substituting in equations (11) for K_x, K_y and K_z,

$$S_z = 0.25K_a^2 \sum_n E_n^2 \tag{12a}$$

$$S_y = 0 \tag{12b}$$

$$S_x = 0.25K_a^2 \sum_n E_n^2 \tag{12c}$$

Thus, when the difference equations are locked-on and the

gain factors of these equations are in the ratios 0.5 : 1.0 : 1.5, the sum-square errors (and the r.m.s. errors) are symmetrical with respect to the y-difference equation error, which ideally is zero. However, the behavior of the errors is different when $K_y > K_a$ than when $K_y < K_a$. For example, if K_y is too large, say $K_y = 10 K_a$, then substitution of K_x, K_y and K_z into equations (11) gives ratios for the r.m.s. errors,

$$R_x : R_y : R_z \quad \text{equal to} \quad 4 : 9 : 14$$

But, if K_y is too small, say $K_y = 0.1 K_a$, then the ratios of the r.m.s. errors are,

$$R_x : R_y : R_z \quad \text{equal to} \quad 19 : 18 : 17$$

Hence, when the y-difference equation gain is greater than the aircraft gain the r.m.s. errors are more widely separated than when the y-difference equation gain is less than that of the aircraft. The decision logic (Ref. page 14) is consequently more likely to detect correctly a requirement to reduce $M_{\delta y}$ (and increase K_v) than to increase $M_{\delta y}$ (and reduce K_v).

After this behavior of the r.m.s. errors was substantiated in the closed loop simulation of the system, advantage was taken of it to ensure that K_v would not unnecessarily be increased, thereby reducing the control system stability. To do this the decision logic to reduce $M_{\delta y}$ was changed from the requirement that $R_x < R_y < R_z$ to the stronger requirement that $(R_y < R_z)$ AND $(3R_x < R_z)$. The results of this change are shown in the next chapter.

Case 2 - Disturbance Inputs Only

Although the primary effect of vertical wind gusts is to cause a change in the aircraft angle of attack (Ref. Appendix B), the only interaction with the control system is through the resulting aircraft pitch rate. Therefore, in this analysis the wind gusts are considered in terms of a disturbance pitch rate, samples of which are represented in Fig. 6 by G_n.

For no pilot commands, $Q_n = 0$ for all n.

Hence,
$$E_n = +K_o P_n \qquad (13)$$

As in the previous case, when the difference equations are locked-on, $K_x = 0.5K_a$, $K_y = K_a$ and $K_z = 1.5K_a$.

Substituting in equations (9) for E_n, K_x, K_y and K_z, the sum-square errors now become,

$$S_z = (1.5K_a K_o + 1)^2 \sum_n r_n^2 \tag{14a}$$

$$S_y = (K_a K_o + 1)^2 \sum_n P_n^2 \tag{14b}$$

$$S_x = (0.5K_a K_o + 1)^2 \sum_n P_n^2 \tag{14c}$$

Since K_a and K_o are positive, $S_x < S_y < S_z$. With this result, the decision logic provides for the gain factor of the y-difference equation to be reduced. This analysis therefore shows that low frequency pitch rate disturbances tend to increase the value of K_v.

IV. Performance of the Gain Computer in the System Simulation

Figures 7 through 20 illustrate the performance of the self-adaptive control system for pilot command inputs. These results were obtained by means of a simulation program which was run on an IBM 7094 computer. Because of the large number of integrations required to simulate the system transfer functions, the program speed was approximately 1/30th. of real time. The results of the computations were stored on magnetic tape, and then subsequently plotted on a Benson-Lehner digital plotter. Details of the program are contained in Appendix A.

The quantities plotted on the graphs are:

a. Pilot command input, $\dot{\theta}_c$ (deg./sec.).

b. Output of the pre-filter model reference, $\dot{\theta}_m$ (deg./sec.).

c. Aircraft pitch rate, $\dot{\theta}_a$ (deg./sec.).

d. Elevator deflection angle δ_e (deg.).

e. Gain error in the control loop relative to the design value (Ref. equations (D.6) and (D.7)) for the particular Flight Condition (F.C.), ΔK_v dB.

For each F.C. the loop gain was initially offset from its design value in order to test the speed and accuracy with which the gain computer returned it to the design value. The amount of initial offset was in some cases restricted. For example, in F.C. 28 the design value of loop gain was achieved when the variable gain element was at its minimum setting, so that the loop gain could never be too low for this F.C. Since the control loop had a design value of gain margin of approximately 12 dB for all F.C., it was not practicable to set in a positive gain error higher than this. Thus, in Fig. 8 the control loop is seen to be just on the verge of instability until the gain error is reduced below 12 dB.

In all cases when the loop gain setting was not grossly in error the aircraft response followed the model response with

negligible error. By comparing the elevator motion for F.C. 28 in Fig. 7 with that for F.C. 32 in Fig. 12, the wide variation in elevator effectiveness between the two F.C. is apparent.

The decision logic which was used in the gain computer to obtain Figures 7 through 12 was that which is described on page 14. With the exception of F.C. 7 (Fig. 10), the gain changing was erratic, although the final gain errors were small; 4 dB for F.C. 28, and less than 2 dB for the other flight conditions.

When a small amplitude dither signal was injected into the control loop to continuously excite the system response, the performance of the gain computer was considerably improved. A comparison of Fig. 13 with Fig. 7 shows that with the dither signal there was less tendency for the gain to stay fixed at too high a value. This is particularly noticable in the first two seconds of each run, when there was no pilot input. In Fig. 14, the effect of modifying the decision logic (Ref. page 22) to prevent unnecessary increases in gain is shown. Thus, both of these changes improved the performance of the gain computer for F.C. 28.

With these two changes, repeats of the computer runs for the other three F.C. were then made. A comparison of Figs. 8 to 12 with Figs. 15 to 19, respectively, shows that in each case the gain errors were reduced, and gain adaption took place more rapidly.

The dither signal which was used in these tests had a frequency of 30 rad./sec. and was inserted into the control loop at the input summing junction. To prevent the elevator motion from becoming excessive in conditions of low elevator effectiveness, the amplitude of the signal was progressively reduced as the identified value of elevator effectiveness became smaller. For F.C. 28, the condition of greatest elevator effectiveness, the amplitude was 0.01 deg./sec., whereas for F.C. 32, the condition of least elevator effectiveness, the amplitude was reduced to 1/5th. of this value. Fig. 20 shows the excessive elevator motion which occurred when a variable amplitude dither signal was not used.

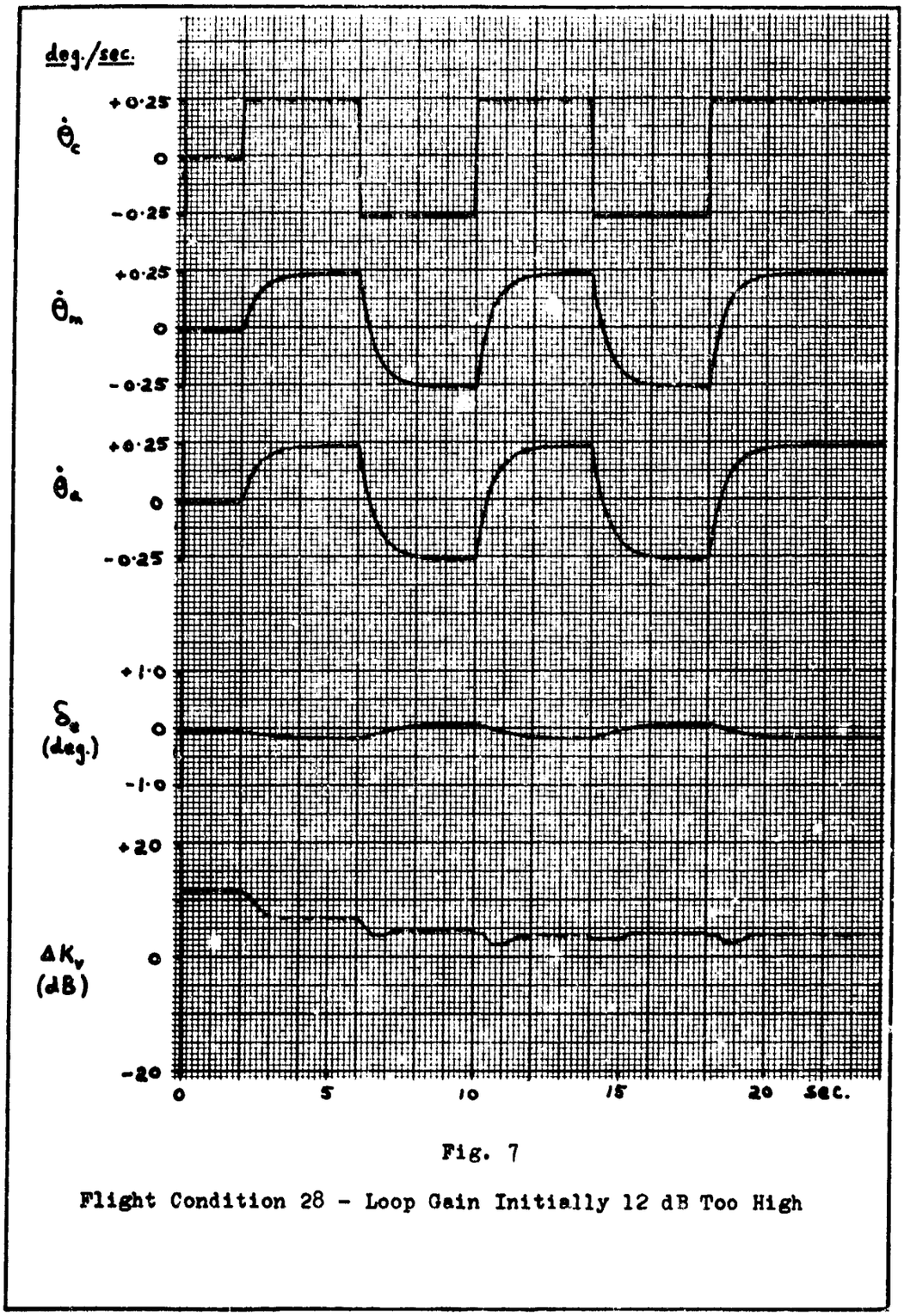

Fig. 7

Flight Condition 28 - Loop Gain Initially 12 dB Too High

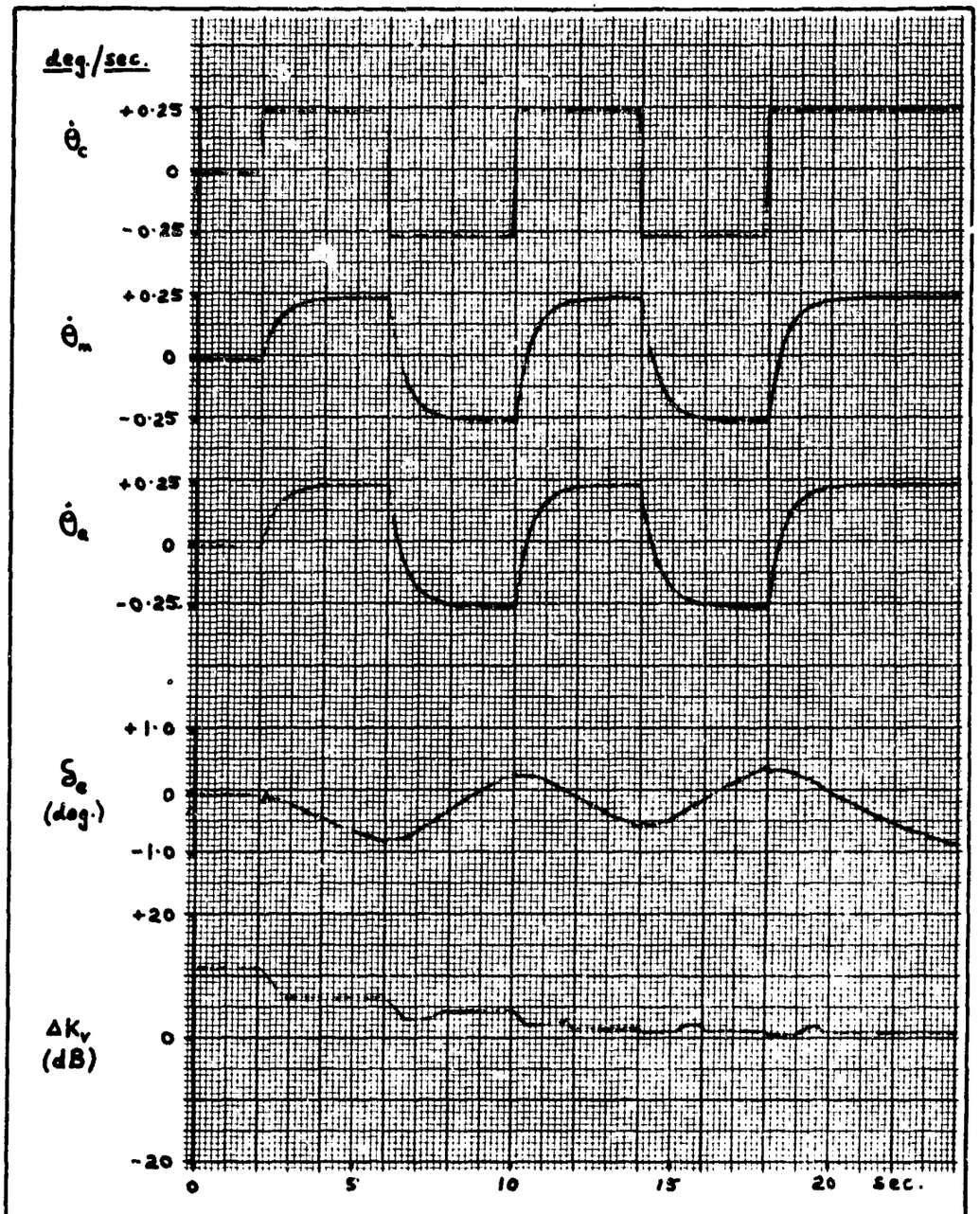

Fig. 8

Flight Condition 7 - Loop Gain Initially 12 dB Too High

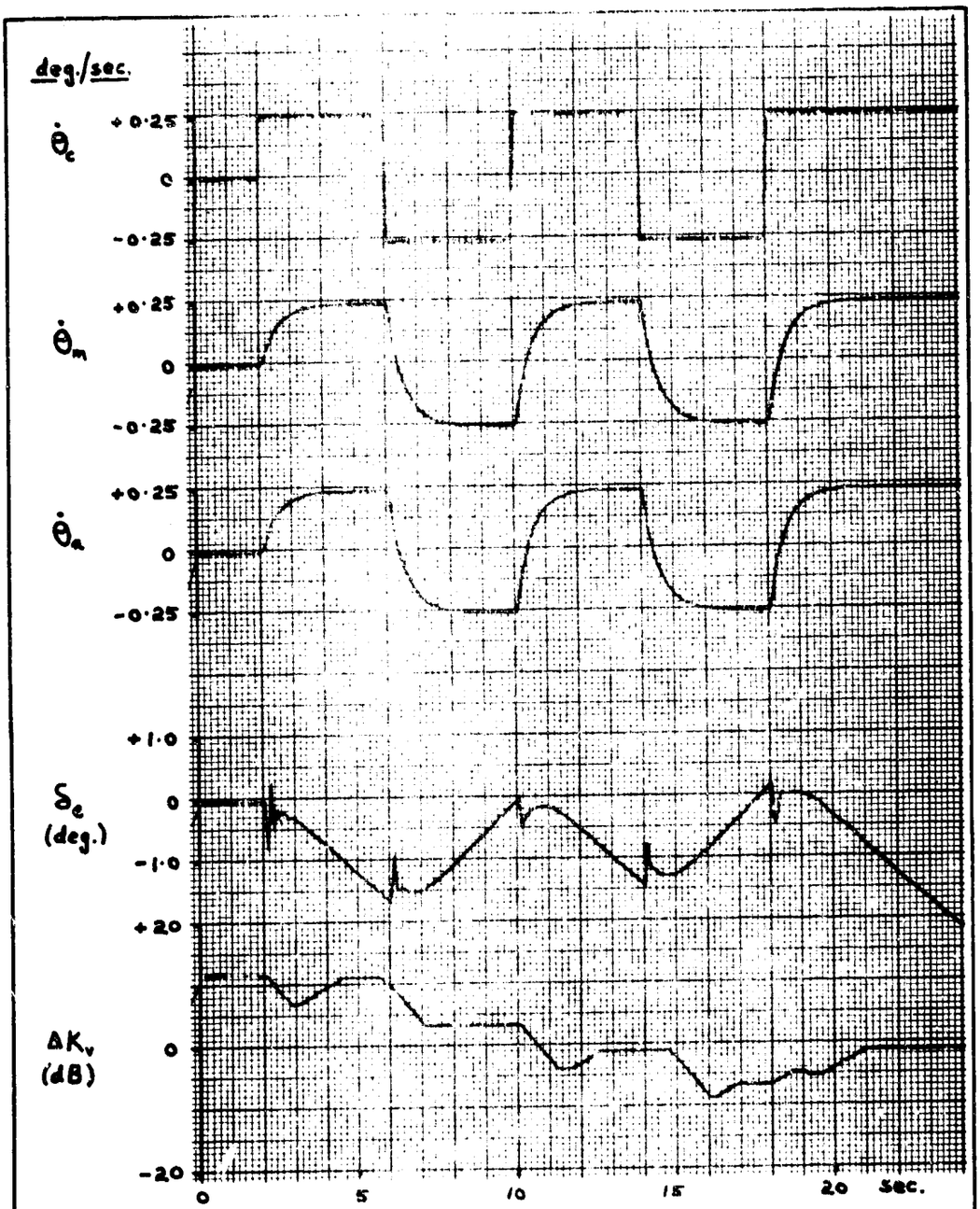

Fig. 9

Flight Condition 24 - Loop Gain Initially 12 dB Too High

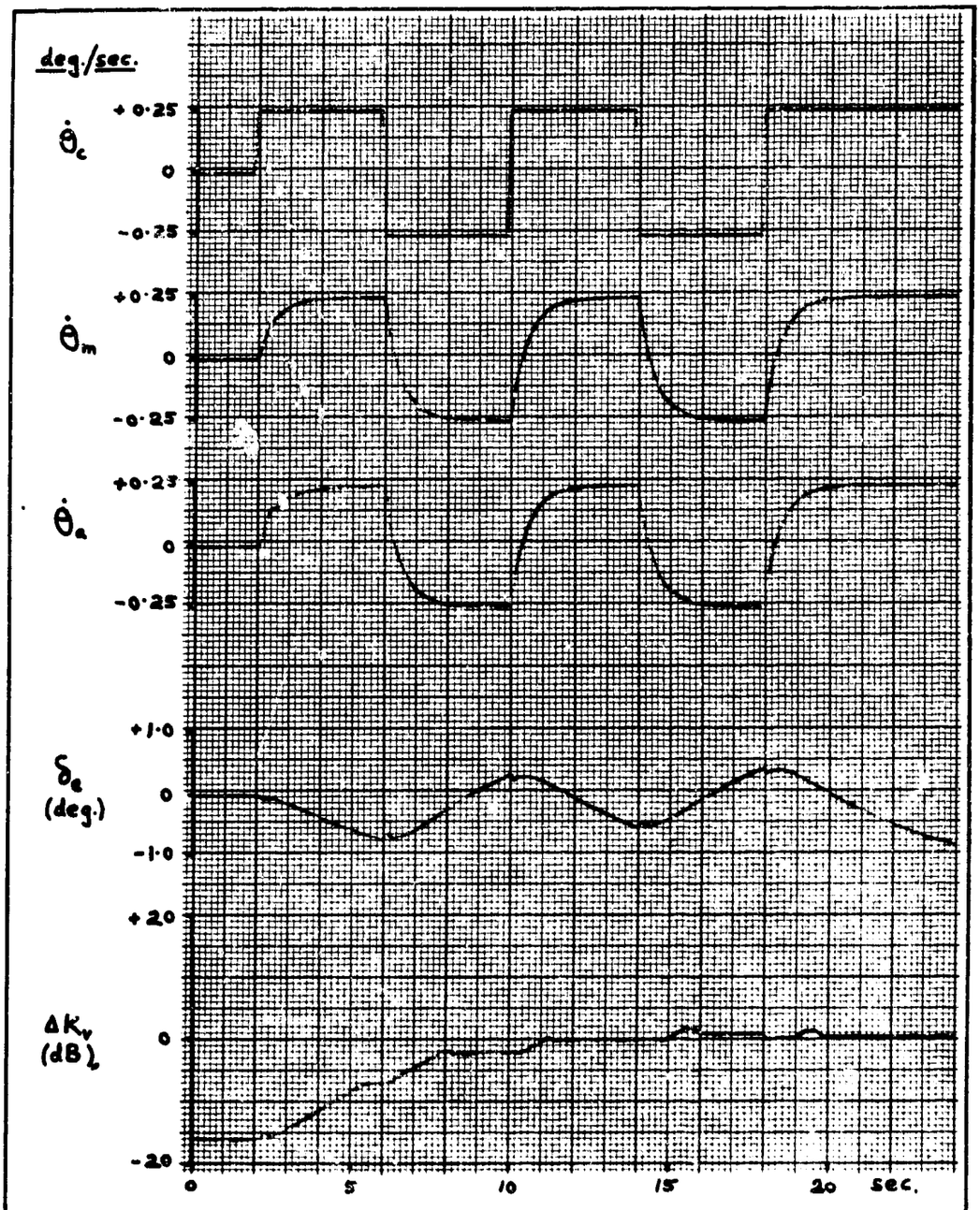

Fig. 10

Flight Condition 7 - Loop Gain Initially 16 dB Too Low

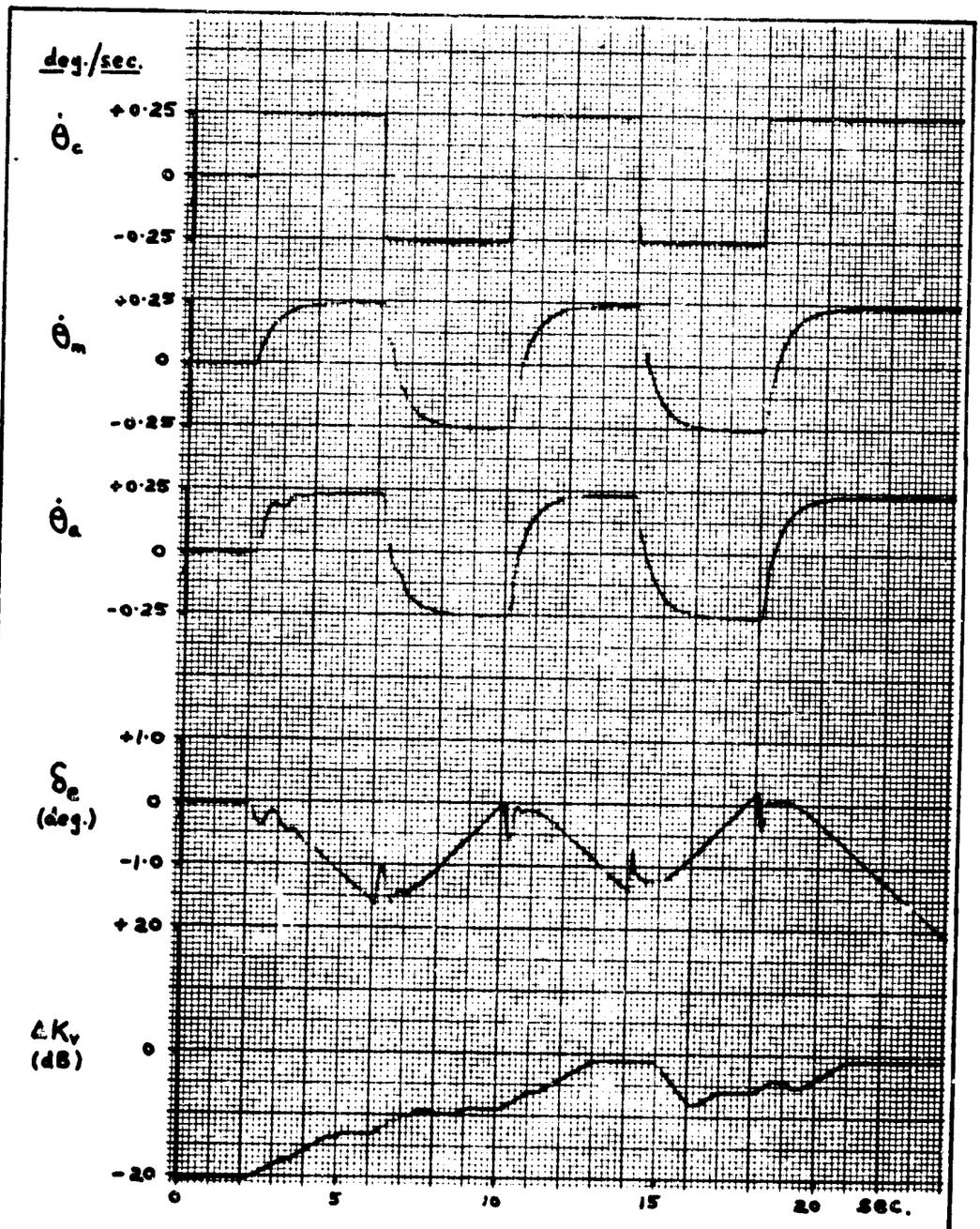

Fig. 11

Flight Condition 24 - Loop Gain Initially 20 dB Too Low

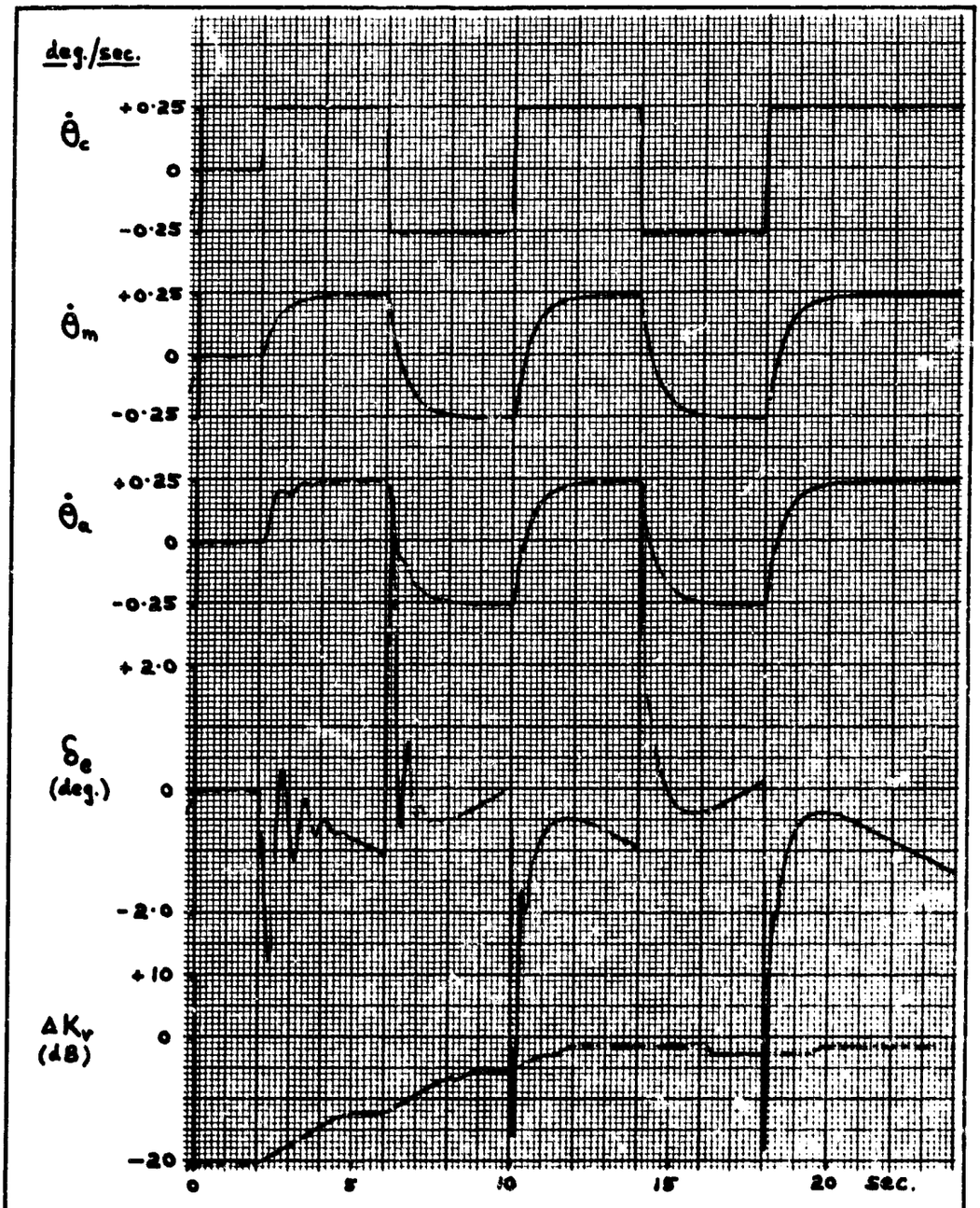

Fig. 12

Flight Condition 32 - Loop Gain Initially 20 dB Too Low

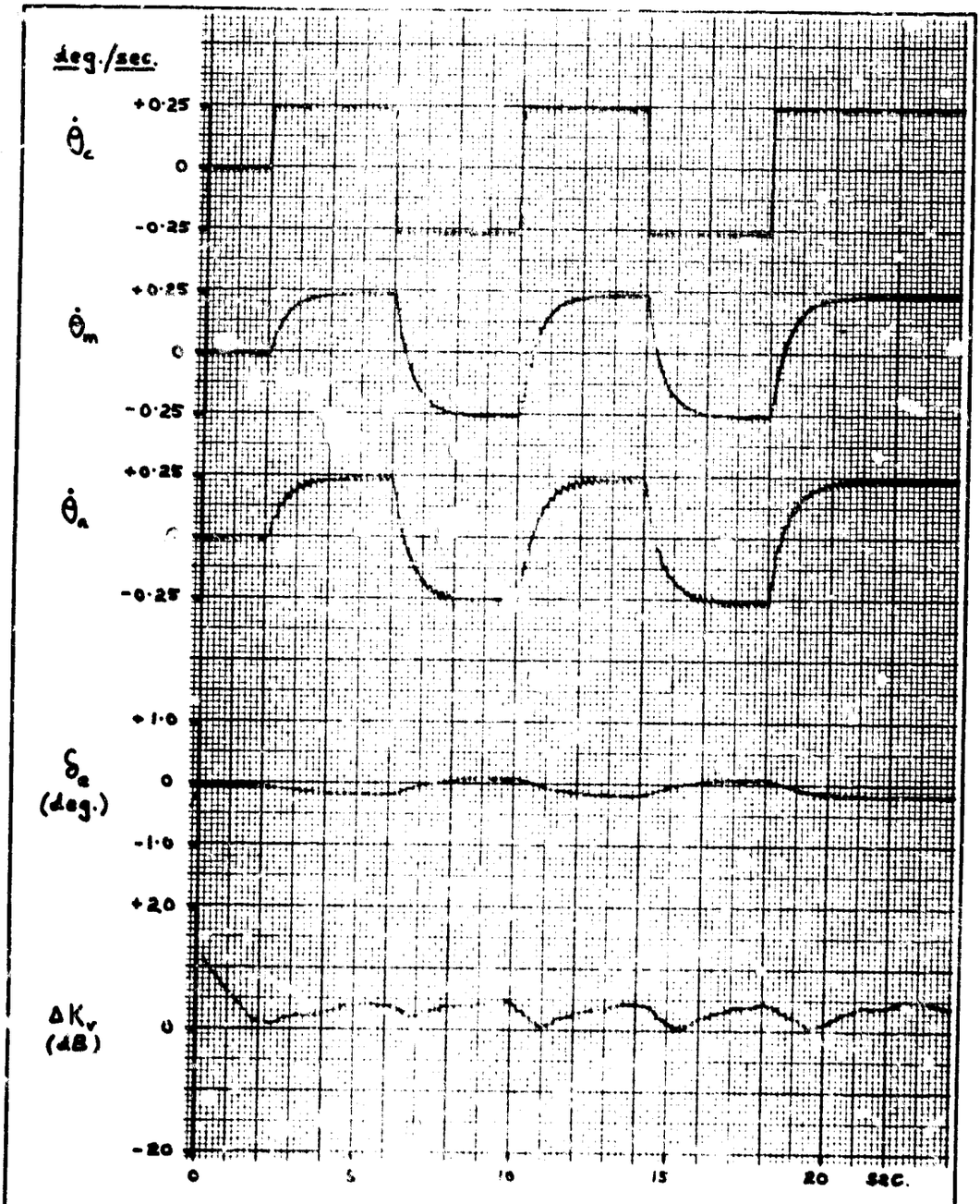

Fig. 14

Flight Condition 28 - With Dither Signal

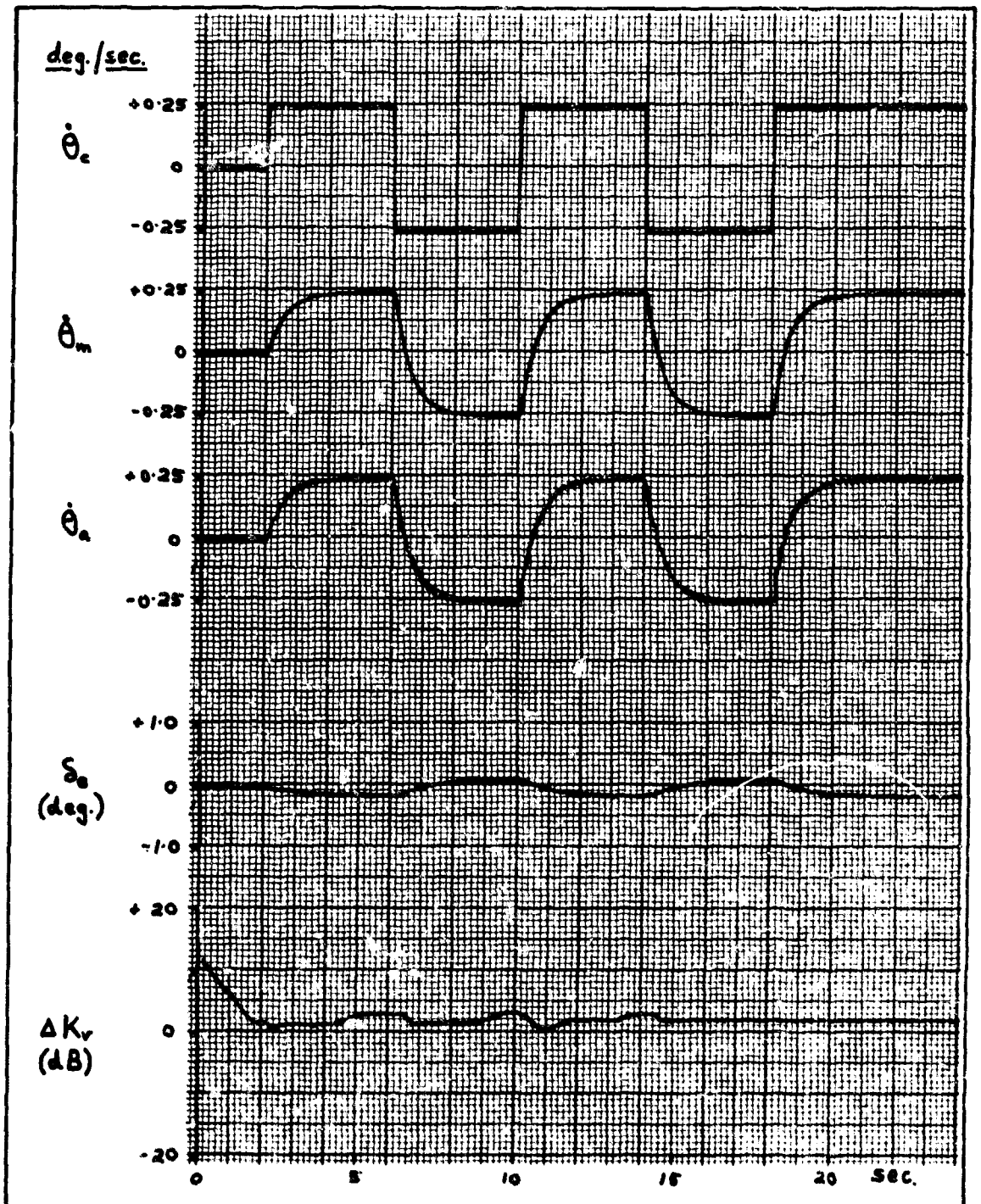

Fig. 14

Flight Condition 28 - With Dither Signal and Improved Decision Logic

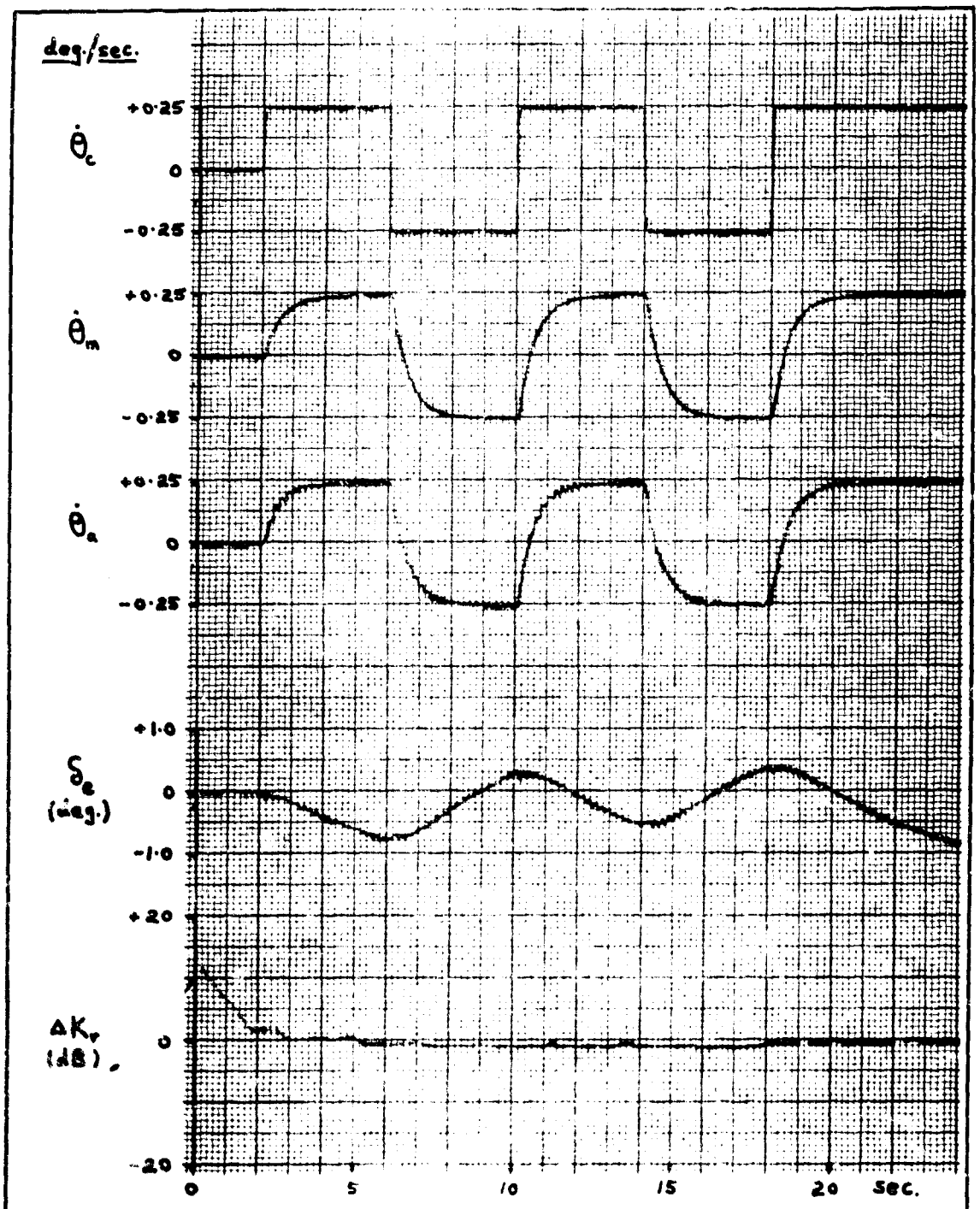

Fig. 15

Flight Condition 7 - With Dither Signal and Improved Decision Logic

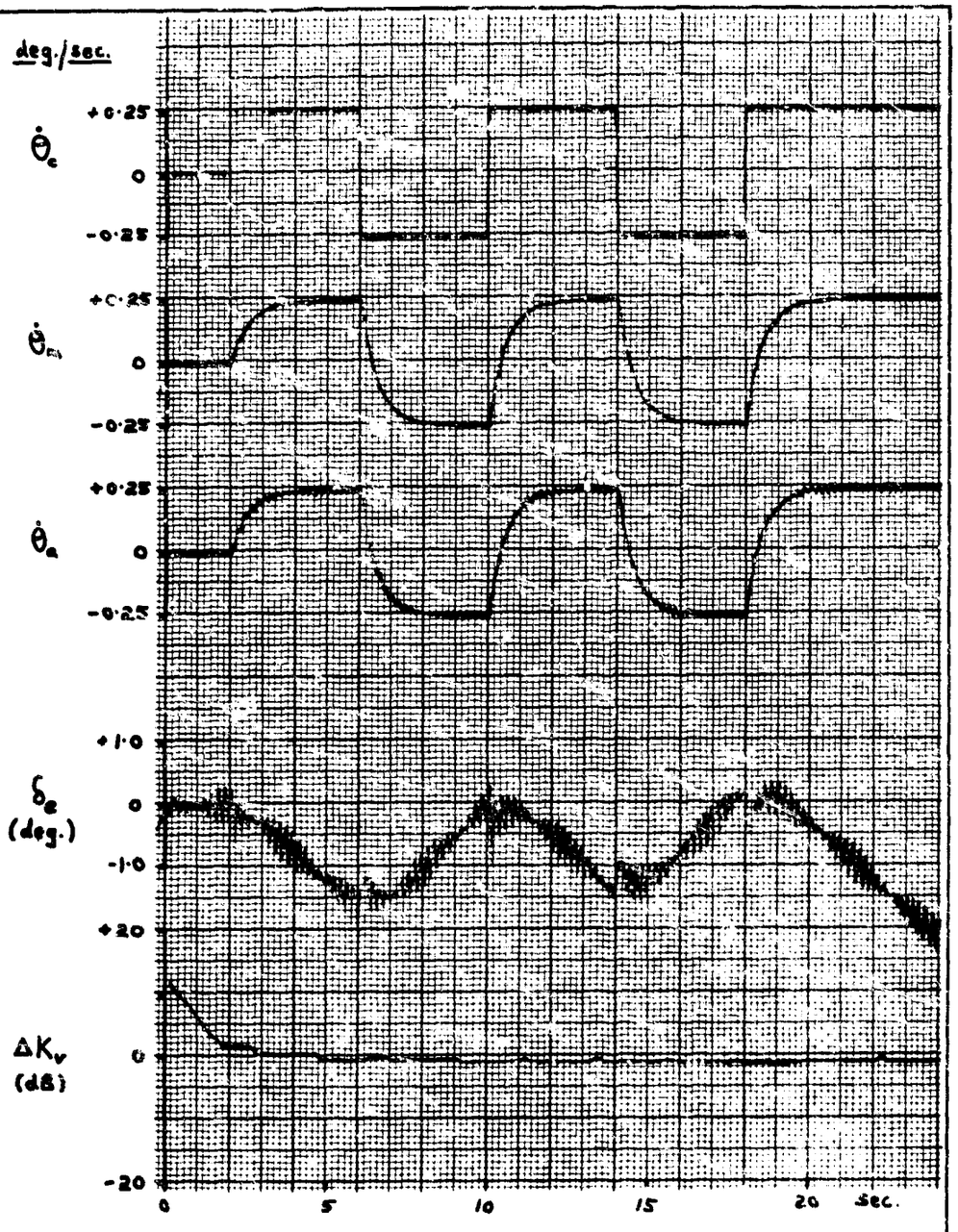

Fig. 16

Flight Condition 24 - With Dither Signal and Improved Decision Logic

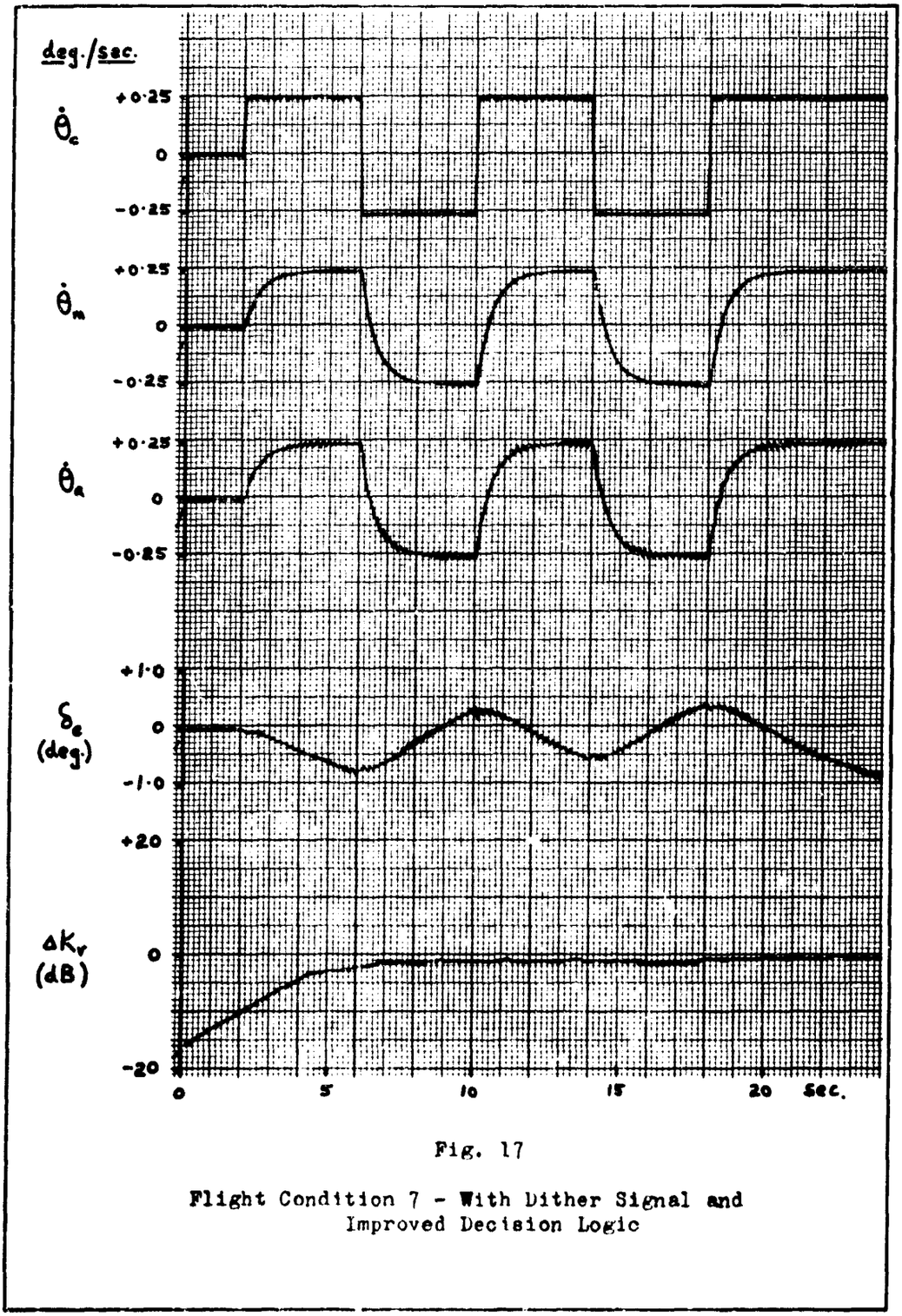

Fig. 17

Flight Condition 7 - With Dither Signal and Improved Decision Logic

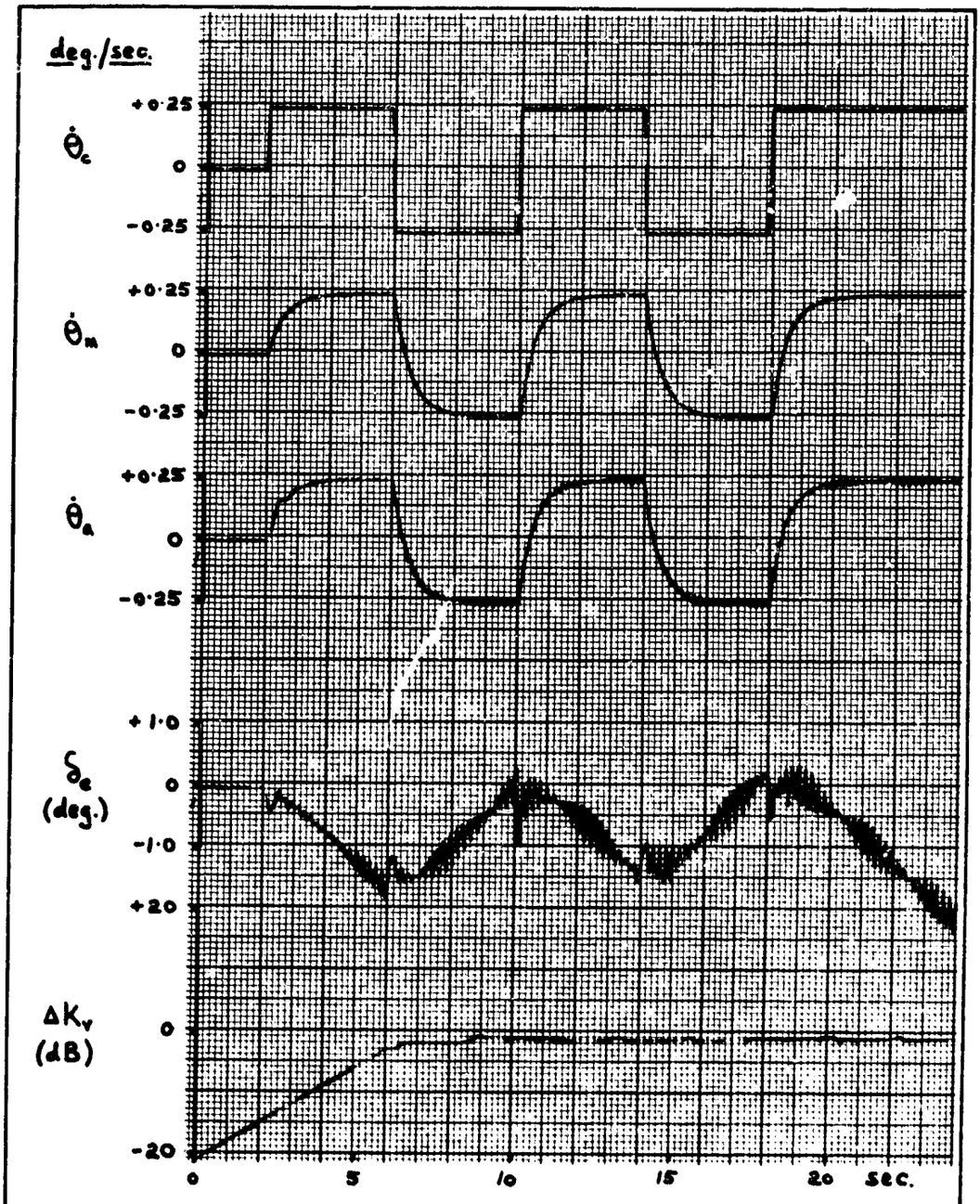

Fig. 18

Flight Condition 24 - With Dither Signal and Improved Decision Logic

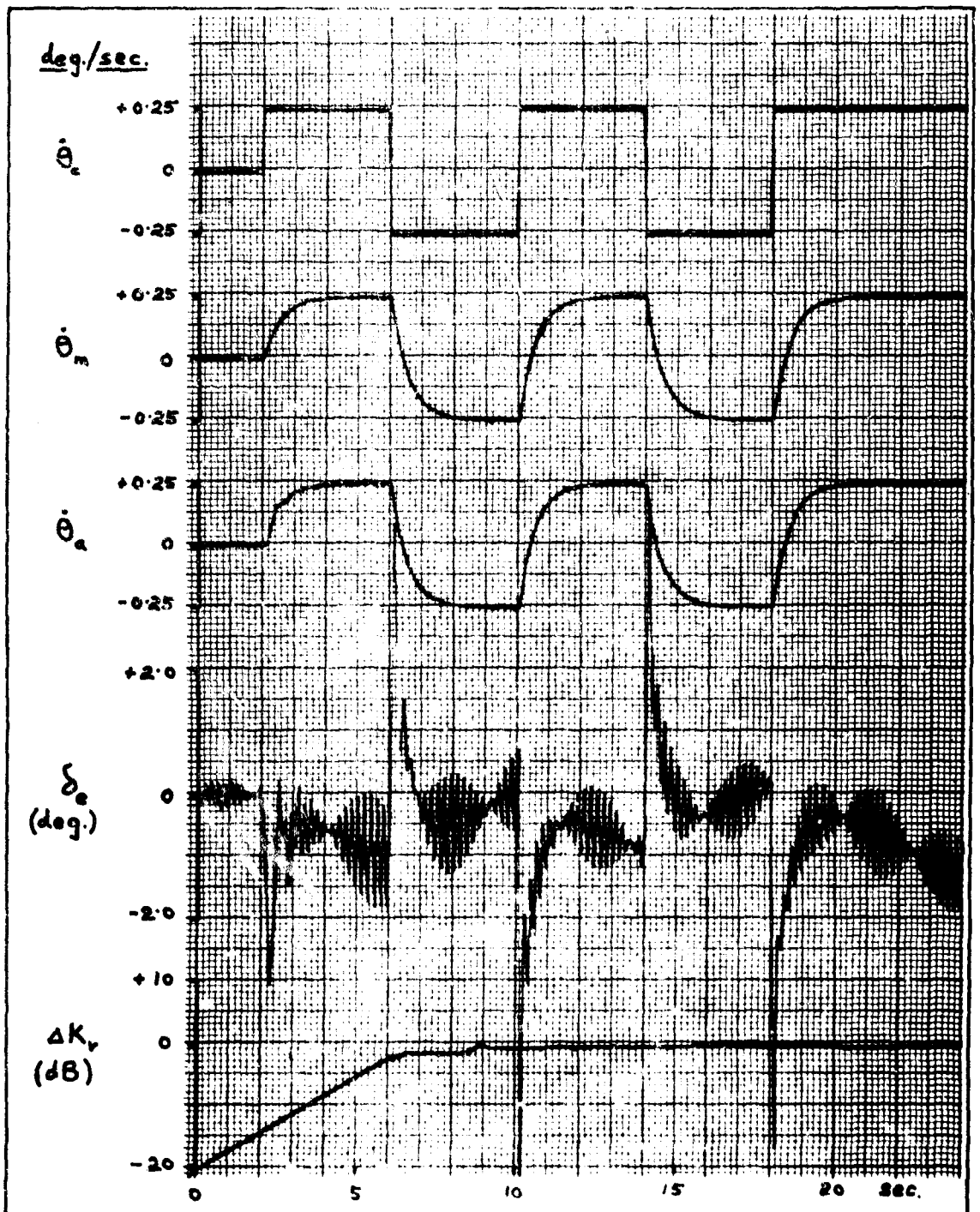

Fig. 19

Flight Condition 32 - With Dither Signal and Improved Decision Logic

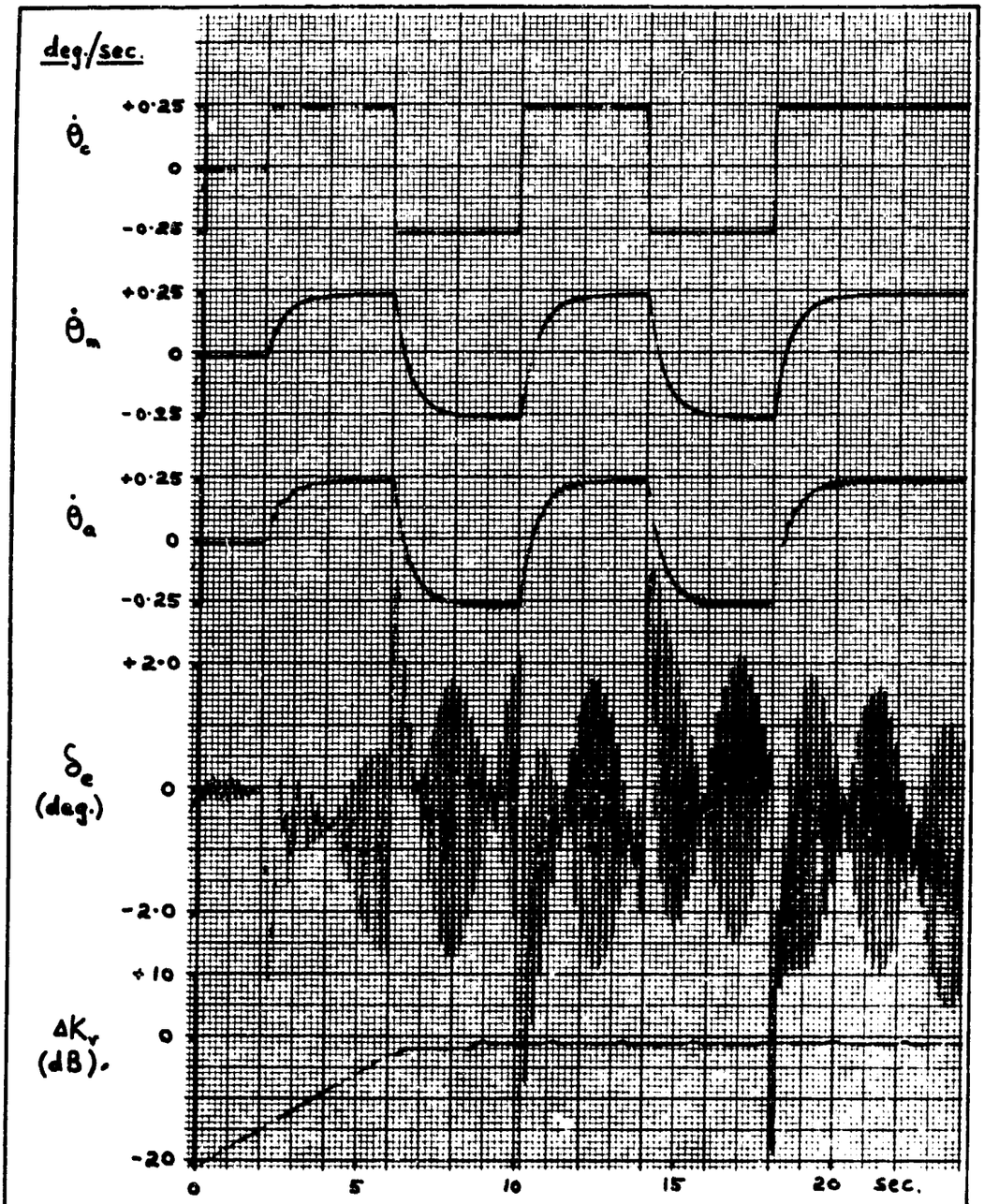

Fig. 20

Flight Condition 32 - Showing Excessive Elevator Motion When a Constant Amplitude Dither Signal was Used

V. Conclusions and Recommendations

Conclusions

1. Identification Accuracy. Difference equations, iterated in an airborne digital computer, may be used to identify the value of elevator effectiveness within approximately ±2 dB, provided that wind gust disturbances are not present and that accurate measurements of elevator deflection and aircraft pitch rate are available.

2. Loop Gain Adjustment. By adjusting a variable gain element in the forward loop inversely to changes in the identified value of elevator effectiveness the gain crossover frequency may be held within the range of 27 to 37 rad./sec. This frequency range is only 0.14 of a decade. In comparison, the gain crossover frequency shifts over approximately 1.7 decades for a fixed gain system, which greatly increases the problem of stabilizing the control loop. The figure of 1.7 decades is calculated by assuming that, for stability, an average gain slope of 28 dB/decade is required in the region of the gain crossover frequency, which shifts as the elevator effectiveness varies over 47.6 dB (240:1).

3. Bandwidth. The design open loop bandwidth (defined by the gain crossover frequency) for the self-adaptive system was set at 31.5 rad./sec. At this value, a fast control response was achieved, and yet the bandwidth was not so high that body bending modes would be significant. If a fixed gain system had been used, with this bandwidth for Flight Condition 32 (M_δ = -0.219), then the bandwidth for Flight Condition 28 (M_δ = -52.9) at a frequency of 1.7 decades higher would have been 470 rad./sec. Although this is an approximate theoretical figure, it is close to the value of 520 rad./sec. which was found to be necessary by Beale and Hellings (Ref. 1:94). In practise, of course, such large bandwidths are quite impossible to realize because of saturation effects in physical components in the control loop, noise pick-up and the destabilizing action of high frequency body bending modes. For the open loop bandwidth of 31.5 rad./sec. the closed loop bandwidth,

measured from the output of the pre-filter model reference to the aircraft pitch rate, was 6 dB down at a frequency of 22 rad./sec.

4. Response Speed. The control system response speed and consistency between the extreme ranges of elevator effectiveness is demonstrated by the following example. For a step pilot command input the output of the pre-filter model reference reached 90 per cent of its steady-state value after 1.15 sec. With this command, the aircraft pitch rate reached 90 per cent of the steady-state value after 1.26 sec. for Flight Condition 28, and after 1.14 sec. (implying a slight overshoot) for Flight Condition 32.

5. Dither Signal. The injection of a small amplitude dither signal into the control loop to continuously excite an aircraft response greatly improved the speed and accuracy of the identification process. The frequency of the dither signal was 30 rad./sec., and its maximum amplitude was 0.01 deg./sec. To prevent excessive elevator motion under conditions of low elevator effectiveness, the amplitude was reduced as a function of the identified elevator effectiveness, so that for Flight Condition 32 the amplitude was only 1/5 of the maximum value. In a practical implimentation of the identification process circuit noise and small disturbances to the aircraft flight path would probably be sufficient to make identification possible without a dither signal. This was found to be true for the General Electric system (Ref. 6:89).

6. Wind Gusts. The presence of wind gusts degraded the accuracy with which the elevator effectiveness was identified. For severe random wind gusts with an r.m.s. magnitude of 20 ft./sec. their effect on the control system was to cause the loop gain to decrease by 4 to 6 dB below its design value. Because of the tolerance of the high gain feedback loop to gain variations of this size, there was no adverse effect on the control response characteristics.

7. Difference Equations. To provide the greatest accuracy when transfer functions are represented by finite difference equations, derivative approximations should be made by means of central difference formulas. For a given test function, central differences

were found to give r.m.s. errors of only 0.01 per cent, compared with errors of approximately 4 per cent for both backward and forward differences.

Recommendations.

1. A low frequency analysis of the behavior of the decision logic indicated that wind gust disturbances acting on the aircraft should cause the loop gain to be increased beyond its design value. However, in the system simulation the gain was found to decrease. Because of lack of time, this phenomenon was not extensively investigated, although it appears likely to be due to failure of the difference equations to respond accurately to high frequency components in the elevator deflection motion. It is therefore recommended that the effect of wind gusts on the performance of the gain computer should be the subject of further investigation.

2. The central difference equation approximation to the aircraft transfer function was found to be very accurate (0.01 per cent r.m.s. error) when the exact aircraft parameters were used in it for test purposes. It is therefore recommended that a study be made to investigate the feasibility of writing a general purpose computer program for the simulation of closed loop control systems on the AFIT IBM 1620 machine. Such a program would use a central difference equation to represent each transfer function in the control loop.

Bibliography

Note: WPAFB - Wright-Patterson Air Force Base.

1. Beale, R. E. and F. J. Hellings. Comparison of High-Gain-Linear and Self-Adaptive Flight Control Systems for a Typical Winged Re-Entry Vehicle. Thesis. WPAFB, Ohio: Air Force Institute of Technology, May 1963.

2. Blakelock, J. H. Automatic Control of Aircraft and Missiles. New York: John Wiley and Sons, Inc., 1965.

3. Clark, D. C., et al. Application of Self-Adaptive Control Techniques to the Flexible Supersonic Transport. Report No. IH-1696-F-5 by Cornell Aeronautical Laboratory, Inc. Also published as ASD-TDR-63-831, Vol. 1. WPAFB, Ohio: Aeronautical Systems Division, August 1963.

4. Dorrity, J. L. Application of Multiple Fixed Compensators to Achieve Invariant Response. Thesis. WPAFB, Ohio: Air Force Institute of Technology, May 1963.

5. Etkin, B. Dynamics of Flight. New York: John Wiley and Sons, Inc., 1965.

6. Farr, J. E., D. P. Hoffman and N. R. Cooper. Evaluation of the General Electric Self-Adaptive Control System on the X-15 Flight Control Simulator. ASD TR 61-81. WPAFB, Ohio: Aeronautical Systems Division, August 1961.

7. Gebhart, C. E. and K. Jakstas. Digital Computer Simulation of Interceptor-Missiles. AL-TDR-64-12, Vol. 1. WPAFB, Ohio: Air Force Avionics Laboratory, January 1964.

8. Gregory, P. C. (Editor). Proceedings of the Self-Adaptive Flight Control Systems Symposium (January 1959). WADC Tech. Report No. 59-49; ASTIA (now Defense Documentation Center) Document No. AD 209369. WPAFB, Ohio: Flight Control Laboratory, March 1959.

9. Hendric, R. C. Design Requirements for Adaptive Flight Control Systems. Unpublished. Minneapolis-Honeywell Regulator Co., Minnesota: Advanced Flight Systems Section, January 1964.

10. Karnopp, D. "Combine Controller Parameters for Better Performance." Control Engineering: pp. 61-65, February 1967.

11. Lee, Y. W. Statistical Theory of Communication. New York: John Wiley and Sons, Inc., 1963.

12. Lindall, J., W. McGuire and M. Reed. Advanced Flight Vehicle

Adaptive Flight Control System. WADD-TR-651. WPAFB, Ohio: Air Force Flight Dynamics Laboratory, Flight Control Division, December 1963.

13. Nixon, F. E. Handbook of Laplace Transformation. New Jersey: Prentice-Hall, Inc., 1960.

14. Notess, C. B. A Triangle - Flexible Airplanes, Gusts, Crew. Memorandum No. 343. Cornell Aeronautical Laboratory, Inc., Buffalo, N. Y., May 1963.

15. ----- and P. C. Gregory. Requirements for the Flight Control System of a Supersonic Transport. Paper No. 679C; presented to National Aero-Nautical Meeting, Washington, D. C., April 1963. Society of Automotive Engineers - Society of Naval Engineers, 1963.

16. Osburn, P. V., H. P. Whitaker and A. Kezer. New Developments in the Design of Model Reference Adaptive Control Systems. IAS Paper No. 61-39. Institute of the Aerospace Sciences, New York, February 1961.

17. Peterson, H. E. and F. J. Sansom. MIMIC - a Digital Simulator Program. Internal Memo. 65-12. WPAFB, Ohio: Directorate of Computation, May 1965.

18. Press, H., M. T. Meadows and I. Hadlock. A Re-Evaluation of Data on Atmospheric Turbulence and Airplane Gust Loads for Application in Spectral Calculations. NACA Report No. 1272. Washington: National Advisory Committee for Aeronautics, 1956.

19. Salvadori, M. G. and M. L. Baron. Numerical Methods in Engineering. New York: Prentice-Hall, Inc., 1961.

20. Schuler, J. M., C. R. Chalk and A. E. Schelhorn. Application and Evaluation of Certain Adaptive Control Techniques in Advanced Flight Vehicles. ASD-TR-61-104, Vol. 1. WBAFB, Ohio: Aeronautical Systems Division, July 1961.

21. Stein, T. T. Difference Equations - Adaptive Controller Design Technique. Thesis. WPAFB, Ohio: Air Force Institute of Technology, June 1966.

22. Zaborsky, J., et al. Development of an Advanced Digital Adaptive Flight Control System. FDL-TDR-64-115. WPAFB, Ohio: Flight Control Laboratory, December 1964.

Appendix A

The System Simulation Program

Input Data

Input data for the program is contained on three cards. The parameters which are required to be specified on these cards are listed below.

Card No. 1

WVEL	A velocity (W_{g_o}) as a starting value for the wind gust samples defined in equation (B.8).
UAC	Aircraft velocity (U); specified in Appendix C, Table II.
TS	Integration step interval (t_s), and also wind gust sample interval.

Card No. 2

GF	Control loop fixed gain factor (K_f).
GV	Initial value for the variable gain factor (K_v).
STOP	Length of simulation run (sec.) required.
K	A switch. If K = 1.0 the program will run normally, but if K = 0.0 then K_v will remain fixed at its initial value.
TEMPG	A dummy variable, which may be ignored.

Card No. 3

MQ	
MALF	The aircraft stability derivatives M_q, M_α,
MDEL	M_δ, L_α, and L_δ, respectively. Numerical
LALF	values are contained in Appendix C, Table I.
LDEL	

Program Organization

A list of the program statements is given at the end of this Appendix. It will be noticed that the complete program is divided into two sections; the first is written in the MIMIC programming

language, and the second in FORTRAN. In general terms, the two sections of the program perform the following operations:

MIMIC

a. Simulation of the aircraft longitudinal equations of motion; equations (C.1) and (C.2).

b. Simulation of the components comprising the control system;

(1) Pre-filter model reference.

(2) Fixed and variable gain elements.

(3) Compensator.

(4) Servo and actuator.

(5) Rate gyro.

c. Generation of inputs to the control system;

(1) Pilot pitch rate commands.

(2) Dither signal to stimulate the adaptive control mechanism in the absence of pilot commands.

(3) Random wind gusts. (Ref. Appendix B)

d. Transmission of data to the airborne digital computer (the gain computer, simulated in the FORTRAN section);

(1) Samples of elevator deflection angle and aircraft pitch rate (as measured by the rate gyro) every 0.01 sec.

(2) The present value of the variable gain setting every 0.1 sec.

e. Output of pilot commands and aircraft responses, etc., for storage on magnetic tape. The tape could then be later transcribed on the Benson-Lehner digital plotter.

FORTRAN

a. Simulation of the airborne digital computer;

(1) Iteration of the three difference equations, and calculation of their root-mean-square errors.

(2) Decision whether or not to change the loop gain.

b. Transmission of output data to the line printer;

(1) Errors in the difference equation solutions.

(2) Control loop gain error, calculated from equation (D.7). It should be noted that this calculation of gain error (ΔK_v) is readily made during simulation, where the true value of elevator effectiveness for the Flight Condition which is being simulated is known precisely.

Program Execution Sequence

Through the use of the MIMIC processor (Ref. 17), which is available on the IBM 7094 computer, differential equations may be set up and solved in a way which closely resembles that used in analog computation. Consider, for example, equation (C.1):

$$\ddot{\theta}_a = M_q \dot{\theta}_a + M_\alpha \alpha + M_\delta \delta_e \qquad (C.1)$$

In the MIMIC program language this equation is written,

```
DQAC    = MQ*QAC+MALF*ALF+MDEL*EL
```

where, DQAC is the program symbol for $\ddot{\theta}_a$, QAC is the symbol for $\dot{\theta}_a$, and the other terms are self-descriptive. Then, to get $\dot{\theta}_a$ from $\ddot{\theta}_a$, the variable DQAC is simply used as the input to a MIMIC integrator, with zero initial conditions:

```
QAC     = INT(DQAC,0.)
```

Unlike an analog computer, however, the digital computer can only perform one integration at a time, so that the integrator outputs must be updated in sequence; this is organized automatically by the MIMIC processor. Normally, the processor also adjusts the integration step interval so that the error at the output of each integrator is held to within 5 parts in 10^6. When the random wind gust inputs were used this latter facility was not available, and instead, a fixed integration step of 0.0005 sec. was used as a compromise between accuracy and speed of computation. This step size dictated the sampling period (t_s) for the wind gusts.

To provide computation time for simulation of the airborne computer, the following time-sharing routine was established in the IBM 7094 computer:

a. The initial value for the setting of the variable gain element (K_v), which was input to the program on a data card, was used in the MIMIC simulation of the control loop during the first 0.1 sec.

b. Every 0.01 sec. the computed values of elevator deflection and aircraft pitch rate were stored and transfered to the FORTRAN section of the program.

c. After the end of the first 0.1 sec. of MIMIC computation (and at subsequent 0.1 sec. intervals) all the outputs of the MIMIC integrators were 'frozen', and computation was transfered to the FORTRAN section.

d. Using the known value of K_v, the best estimate of computed elevator effectiveness (M_{δ_y}) was established from the relationship between these two variables defined by equation (D.6).

e. Coefficients for the three difference equations were calculated from M_{δ_y}, as described in Appendix E.

f. The difference equations were initialized and then iterated, using the stored values of elevator deflection as inputs.

g. A calculation of the root-mean-square errors of the difference equations was made by comparing the iterated solutions with the stored values of aircraft pitch rate.

h. Based on the relative magnitudes of the r.m.s. errors (R_x, R_y, and R_z), a decision was made whether or not to change the loop gain:

(1) $R_x < R_y < R_z$; K_v increased by 0.3 dB.

(2) $R_x > R_y > R_z$; K_v decreased by 0.6 dB.

(3) $R_x > R_y$ and $R_z > R_y$; K_v unchanged.

i. MIMIC simulation for a further 0.1 sec. was continued, with the new value of K_v, and the routine was repeated until the required program running time had been completed. It may be noted that equation (D.6) was always used to relate K_v and M_{δ_y} when the computation was transfered from the MIMIC section to the FORTRAN section, or vice-versa.

Output Data

A short sample of printed output data from the IBM 7094 computer is given in Fig. A.1. These results were obtained by the application of a 0.5 deg./sec. step command input to the control system, with the aircraft in Flight Condition 24, and with an initial gain error (ΔK_v) of 6 dB.

Printed across the page are values of the aircraft pitch rate (from the rate gyro) at 0.01 sec. intervals, and underneath them are the corresponding errors in the difference equation solutions. It can be seen that the difference equations were restarted every 0.1 sec., using two samples of the aircraft pitch rate to set in the initial conditions. The extreme right hand column contains the final values of the difference equation errors at the end of each 0.1 second computation cycle (i.e. after eight iterations). Also in this column is the gain error, which decreased from 6 dB to 3 dB over the period of 0.7 sec. To the left of this column are three offset columns containing the root-mean-square (r.m.s.) errors of the difference equations over each computation cycle: to obtain comparable numbers for the r.m.s. errors, they have been normalized with respect to the r.m.s. change in aircraft pitch rate from its value at the begining of the relevant computation cycle.

At the end of the first three computation cycles the r.m.s. error of the z-difference equation was less than that of the other two, so that ΔK_v was reduced to 4.2 dB in three steps of 0.6 dB. However, at the end of the fourth cycle the y-difference equation had the smallest error, and consequently no gain change was made. It may be expected that this will happen occasionally because of the approximations made in the difference equations. For the remaining three computation cycles shown in the figure further decreases in gain were correctly generated.

Over the same period (but not shown in the print-out) it follows from equation (D.6) that the values of elevator effectiveness used in the difference equations (M_{δ_x}, M_{δ_y}, M_{δ_z}) were all <u>increased</u> by 3 dB, so that M_{δ_y} approached the true value of the

aircraft elevator effectiveness. Thus, at the begining of the simulation run M_{δ_y} was 6 dB too small, but after 0.7 sec. it was only 3 dB too small. The closer matching of M_{δ_y} to the true elevator effectiveness is reflected in greater accuracy in the difference equation solutions. For example, at the end of the first computation cycle the y-difference equation error was 49 per cent (0.0488/0.0991), whereas at the end of the seventh cycle it was only 0.76 per cent (0.0030/0.3926); both the percentage error, with respect to the aircraft pitch rate, and the absolute error were reduced.

TIME

0.1					
AIRCRAFT PITCH RATE	0.0000	0.0019	0.0100	0.0256	0.0
X DIFF. EQN. ERROR	0.	0.	-0.0047	-0.0152	-0.0
Y DIFF. EQN. ERROR	0.	0.	-0.0030	-0.0103	-0.0
Z DIFF. EQN. ERROR	0.	0.	-0.0014	-0.0054	-0.0
0.2					
AIRCRAFT PITCH RATE	0.1022	0.1054	0.1093	0.1137	0.1
X DIFF. EQN. ERROR	0.	0.	-0.0004	-0.0013	-0.0
Y DIFF. EQN. ERROR	0.	0.	-0.0003	-0.0008	-0.0
Z DIFF. EQN. ERROR	0.	0.	-0.0001	-0.0003	-0.0
0.3					
AIRCRAFT PITCH RATE	0.1663	0.1768	0.1875	0.1979	0.2
X DIFF. EQN. ERROR	0.	0.	-0.0001	0.0001	0.0
Y DIFF. EQN. ERROR	0.	0.	-0.0001	-0.0000	0.0
Z DIFF. EQN. ERROR	0.	0.	-0.0001	-0.0001	-0.0
0.4					
AIRCRAFT PITCH RATE	0.2403	0.2415	0.2423	0.2429	0.2
X DIFF. EQN. ERROR	0.	0.	0.0004	0.0009	0.0
Y DIFF. EQN. ERROR	0.	0.	0.0003	0.0007	0.0
Z DIFF. EQN. ERROR	0.	0.	0.0001	0.0004	0.0
0.5					
AIRCRAFT PITCH RATE	0.2683	0.2763	0.2850	0.2938	0.3
X DIFF. EQN. ERROR	0.	0.	-0.0004	-0.0011	-0.0
Y DIFF. EQN. ERROR	0.	0.	-0.0003	-0.0007	-0.0
Z DIFF. EQN. ERROR	0.	0.	-0.0001	-0.0003	-0.0
0.6					
AIRCRAFT PITCH RATE	0.3323	0.3326	0.3321	0.3310	0.3
X DIFF. EQN. ERROR	0.	0.	0.0006	0.0017	0.0
Y DIFF. EQN. ERROR	0.	0.	0.0004	0.0010	0.0
Z DIFF. EQN. ERROR	0.	0.	0.0001	0.0003	0.0
0.7					
AIRCRAFT PITCH RATE	0.3367	0.3421	0.3484	0.3555	0.3
X DIFF. EQN. ERROR	0.	0.	-0.0006	-0.0017	-0.0
Y DIFF. EQN. ERROR	0.	0.	-0.0003	-0.0008	-0.0
Z DIFF. EQN. ERROR	0.	0.	0.0000	0.0001	0.0

Fig. A.1

Sample of the Simulation Program Print-Out

				RMSX	RMSY	RMSZ	GAIN	ERROR(DB)
				0.6824	0.4963	0.3111		6.0
0.0019	0.0100	0.0256	0.0453	0.0643	0.0793	0.0893	0.0954	0.0991
0.	-0.0047	-0.0152	-0.0292	-0.0427	-0.0534	-0.0602	-0.0639	-0.0658
0.	-0.0030	-0.0103	-0.0203	-0.0303	-0.0384	-0.0438	-0.0470	-0.0488
0.	-0.0014	-0.0054	-0.0114	-0.0178	-0.0234	-0.0274	-0.0301	-0.0319
				0.3121	0.1900	0.0722		5.4
0.1054	0.1093	0.1137	0.1187	0.1244	0.1308	0.1382	0.1467	0.1561
0.	-0.0004	-0.0013	-0.0025	-0.0042	-0.0065	-0.0095	-0.0132	-0.0176
0.	-0.0003	-0.0008	-0.0015	-0.0026	-0.0040	-0.0058	-0.0080	-0.0107
0.	-0.0001	-0.0003	-0.0006	-0.0010	-0.0015	-0.0022	-0.0030	-0.0041
				0.1754	0.0992	0.0197		4.8
0.1768	0.1875	0.1979	0.2076	0.2164	0.2239	0.2301	0.2348	0.2381
0.	-0.0001	0.0001	0.0006	0.0019	0.0040	0.0071	0.0113	0.0165
0.	-0.0001	-0.0000	0.0003	0.0009	0.0021	0.0039	0.0063	0.0094
0.	-0.0001	-0.0001	-0.0002	-0.0001	0.0001	0.0005	0.0012	0.0021
				0.2340	0.1042	0.1633		4.2
0.2415	0.2423	0.2429	0.2438	0.2451	0.2473	0.2507	0.2553	0.2612
0.	0.0004	0.0009	0.0014	0.0015	0.0010	-0.0002	-0.0023	-0.0053
0.	0.0003	0.0007	0.0011	0.0014	0.0014	0.0010	0.0001	-0.0012
0.	0.0001	0.0004	0.0007	0.0011	0.0015	0.0019	0.0022	0.0024
				0.0692	0.0337	0.0223		4.2
0.2763	0.2850	0.2938	0.3025	0.3105	0.3176	0.3235	0.3279	0.3308
0.	-0.0004	-0.0011	-0.0015	-0.0016	-0.0010	0.0004	0.0029	0.0064
0.	-0.0003	-0.0007	-0.0010	-0.0012	-0.0009	-0.0002	0.0010	0.0029
0.	-0.0001	-0.0003	-0.0006	-0.0008	-0.0010	-0.0012	-0.0012	-0.0010
				1.2100	0.9569	0.6846		3.6
0.3326	0.3321	0.3310	0.3296	0.3285	0.3278	0.3281	0.3296	0.3324
0.	0.0006	0.0017	0.0029	0.0041	0.0050	0.0053	0.0049	0.0035
0.	0.0004	0.0010	0.0019	0.0027	0.0035	0.0040	0.0042	0.0040
0.	0.0001	0.0003	0.0007	0.0012	0.0018	0.0025	0.0032	0.0040
				0.1310	0.0706	0.0192		3.0
0.3421	0.3484	0.3555	0.3630	0.3705	0.3776	0.3838	0.3889	0.3926
0.	-0.0006	-0.0017	-0.0030	-0.0044	-0.0055	-0.0061	-0.0059	-0.0048
0.	-0.0003	-0.0008	-0.0015	-0.0022	-0.0028	-0.0032	-0.0033	-0.0030
0.	0.0000	0.0001	0.0000	-0.0001	-0.0003	-0.0006	-0.0010	-0.0014

1

Program Print-Out

B

```
**** ADAPTIVE CONTROL SYSTEM SIMULATION PROGRAM ****

*      MIMIC SECTION

$SETUP 15       DISK,1496
$DATA
                    PAR(WVEL,UAC,TS)
                    PAR(GF,GV,STOP,K,TEMPG)
                    PAR(MQ,MALF,MDEL,LALF,LDEL)
          DT      = 0.002
          DTMIN   = TS
          DTMAX   = TS
WIND GUST GENERATOR
          TC      = 666./UAC
          SD      = SQR(400.0*(1.-EXP(-2.*(TS/TC))))
          SNO     = 145.91
          RAN     = SR2(0.,SD,SNO,T)
          WVEL    = RAN+WVEL*EXP(-TS/TC)
          ALFN    = -WVEL/UAC
PILOT INPUT
          QC      = 0.0
MODEL
          QMOD    = FTR(QC,.5)
ERROR SUMMATION
          EPSY    = QMOD-QGYRO+AMPL*SIN(30.0*T)
COMPENSATOR
          COMOP   = 10.*EPSY -9.*FTR(EPSY,.005)
FIXED GAIN
          KFOP    = -GF*COMOP
VARIABLE GAIN
          KVOP    = KFOP*GV
SERVO/ACTUATOR
          DDDEL   = -180.*DDEL-3.24E4*(DEL-KVOP)
          DDEL    = INT(DDDEL,0.)
          DEL     = INT(DDEL,0.)
          EL      = INT(DEL,0.)
AIRCRAFT SHORT-PERIOD DYNAMICS
          DQAC    = MQ*QAC+MALF*ALF+MDEL*EL
          QAC     = INT(DQAC,0.)
          DALF    = QAC-LALF*ALF-LDEL*EL
          ALF     = INT(DALF,0.)+ALFN*57.3
          DGAMA   = QAC-DALF
          NZG     = (DGAMA*UAC)/(57.3*32.2)
RATE GYRO
          DDGYRO  = -400.*DGYRO-1.6E5*(QGYRO-QAC)
          DGYRO   = INT(DDGYRO,0.)
          QGYRO   = INT(DGYRO,0.)
E-FILTER
          E       = EL
Q-FILTER
          Q       = QGYRO
```

```
MIMIC-FORTRAN COMMUNICATION
          GV        SR1(E,Q,GV,MDEL,TEMPG,K)
          GVERR  =  TEMPG+T-T
                    FIN(T,STOP)
OUTPUT TO PLOTTER
                    PLO(T,GVERR,EL,QAC,NZG)
                    ZER(5.0,6.0,9.0,12.0,15.0)
                    SCA(0.5,5.0,10.0,0.1,0.1)
                    PLO(T,ALF,WVEL)
                    ZER(5.0,18.0,21.0)
                    SCA(0.5,5.0,40.0)
                    END

C**** FORTRAN SECTION

$IBFTC MM13
      SUBROUTINE SR1(A,B,C,D,GVERR,ADJGVK,GV)
      DIMENSION P(95),R(2500),S(2500),FF(9100)
      COMMON P,R,S,FF,IOUT,IPAR,INOUT,IHDR,IFIN,IEND,
     C       NPAR,LKDR,LKDR2,ILC,IPC,IS,ICOUNT,ISKIP
      DIMENSION E(10),Q(10),X(10),Y(10),Z(10)
      DIMENSION XERR(10),YERR(10),ZERR(10)
      DIMENSION EA(50), QB(50)
      DATA I/0/
      IF(IOUT.NE.1) RETURN
      IF(R(1).NE.0.) GO TO 50
      I=0
      CMDEL=-D
      GV=C
      REQDGV=52.95/CMDEL
      GVRAT=GV/REQDGV
      IF(GVRAT-1.) 1,2,3
 1    GVERR= -8.686*ALOG(1./GVRAT)
      GO TO 4
 2    GVERR=0.
      GO TO 4
 3    GVERR=8.686*ALOG(GVRAT)
 4    K=ADJGVK
      WRITE(6,20)
 20   FORMAT(/,5H TIME,75X,4HRMSX,6X,4HRMSY,6X,4HRMSZ,
     C       16H  GAIN ERROR(DB),//)
      RETURN
 50   I=I+1
C**** RECEIVE DATA FROM MIMIC SECTION
      EA(I)=A
      QB(I)=B
      IF(I.NE.50)RETURN
C**** SAMPLES FOR THE DIFFERENCE EQNS.
      J=0
      DO 70 L=1,46,5
      J=J+1
      E(J)=EA(L)
 70   Q(J)=QB(L)
```

```
C**** COMPUTED VALUES OF AIRCRAFT CONSTANTS
      SUMSDQ=0.
      SUMSQX=0.
      SUMSQY=0.
      SUMSQZ=0.
      DMY=52.95/GV
      DMX=DMY/2.0
      DMZ=DMY*1.5
      DBMY=8.686*ALOG(DMY/.2193)
      DBMX=DBMY-6.
      DBMZ=DBMY+3.522
      IF(GV.GT.120.7)DBMX=0.0
      IF(GV.LT.1.5)DBMZ=47.66
      ZWAX=.002*EXP(.1518*DBMX)
      ZWAY=.002*EXP(.1518*DBMY)
      ZWAZ=.002*EXP(.1518*DBMZ)
      WAX=OMEGA(DBMX)
      WAY=OMEGA(DBMY)
      WAZ=OMEGA(DBMZ)
C**** COEFFICIENTS FOR THE CENTRAL DIFFERENCE EQUATIONS
      DMX=-DMX
      DMY=-DMY
      DMZ=-DMZ
      CX=1./(1.+.01*ZWAX)
      CXE31=.005*DMX*CX
      CXE2=.0001*DMX*ZWAX*CX
      CX2=(2.-.0001*WAX*WAX)*CX
      CX1=(1.0-0.01*ZWAX)*CX
C
      CY= 1./(1.+.01*ZWAY)
      CYE31=.005*DMY*CY
      CYE2=.0001*DMY*ZWAY*CY
      CY2=(2.-.0001*WAY*WAY)*CY
      CY1=(1.0-0.01*ZWAY)*CY
C
      CZ=1./(1.+.01*ZWAZ)
      CZE31=.005*DMZ*CZ
      CZE2=.0001*DMZ*ZWAZ*CZ
      CZ2=(2.-.0001*WAZ*WAZ)*CZ
      CZ1=(1.0-0.01*ZWAZ)*CZ
C**** ITERATION OF THE DIFFERENCE EQUATIONS
      DO 100 J=1,2
      X(J)=Q(J)
      Y(J)=X(J)
 100  Z(J)=Y(J)
      DO 200 J=1,8
      X(J+2)=CXE31*(E(J+2)-E(J))+CXE2*E(J+1)+CX2*X(J+1)-CX1*X(J)
      Y(J+2)=CYE31*(E(J+2)-E(J))+CYE2*E(J+1)+CY2*Y(J+1)-CY1*Y(J)
      Z(J+2)=CZE31*(E(J+2)-E(J))+CZE2*E(J+1)+CZ2*Z(J+1)-CZ1*Z(J)
      SUMSQX=SUMSQX+(X(J+2)-Q(J+2))**2
      SUMSQY=SUMSQY+(Y(J+2)-Q(J+2))**2
      SUMSQZ=SUMSQZ+(Z(J+2)-Q(J+2))**2
      SUMSDQ=SUMSDQ+(Q(J+2)-Q(2))**2
```

```
C**** CALCULATION OF RMS ERRORS
      RMSX=SQRT(SUMSQX/SUMSDQ)
      RMSY=SQRT(SUMSQY/SUMSDQ)
      RMSZ=SQRT(SUMSQZ/SUMSDQ)
C**** DECISION WHETHER TO CHANGE GAIN
      PRERR=GVERR
      IF(K-1)16,30,16
 30   IF((RMSX.GT.RMSY).AND.(RMSY.GT.RMSZ))GO TO 9
      IF((RMSX.LT.RMSY).AND.(RMSY.LT.RMSZ))GO TO 11
      GO TO 16
C**** GAIN WAS TOO HIGH
 9    GV=GV/1.072
      IF(GV-1.) 10,8,8
 10   GV=1.
      GO TO 8
 11   IF(RMSZ.LT.(3.0*RMSX))GO TO 16
C**** GAIN WAS TOO LOW
      GV=GV*1.035
      IF(GV-241.4) 8,8,12
 12   GV=241.4
 8    GVRAT=GV/REQDGV
      IF(GVRAT-1.) 13,14,15
 13   GVERR= -8.686*ALOG(1./GVRAT)
      GO TO 16
 14   GVERR=0.
      GO TO 16
 15   GVERR=8.686*ALOG(GVRAT)
C**** OUTPUTS TO BE PRINTED
 16   DO 300 M=1,10
      XERR(M)=X(M)-Q(M)
      YERR(M)=Y(M)-Q(M)
 300  ZERR(M)=Z(M)-Q(M)
      WRITE(6,22)R(1),RMSX,RMSY,RMSZ,PRERR
 22   FORMAT(F4.1,70X,3F10.4,F16.1)
      WRITE(6,60)(Q(M),M=1,10)
 60   FORMAT(20H AIRCRAFT PITCH RATE,10F10.4)
      WRITE(6,61)(XERR(M),M=1,10)
 61   FORMAT(20H X DIFF. EQN. ERROR ,10F10.4)
      WRITE(6,62)(YERR(M),M=1,10)
 62   FORMAT(20H Y DIFF. EQN. ERROR ,10F10.4)
      WRITE(6,63)(ZERR(M),M=1,10)
 63   FORMAT(20H Z DIFF. EQN. ERROR ,10F10.4,//)
      I=0
      RETURN
      END
$IBFTC OME
      FUNCTION OMEGA(DBGEN)
      IF(DBGEN.GT.11.) GO TO 53
      OMEGA=.5+.03*DBGEN
      RETURN
 53   IF(45.5.GE.DBGEN) GO TO 56
      OMEGA=DBGEN-40.6
      RETURN
```

```
 56    OMEGA=-.57+.121*DBGEN
       RETURN
       END
       SUBROUTINE SR2(XMEAN,STD,ISTART,D,E,F,ANS)
       ISTART=ISTART*30517578125
       ANS=OR(ARS(ISTART,8),2**34)
       CALL MIMRN(XMEAN,STD,ANS)
       RETURN
       END
```

Appendix B

Digital Simulation of the Effect of Vertical Random Wind Gusts on the Performance of the Gain Computer

Effect of Gusts on the Airframe

For flight through atmospheric turbulence only the vertical components of wind velocity (W_g) have any influence on the aircraft longitudinal motion. The principle effect is that a downdraft (positive in the NACA axis convention) results in a negative incremental change (α_g) in the angle of attack, owing to a change in direction of the relative wind.

$$\alpha_g = -57.3 \frac{W_g}{U} \quad \text{(deg.)} \qquad \text{(B.1)}$$

where U is the aircraft forward velocity.

Spectral Density of Turbulance

Over a short period of time variations in atmospheric turbulence may be assumed to have a stationary Gaussian distribution within a local region of the atmosphere. This assumption implies that the region or time is small relative to the entire flight path or flight duration, but is large enough for statistical equilibrium to be achieved (Ref. 18:5). At any instant within such a region along the flight path the vertical components of wind velocity are characterized by the root-mean-square (r.m.s.) intensity, and by the spatial distribution of velocity. By Fourier analysis, this spatial distribution may be decomposed into sine waves, each of which has an associated wave number. The predominant wavelength, the one which contains the largest turbulence energy, has typically a length (λ_p) of 0.8 miles, so that the frequency (f_p) at which an aircraft traverses these waves is,

$$f_p = \frac{U}{\lambda_p} \qquad \text{(B.2)}$$

An approximate expression (Ref. 15:2) for gust power spectral density ($\phi_g(w)$, ft^2/sec^2 per radian/sec.) which reflects the influence of flight speed on the received distribution of gust velocity

is given below,

$$\phi_g(w) = \frac{4\,T_g\,\overline{w_g^2}}{1 + w^2T_g^2} \qquad \text{for } 0 < w < \infty \qquad (B.3)$$

where, $w = 2\pi f$ (rad./sec.)

$\overline{w_g^2}$ = mean-square gust velocity ($ft.^2/sec.^2$)

and, $T_g = \frac{\lambda p}{2\pi U} = \frac{666}{U}$ (sec., for U in ft./sec.)

Equation (B.3) has been used by Cornell Aeronautical Laboratory (Ref. 3:25) for testing the gust response of a proposed supersonic transport aircraft, and is the expression for spectral density which was used in this simulation.

Analog Simulation of Gusts

Before the digital simulation of gusts is described the more familiar problem of analog simulation will be mentioned, because it illustrates the relative simplicity of all-digital simulation. Equation (B.3) may be written,

$$\phi_g(w) = 4\,T_g\,\overline{w_g^2}\left|\frac{1}{1 + jwT_g}\right|^2 \qquad (B.4)$$

From the form of equation (B.4) it is clear that the required spectral distribution could be obtained by analog means by passing white noise of (uniform) power density $4T_g\overline{w_g^2}$ through a first order filter of time constant T_g. Although the bandwidth of practical white noise generators is necessarily restricted (e.g. DC to 40 cycles/sec. for Model 401 from Electronic Associates Inc.), the filter output approximates the required noise characteristics sufficiently accurately for most purposes as long as the noise generator has a uniform power output up to a frequency of a decade or more above the filter cut-off frequency.

One method of obtaining samples of band-limited noise for use in a digital computer program is to record the filter output on magnetic tape via an analog-to-digital converter, but there are several disadvantages to this technique:

a. The sampling time intervals (t_s) used in making the tape

determine the integration step interval which must be used in the program, and hence the accuracy of the simulation. Any difference between the two time scales alters the effective cut-off frequency of the filter, and so changes the noise characteristics.

b. A new tape is required for each Flight Condition, since the filter cut-off frequency is a function of the aircraft velocity.

c. There is a physical problem involved in making the tapes and ensuring compatibility with the computer installation.

Digital Simulation of Gusts

A simple method of generating band-limited noise samples by means of program statements is to employ the Gaussian random number subroutine. The method outlined below ensures that the resulting wind gust samples (W_{g_n}, n = 0, 1, 2, ...) have the required spectral density, as specified by equation (B.3).

Although the physically measurable wind gust spectral density exists only over the range of positive frequencies, it is usual and convenient for the purpose of mathematical analysis to define a spectral density function $\phi'(w)$, such that,

$$\phi'(w) = \begin{cases} 1/2\ \phi_g(w) & \text{for } 0 \leq w < \infty \\ 1/2\ \phi_g(-w) & \text{for } -\infty < w \leq 0 \end{cases} \qquad (B.5)$$

so that $\phi'(w)$ is an even function.

The autocorrelation function for $\phi'(w)$ is defined as,

$$R_g(\tau) = \frac{1}{2\pi}\int_{-\infty}^{\infty} \phi'(w)\, e^{jw\tau}\, dw \qquad (B.6)$$

$$= \frac{1}{\pi} T_g\, \overline{w_g^2} \int_{-\infty}^{\infty} \frac{\exp(jw\tau)}{1 + w^2 T_g^2}\, dw$$

Hence, by the use of contour integration,

$$R_g(\tau) = \overline{w_g^2}\, \exp(-|\tau| / T_g) \qquad (B.7)$$

In equation (B.7) the absolute value of τ has been taken because the autocorrelation function is always even. It may be noted that the value of the autocorrelation function for $\tau = 0$ yields the mean-square gust velocity. A further useful property of the autocorrelation function, which will now be used, derives from the fact that all waveforms which have the same power spectral density distribution also have the same autocorrelation function (Ref. 11:58).

Suppose that the wind gust samples are formed at time intervals t_s from the sequence of random numbers N_n ($n = 0, 1, 2, \ldots$), having a specified varience σ^2 and zero mean, in the following way:

$$W_{g_{n+1}} = N_{n+1} + W_{g_n} \exp(-\beta t_s) \tag{B.8}$$

where the term $\exp(-\beta t_s)$ represents a decay factor for the previous gust sample, and the starting value W_{g_o} may be arbitrarily chosen. It may be shown (Ref. 7:1-130,1-131) that at the discrete delay times given by $\tau = nt_s$ the autocorrelation function for the samples W_{g_n} is,

$$R(\tau) = \frac{\sigma^2 \exp(-\beta|\tau|)}{1 - \exp(-2\beta t_s)} \tag{B.9}$$

Hence, if $R(\tau)$ is to be identical to $R_g(\tau)$ it is necessary that,

$$W_g^2 \exp(-|\tau|/T_g) = \frac{\sigma^2 \exp(-\beta|\tau|)}{1 - \exp(-2\beta t_s)} \tag{B.10}$$

Thus, $$\beta = 1/T_g$$

and, $$\sigma^2 = W_g^2 \left[1 - \exp(-2t_s/T_g)\right] \tag{B.11}$$

Use of the Wind Gust Equations

To test the performance of the gain computer in the presence of random inputs a wind gust intensity of r.m.s. value 20 ft./sec. was selected, since this magnitude was used by Honeywell (Ref. 9:4) in the development of adaptive control systems for the X-15 and X-20 (Dyna Soar) vehicles. For the integration step interval (t_s) used in the MIMIC simulation program a size of 0.0005 sec. was chosen as

a compromise between accuracy of computation and time taken by the IBM 7094 computer to complete a simulation run. Then, for each Flight Condition the time constant T_g was calculated from the aircraft velocity, as shown under equation (B.3). Substitution of the values for $\overline{w_g^2}$, t_s, and T_g into equation (B.11) gave the varience required for the random number subroutine. The wind gust samples were then calculated from the random numbers by the use of equation (B.8). Finally, samples of the disturbance angle of attack were found by substituting the wind gust values into equation (B.1).

Results of the Simulation

Figures B.1 through B.4 show the aircraft response and performance of the gain computer in the presence of random wind gusts. The dither signal was used, but there were no pilot command inputs. It should be noted that the vertical scales in Fig. B.4 are different from those in the other three figures, and in all four the scale of ΔK_v ic twice that which was earlier used, so that the finite step changes in gain are visible. Starting from the top trace, the curves are:

a. Wind gust velocity, W_g.

b. Incremental change in angle of attack, α.

c. Normal acceleration, n_z.

d. Aircraft pitch rate, $\dot{\theta}_a$.

e. Elevator deflection angle, δ_e.

f. Control loop gain error, ΔK_v.

Aircraft gust sensitivity, in terms of its normal acceleration and pitch rate responses, is known (Ref. 14:18) to be primarily dependent on the lift curve slope (proportional to L_α) and the static stability (proportional to M_α), respectively. These relationships are apparent when the n_z and $\dot{\theta}_a$ curves are compared with the magnitudes of the L_α and M_α stability derivatives (Appendix C, Table I) for each of the Flight Conditions. For example, in Flight Condition 28 (Fig. B.1), where L_α takes on its largest value, the normal acceleration response is also the greatest of the four, with

peaks of ± 2.5g. For a manned aircraft this acceleration level is obviously unacceptable, and in practise is unlikely to arise, because:

a. An r.m.s. gust intensity of 20 ft./sec. represents severe atmospheric turbulence, for which the probability that it will be encountered is less than 0.01 per cent (Ref. 15:3).

b. In simulating the aircraft dynamics it was assumed that the $\dot{\alpha}$ stability derivatives were negligibly small (Appendix C). This assumption implies that the pressure distribution over the wing changes instantaneously when the angle of attack is suddenly changed (Ref. 5:158). For pilot commands transmitted through the pre-filter model reference the rate of change of angle of attack is sufficiently slow for the assumption to be valid. However, as the Figures show, wind gusts can cause very rapid changes in the angle of attack, and the assumption is then no longer strictly correct. Qualitatively, if the aerodynamic lag is taken into consideration, it may be seen that the peaks on the curves in Figs. B.1 through B.4 would be considerably smoothed.

To ensure that the aircraft and control system had achieved a 'steady-state' all the simulation runs with wind gust inputs were made 15 sec. long, of which the Figures show only the first 6 sec. The aircraft responses for the first 6 sec. are representative of the complete run, but except for Flight Condition 28 the loop gain decreased further. For Flight Conditions 7 and 24 the average gain error was approximately -6 dB, and for Flight Condition 32 was -4 dB. The gain for Flight Condition 28 could not decrease below its design value, as defined by equation (D.6), since the variable gain setting (K_v) was then on its lower end stop for this condition of maximum elevator effectiveness. It may be noted that in Figs. B.1 through B.4 the dither signal is not apparent on the pitch rate curves because of its small amplitude (Ref. page 25).

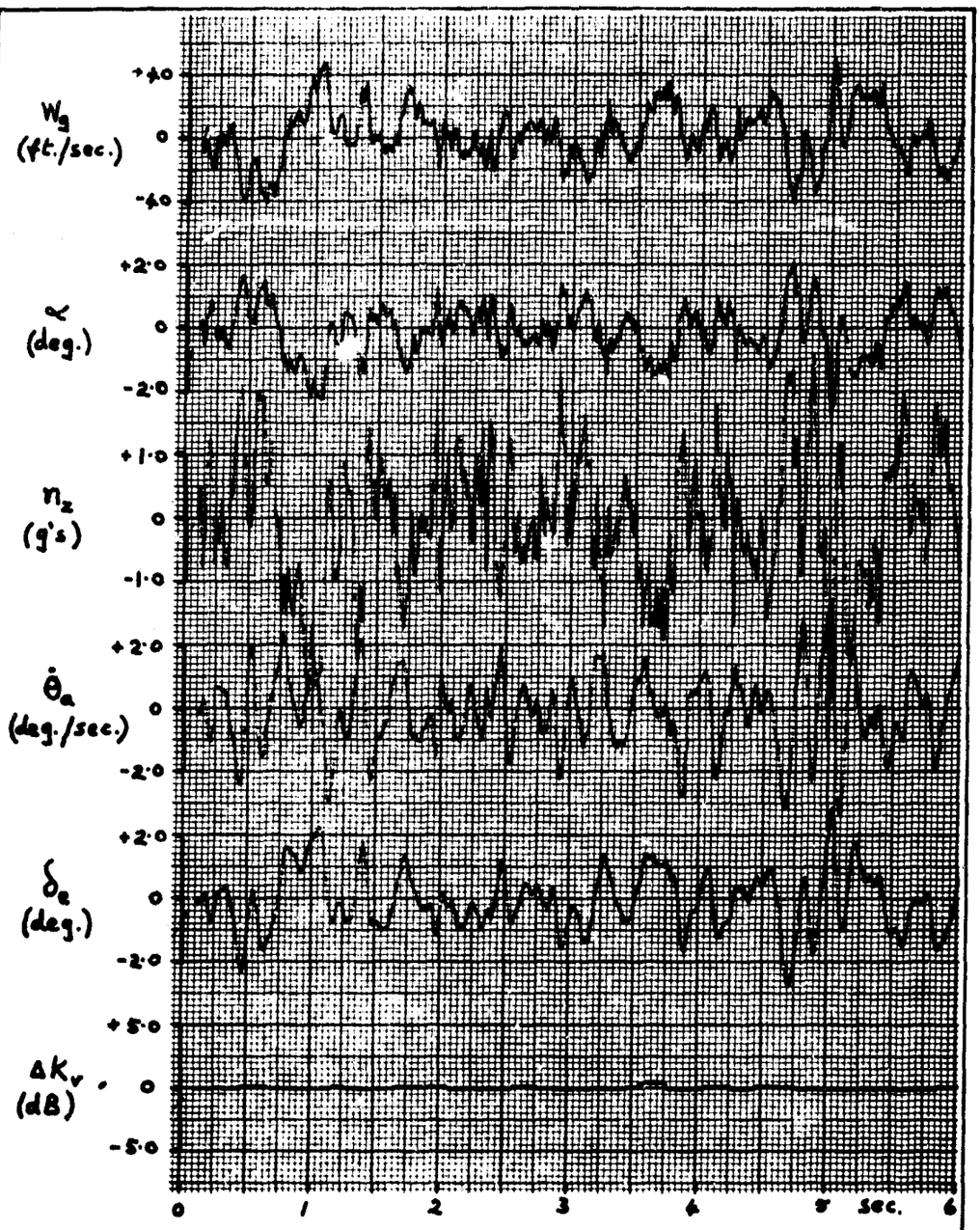

Fig. B.1

Flight Condition 28 - Aircraft Response and Performance of the Gain Computer for Random Wind Gust Disturbances

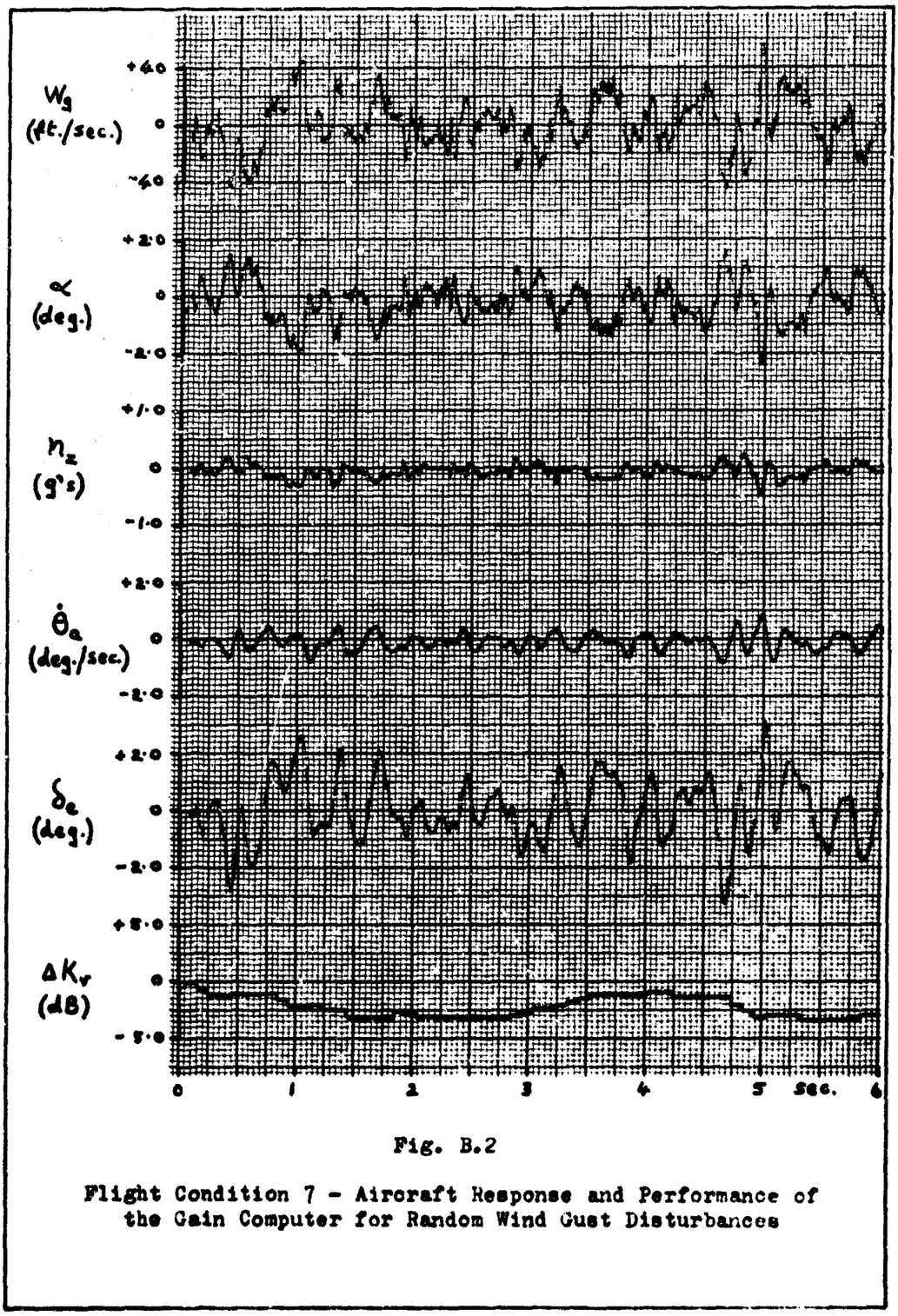

Fig. B.2

Flight Condition 7 - Aircraft Response and Performance of the Gain Computer for Random Wind Gust Disturbances

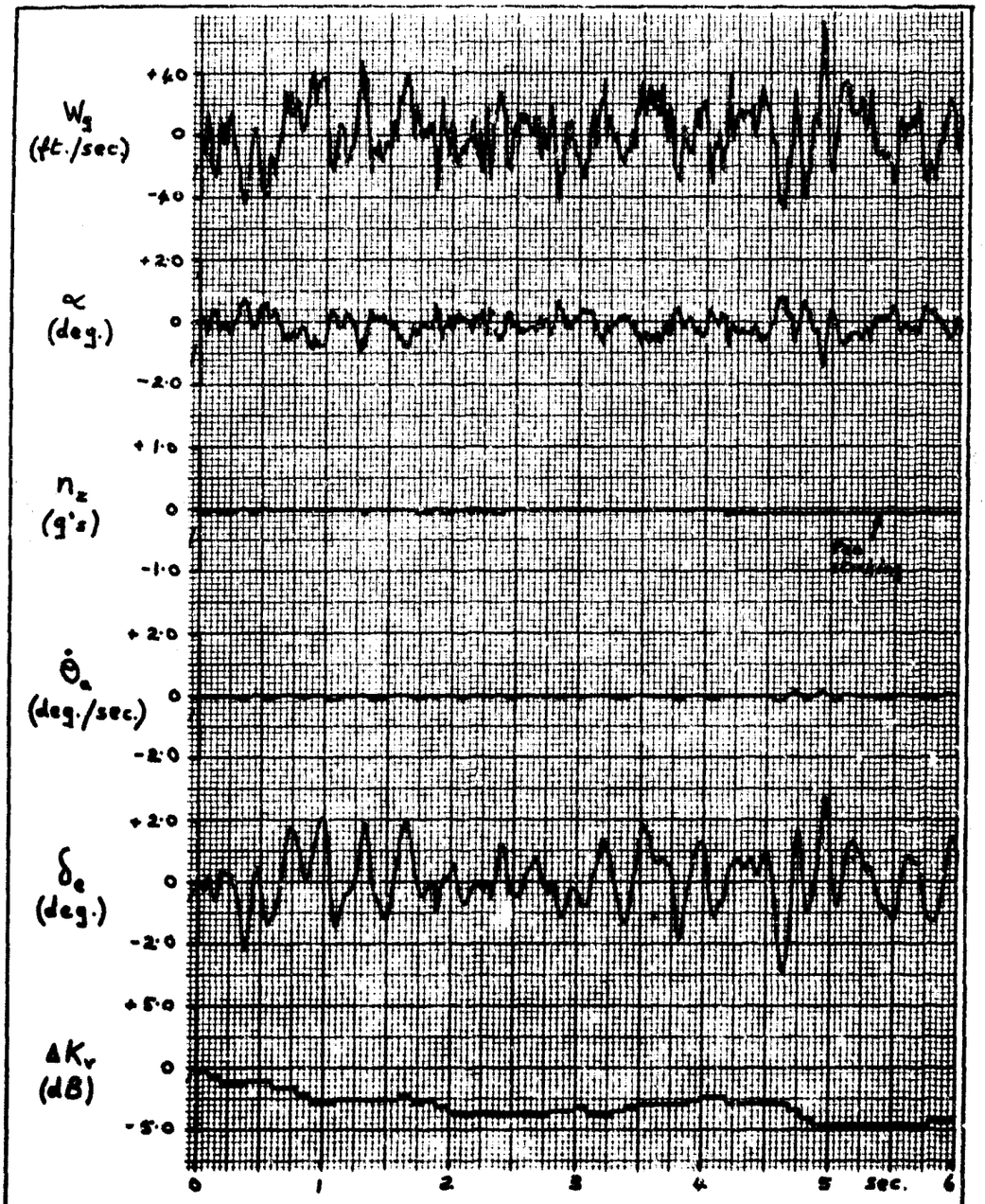

Fig. B.3

Flight Condition 24 - Aircraft Response and Performance of the Gain Computer for Random Wind Gust Disturbances

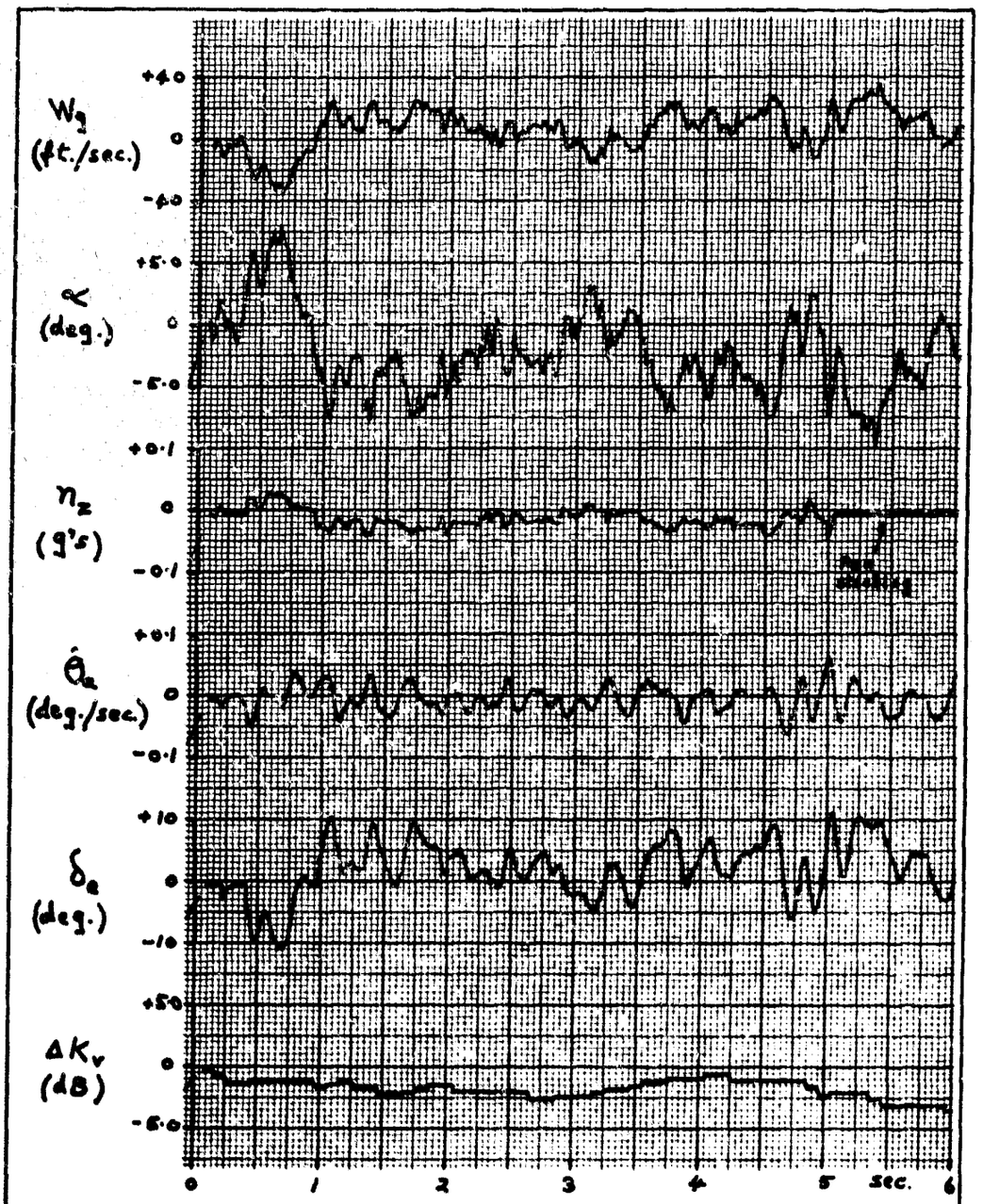

Fig. B.4

Flight Condition 32 - Aircraft Response and Performance of the Gain Computer for Random Wind Gust Disturbances

Appendix C

Aircraft Short-Period Equations of Motion and Transfer Functions in Terms of the Pitch Stability Derivatives

The Basic Equations of Motion

A complete development (e.g. Refs. 2 and 5) of the general, linearised aircraft equations of motion involves the use of a considerable number of approximations and qualifying statements, and is quite long. Consequently, only a brief outline is given, together with an indication of the principal assumptions.

From the point of view of the control system designer it is convenient if the equations are ultimately expressed in transfer function form. A complication which is often encountered is that the equations are written in non-dimensional form. However, for supersonic flight the variations in magnitude of the non-dimensional stability derivatives (coefficients of the differential equations) as a result of Mach Number effects cannot be ignored; in this event the most straightforward approach is to associate with a number of reference Flight Conditions a distinct set of numerical values for the stability derivatives.

The basic equations of motion may be derived in the following way:

a. A body axis system is assumed to be rigidly fixed to the airframe; the axes are known as stability axes if, when the aircraft is flying straight and level, the x-axis is directed along the aircraft velocity vector, the y-axis along the starboard wing, and the z-axis downwards. The use of these axes enables the equations to be derived in their simplest form.

b. Euler's equations of motion for a rotating rigid body and Newton's equations for motion of the center of mass are written as the moment and force equations, respectively. The external forces acting on the airframe are due to aerodynamic forces and gravity forces, while the external moments about the center of mass are due to aerodynamic forces alone.

c. Each of the forces and moments is assumed to consist of two components; one a constant component, determined by the particular reference Flight Condition, and the other a perturbation component which arises when the aircraft is disturbed from the reference. The perturbation values of the aerodynamic forces and moments are assumed to be linear functions of the disturbances, a concept which gives rise to the definition of the stability derivatives.

d. The steady-state values of the forces and moments are subtracted from both sides of the resulting equations, and products of small angles and angular rates are neglected. When this is done, it is found that the linearised longitudinal equations are decoupled from the lateral equations. A further simplification of the equations results if the airflow around the wing and tail is assumed to be quasi-steady. (e.g. Ref.2:21, eqns. (1-59). For the X-15 the non-dimensional derivative C_{z_q} is zero, and the last assumption implies that $C_{z_{\dot{\alpha}}}$ and $C_{m_{\dot{\alpha}}}$ are negligibly small.)

e. When only the short-period mode is considered (i.e. if the comparatively low frequency phugoid mode is ignored) the small variations which occur in the aircraft forward velocity are insignificant. Finally, if it is assumed that incremental changes in gravity forces which result from small changes in pitch attitude are negligible compared with the incremental aerodynamic forces, then the following basic equations of motion apply:

$$\ddot{\theta}_a = M_q \dot{\theta}_a + M_\alpha \alpha + M_\delta \delta_e \qquad (C.1)$$

$$\dot{\alpha} = \dot{\theta}_a - L_\alpha \alpha - L_\delta \delta_e \qquad (C.2)$$

where, $\dot{\theta}_a$ = pitch rate (deg./sec.)

α = incremental change in angle of attack from the reference value (deg.)

δ_e = elevator deflection angle, measured from the trim position (deg.)

Values of the moment (M) and lift (L) stability derivatives in equations (C.1) and (C.2) for the four Flight Conditions (F.C.) which were studied are given in Table I. Details of the reference conditions for which the stability derivatives were obtained are listed in Table II (data from Ref. 12).

Table I

Stability Derivatives

Derivative:	M_q	M_α	M_δ	L_α	L_δ
Dimensions:	$(sec.^{-1})$	$(sec.^{-2})$	$(sec.^{-2})$	$(sec.^{-1})$	$(sec.^{-1})$
F.C. 28	-2.456	-49.93	-52.95	2.527	0.5801
F.C. 7	-0.2299	-11.18	-9.097	0.2529	0.04364
F.C. 24	-0.0342	-3.520	-1.741	0.0546	0.007145
F.C. 32	-0.05202	-0.2587	-0.2193	0.04999	0.01218

Table II

Reference Flight Conditions

Condition:	Altitude	Mach No.	Angle of Attack	Velocity U	Dynamic Pressure
Dimensions:	(ft.)	-	(deg.)	(ft./sec.)	$(lb./ft^2)$
F.C. 28	10,000	1.2	0.5	1078	1467
F.C. 7	50,000	1.5	5.0	1453	381
F.C. 24	100,000	3.0	11.4	3014	142
F.C. 32	0	0.2	17.0	223	59

The Short-Period Transfer Functions

When the Laplace transforms of equations (C.1) and (C.2) are taken and the variable α is eliminated, the transfer function which relates pitch rate to elevator deflection angle is obtained:

$$\frac{\dot{\theta}_a(s)}{\delta_e(s)} = M_\delta \frac{s + (L_\alpha - M_\alpha L_\delta / M_\delta)}{s^2 + (L_\alpha - M_q)s + (-M_\alpha - M_q L_\alpha)} \qquad (C.3)$$

It is convenient to write this equation in an alternative form, in which the aircraft short-period time constant (T_a), damping

factor (ζ_a), and natural frequency (w_a) appear explicitly:

$$\frac{\dot{\theta}_a(s)}{\delta_e(s)} = M_\delta \frac{s + 1/T_a}{s^2 + 2\zeta_a w_a s + w_a^2} \qquad (C.4)$$

where, $w_a^2 = -M_\alpha - M_q L_\alpha$ $(rad.^2/sec.^2)$

$2\zeta_a w_a = L_\alpha - M_q$ (rad./sec.)

and, $1/T_a = L_\alpha - M_\alpha L_\delta / M_\delta$ $(sec.^{-1})$

The following table is then obtained by substituting numerical values for the stability derivatives into the above equations.

Table III

Pitch Rate Characteristics

Parameter:	Aerodynamic Gain (M_δ)	Natural Frequency	Damping Factor	Time Constant
Dimensions:	$(sec.^{-2})$	(rad./sec.)	-	(sec.)
F.C. 28	-52.95	7.492	0.3325	0.4829
F.C. 7	-9.097	3.353	0.0720	5.017
F.C. 24	-1.741	1.877	0.0237	24.91
F.C. 32	-0.2193	0.5111	0.0997	28.06

A variable $\dot{\gamma}$ is defined by,

$$\dot{\gamma} = \dot{\theta}_a - \dot{\alpha} \qquad (C.5)$$

The normal acceleration (n_z, positive for eyeballs down) of the center of mass of the aircraft is related to $\dot{\gamma}$ by (Ref. 20:141),

$$n_z = \frac{U\dot{\gamma}}{57.3g} \quad (g's) \qquad (C.6)$$

From equation (C.6), it may be seen that the normal acceleration is not simply proportional to pitch rate while the angle of attack is changing. This important fact is emphasized by solving equations (C.1), (C.2), and (C.3) for the transfer function which relates normal acceleration to pitch rate.

$$\frac{n_z(s)}{\dot{\theta}_a(s)} = \frac{U}{57.3g} \frac{L_\delta}{M_\delta} \frac{s^2 - M_q s + (-M_\alpha + M_\delta L_\alpha / L_\delta)}{s + 1/T_a} \qquad (C.7)$$

The behavior of the normal acceleration response with respect to the pitch rate response is illustrated by considering two approximations to equation (C.7):

a. For a step command input, the initial pitch rate response may be approximated by a ramp function. This assumption implies that $\ddot{\theta}_a(t_o^+)$ is a constant, and hence, by applying the initial value theorem to equation (C.7), the normal acceleration in the region of time zero is obtained,

$$n_z(t_o^+) = \frac{U}{57.3g} \frac{L_\delta}{M_\delta} \ddot{\theta}_a(t_o^+) \qquad (C.8)$$

Therefore, since L_δ is positive and M_δ is negative, the initial sense of n_z is anti-phase to that of the change in pitch rate. This non-minimum phase phenomenon has a simple physical explanation. For example, to initiate a climb a positive pitch rate is required, which is produced by a negative elevator deflection angle. The immediate result is a reduction in the lift component generated by the tail, and until the angle of attack is increased sufficiently for the wing to provide correspondingly more lift, the direction of the normal acceleration is opposite to that required.

b. If T_a is large, there is a period of time after an initial transient when the numerator dynamics associated with equation (C.7) may be ignored. In this event the equation is approximated by,

$$\frac{n_z(s)}{\theta_a(s)} = \frac{K}{s + 1/T_a} \qquad (C.9)$$

where K is a (positive) factor of proportionality. Thus, the normal acceleration follows the pitch rate, but with a lag; only in the steady-state is the normal acceleration directly proportional to the pitch rate, and even then the proportionality factor is a function of the aircraft velocity. It is generally accepted that pilot opinion of aircraft handling qualities is strongly influenced by the form of the normal acceleration response. Consequently, an aircraft which has

a pitch rate command control system which does not overshoot for a step input is likely to be rated 'sluggish' (Ref. 20:20).

Aircraft Response Curves for a Step Input

Figures C.1, C.2, and C.3 show the aircraft response curves for a step command input of 0.5 deg./sec. For each Flight Condition the loop gain was set at its design value (defined in Appendix D), so that the phase and gain margins were the same for all three conditions. Starting from the top trace, the curves are:

a. Output of the pre-filter model, $\dot{\theta}_m$.

b. Aircraft pitch rate, $\dot{\theta}_a$.

c. Difference between pitch rate and rate of change of angle of attack, $\dot{\gamma}$.

d. Elevator deflection angle, δ_e.

The pitch rate curves show that, if the gain computer is able to identify the elevator effectiveness and set the loop gain accordingly, the aircraft will follow the model reference with negligible error. When the normal acceleration curves (proportional to $\dot{\gamma}$) are compared, the effect of the large time constants (T_a) in Flight Conditions 7 and 32 on the lag of acceleration with respect to pitch rate is seen. Also, in Fig. C.3 the non-minimum phase characteristic of the normal acceleration response is apparent.

An inspection of the numerator of equation (C.4) indicates that the pitch rate response may be considered to consist of two components: one proportional to the derivative of the elevator deflection angle, and the other proportional to $1/T_a$ times the magnitude of the angle. Thus, for values of T_a significantly greater than unity the derivative component is dominant, and this effect is particularly noticeable in Flight Condition 32 (T_a = 28.06), where the elevator rate remained almost constant for about twenty seconds.

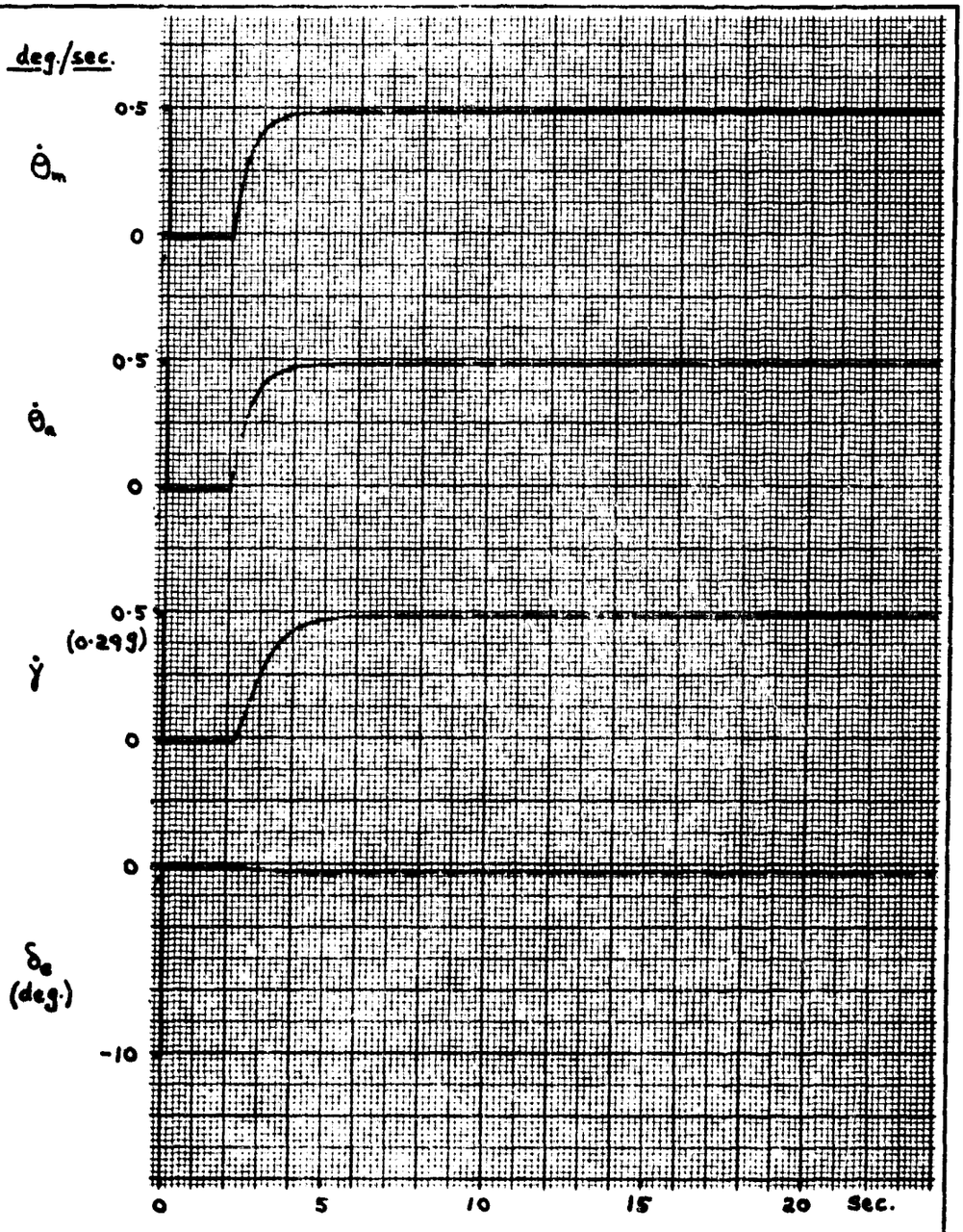

Fig. C.1

Flight Condition 28 - Aircraft Response to a Step Command Input with the Loop Gain Set at its Design Adaptive Value (K_f = 10.0, K_v = 1.0)

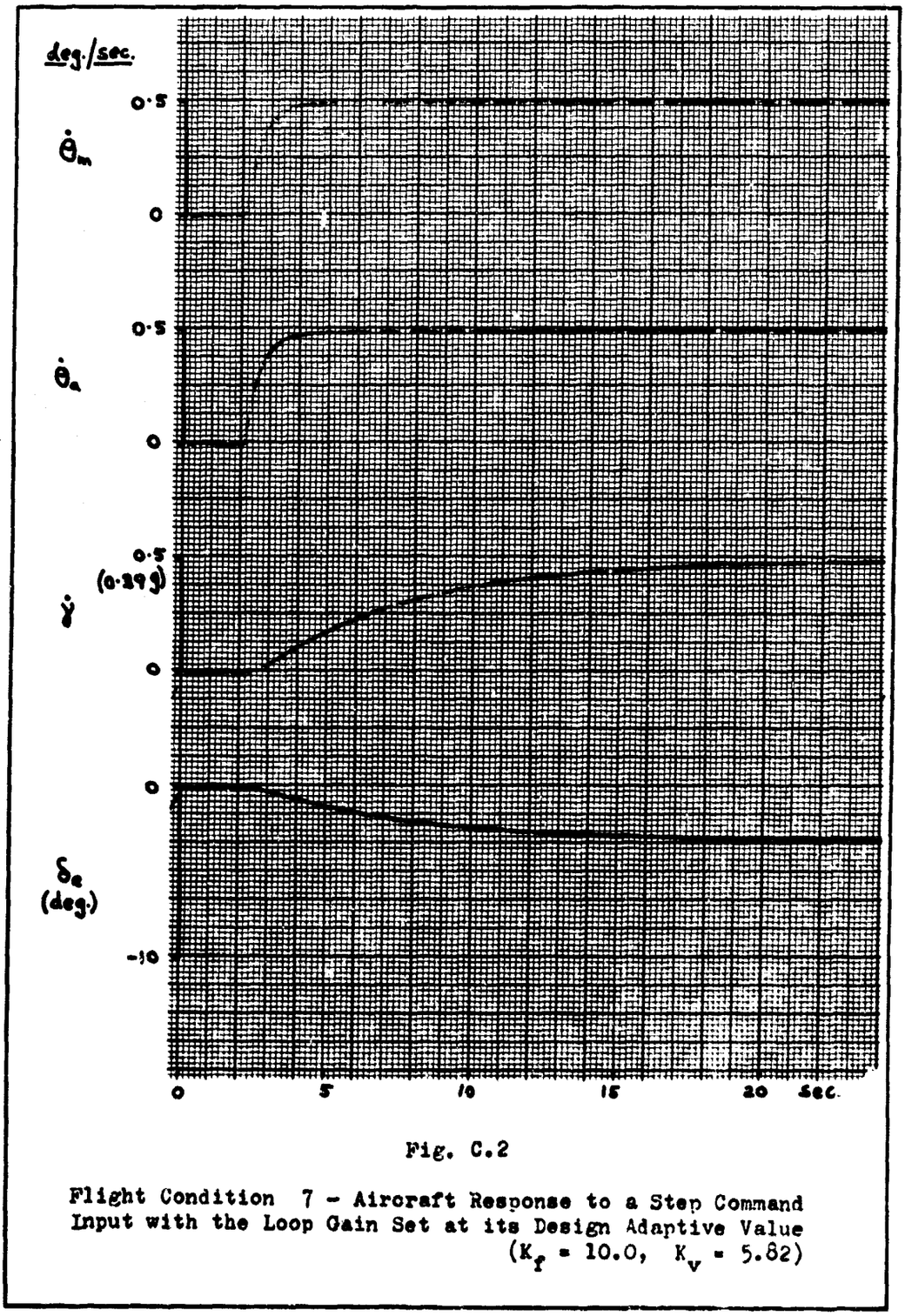

Fig. C.2

Flight Condition 7 - Aircraft Response to a Step Command Input with the Loop Gain Set at its Design Adaptive Value (K_f = 10.0, K_v = 5.82)

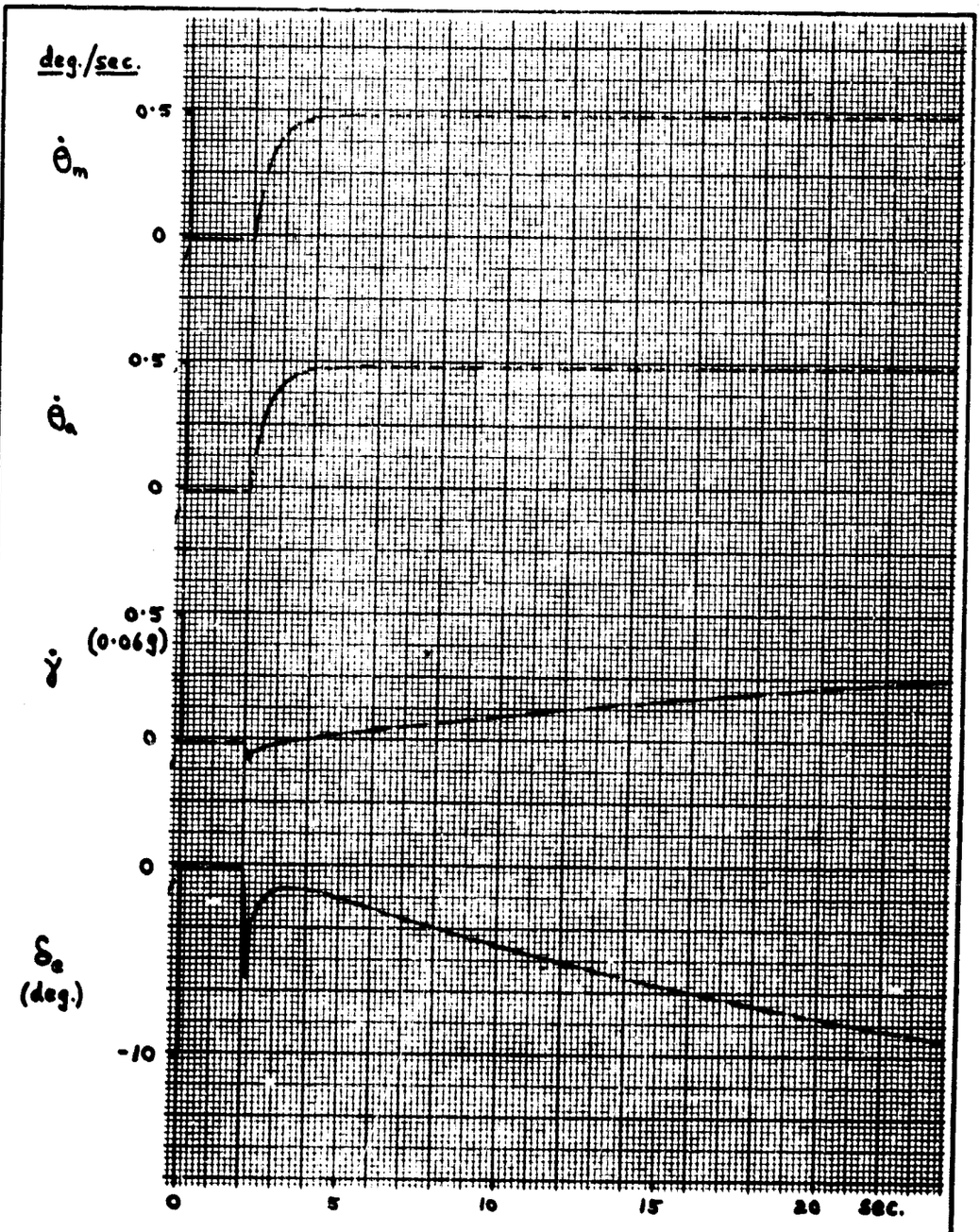

Fig. C.3

Flight Condition 32 - Aircraft Response to a Step Command Input with the Loop Gain Set at its Design Adaptive Value (K_c = 10.0, K_v = 242)

Appendix D

Design of a Compensator for the Control System

Design Requirements

A block diagram of the complete control system is shown in Fig. 1., in which the pre-filter model reference is a simple first order lag, with a break frequency of 2 rad./sec. The object of the design was to make the overall response, from pilot command input to aircraft pitch rate, follow the output of the model reference. This may be achieved by making the bandwidth of the closed loop portion of the control system five to eight times that of the model for all Flight Conditions.

Control Loop Components

Aircraft. Phase angle - frequency curves for the aircraft elevator deflection to pitch rate transfer function are shown in Fig. D.1. The steep slope of these curves in the region of the aircraft natural frequency is indicative of the low damping of the airframe without pitch stability augmentation. For frequencies above 20 rad./sec. the aircraft transfer function, given by equation (C.4), may be approximated by,

$$\frac{\dot{\theta}_a(jw)}{\delta_e(jw)} = \frac{M_\delta}{jw} \qquad (D.1)$$

Thus, the high frequency gain of the aircraft transfer function is directly related to the value of M_δ. As a result, the gain cross-over frequency (where the loop phase shift is -180 deg.) and the gain margin may be held constant for all Flight Conditions by adjusting the variable gain element (K_v) inversely to M_δ. Further, since equation (D.1) shows that the aircraft high frequency phase angle is the same for all Flight Conditions, the phase margin will also be constant. Hence, the gain computer is required to 'measure' the value of M_δ as accurately as possible.

Servo/Actuator Combination. The servo-cylinder and power actuator transfer functions (Ref. 12:69) are shown in Fig. D.2,

where phase angle - frequency curves are plotted for three values of servo gain and feedback. In each case the servo gain was selected to give a servo natural frequency of 180 rad./sec., and except for the case of unity feedback which was not used, the feedback transfer function was chosen to cancel the actuator lag. For the non-integrating (K_2 and H_2 in Fig. D.2) and integrating (K_3, H_3) servos the transfer functions for the servo/actuator combination are,

Non-Integrating Servo:
$$\frac{\delta_e(s)}{v_o(s)} = 6.67 \frac{31200}{s^3 + 180s^2 + 32400s + 31200} \qquad (D.2)$$

Integrating Servo:
$$\frac{\delta_e(s)}{v_o(s)} = \frac{6.67}{s} \frac{180^2}{s^2 + 180s + 180^2} \qquad (D.3)$$

The first tests on the closed loop control system were carried out with the non-integrating servo, but because a droop occurred in the pitch rate response (Fig. D.7) all subsequent simulation was done with the integrating servo. It should be noted that for the purpose of simulation the factor 6.67 associated with the servo/actuator combination has been incorporated in the fixed gain element (K_f).

Rate Gyro. From Figs. D.1 and D.2 it may be seen that for frequencies above 20 rad./sec. the aircraft and servo/actuator angles contribute close to -180 deg., or more. A high frequency rate gyro was therefore chosen, so that it would have only a small phase shift in the region of 20 rad./sec. up to the gain crossover frequency. The rate gyro phase angle - frequency curve is shown in Fig. D.2, and its transfer function is given below,

$$\frac{\dot{\theta}_g(s)}{\dot{\theta}_a(s)} = \frac{400^2}{s^2 + 400s + 400^2} \qquad (D.4)$$

The Complete Control Loop

Phase angle - frequency curves for the uncompensated control loop (with non-integrating servo) are given in Fig. D.3, and in Fig. D.4 the corresponding gain - frequency curves are presented. These Figures also show the phase and gain characteristics of the chosen compensator, whose transfer function is,

$$\frac{v_o(s)}{v_i(s)} = \frac{10(s + 20)}{s + 200} \qquad (D.5)$$

The requirements which dictated the use of this compensator were:

a. An inspection of the open loop phase angle curves in Fig. D.3 showed that a lead network was necessary to obtain the required bandwidth.

b. The upwards break-frequency and the attenuation factor had to be as small as possible. This was to ensure that high frequency noise would not become troublesome.

c. A lower limit for the upwards break-frequency was determined by the resonance peak at 7 rad./sec. in the gain - frequency curve for Flight Condition 28. In the uncompensated case (Fig. D.4) there was a 15 dB decrease in gain in the octave between 8 and 16 rad./sec. By placing the compensator upwards break-frequency at 20 rad./sec. it was possible to realize a 13 dB gain roll-off in this octave (Fig. D.6), which enabled a satisfactory gain margin to be achieved in conjunction with a high loop gain at the lower frequencies.

The design value of the control loop gain setting was then established in the following way:

a. The gain - frequency curve for Flight Condition 28 was taken as a reference when both the variable gain (K_v) and the fixed gain (K_f) were set to unity.

b. It was assumed that the gain computer would normally be capable of correctly identifying the true value of elevator effectiveness for any Flight Condition, so that it would be able to set the gain correctly at its design value.

c. The variable gain was changed as a function of the computed elevator effectiveness (M_{δ_y}) by the relation,

$$K_v = \frac{M_\delta \text{ for F.C. 28 } (= 52.95)}{\text{Computed elevator effectiveness}} \qquad (D.6)$$

d. Thus, the design value of K_v for Flight Condition 28 was defined to be unity. Also, for example, the design value for Flight Condition 24 is given by,

$$K_v \text{ (F.C. 24)} = 52.95/1.741 = 30.42 = 29.7 \text{ dB}$$

where the true elevator effectiveness for Flight Condition 24 (from Appendix C, Table III) has been substituted into the denominator of equation (D.6). It follows that, if the computed elevator effectiveness is in error from the true value, then the setting of K_v will be correspondingly in error from its design value. Hence, in order to assess the accuracy of the gain computer, a loop gain error (ΔK_v) is defined;

$$\Delta K_v = 20 \log \frac{K_v \text{ (actual)}}{K_v \text{ (design)}} \quad \text{(dB)} \qquad \text{(D.7)}$$

e. In Fig. D.4 it can be seen that the effect of increasing the loop gain for Flight Condition 24 by the design value of K_v (29.7 dB) is to cause the gain curve for frequencies above 20 rad./sec. to become co-incident with that for Flight Condition 28. The same result applies to all other Flight Conditions.

f. The fixed gain factor was then set at a value of 10 (K_f = 20 dB), which provided the maximum attainable phase margin, and a gain margin of 11.5 dB. Phase and gain curves which illustrate the net effect of lead compensation and gain adjustment are contained in Figs. D.5 and D.6.

Control System Bandwidth

It was mentioned earlier that the (major) portion of the control system which follows the model reference should have a closed loop bandwidth of five to eight times that of the model (i.e. 10 to 16 rad./sec.). To confirm that this condition was satisfied, a closed loop frequency response calculation was made for Flight Condition 28, with the non-integrating servo included in the loop. It was found that the closed loop gain from model response ($\dot{\theta}_m$) to aircraft response ($\dot{\theta}_a$), measured with respect

to the zero frequency gain, was 3 dB down at 12 rad./sec. and 6 dB down at 22 rad./sec., and was therefore considered satisfactory.

Aircraft Response Curves for a Step Input

When the non-integrating servo was used, the control loop was Type Zero, and consequently, a steady-state error in the final value of the pitch rate response was expected. This error appears as a droop in the pitch rate response, as shown in Fig. D.7. Since it was not practicable to increase the loop gain any further, an integrating servo was adopted. The improved response with the integrating servo is shown in Fig. D.8. The significance of the plots of the term $\dot{y}$ in these two Figures is explained in Appendix C, where curves showing the step responses for the other three Flight Conditions are contained.

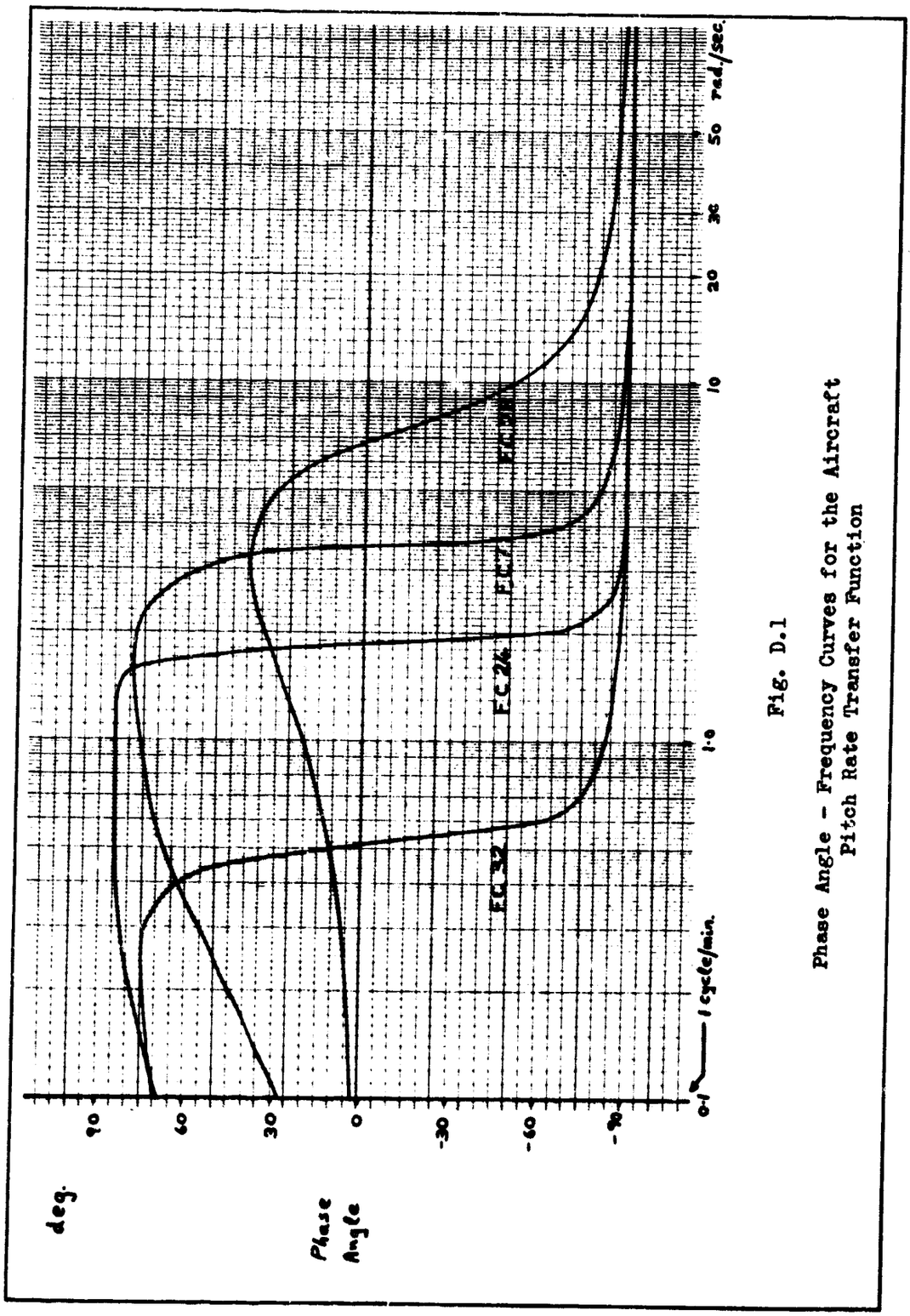

Fig. D.1

Phase Angle - Frequency Curves for the Aircraft
Pitch Rate Transfer Function

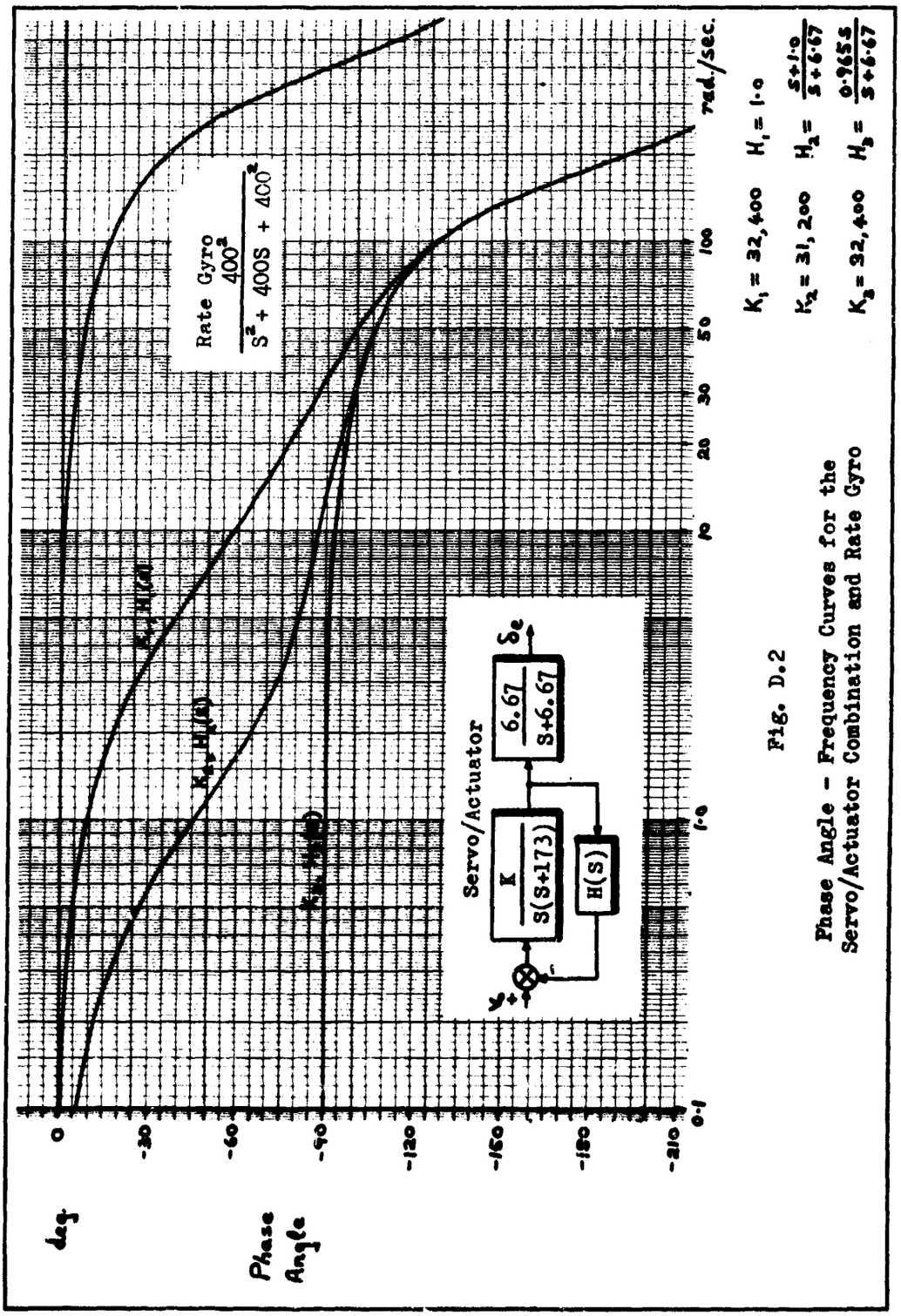

$K_1 = 32,400$ $H_1 = 1.0$

$K_2 = 31,200$ $H_2 = \frac{S+1.0}{S+6.67}$

$K_3 = 32,400$ $H_3 = \frac{0.965S}{S+6.67}$

Fig. D.2

Phase Angle - Frequency Curves for the Servo/Actuator Combination and Rate Gyro

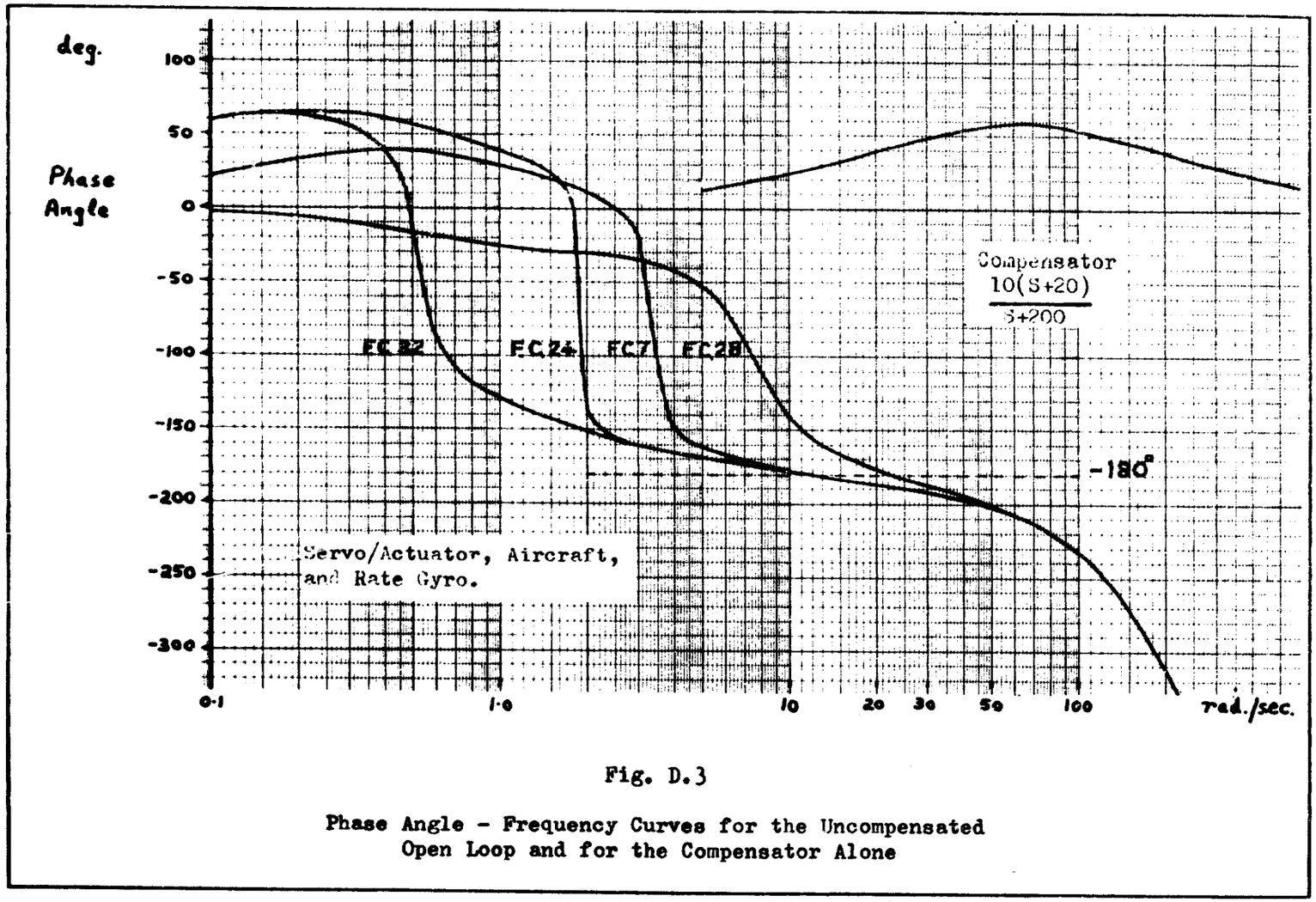

Fig. D.3

Phase Angle - Frequency Curves for the Uncompensated Open Loop and for the Compensator Alone

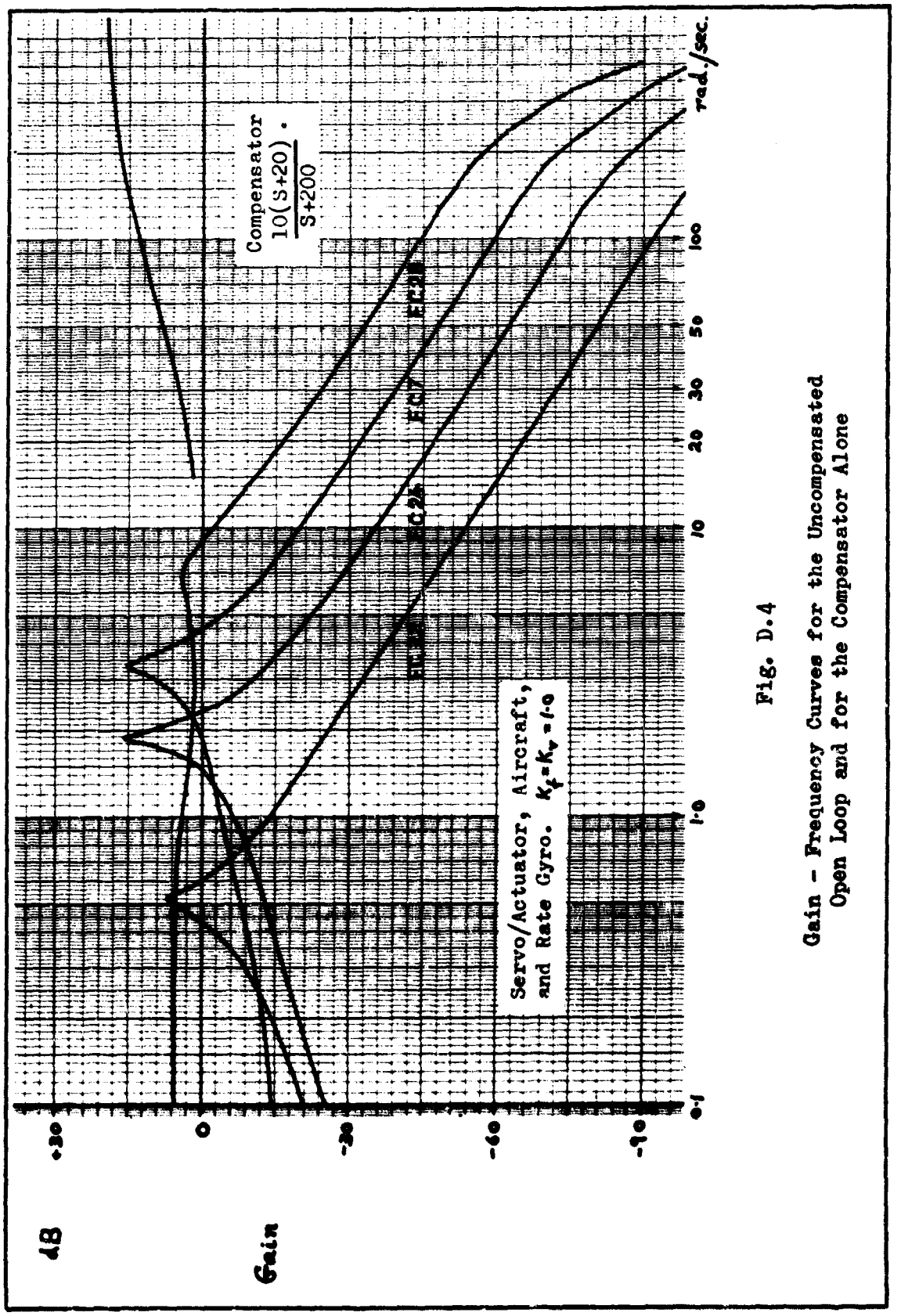

Fig. D.4

Gain - Frequency Curves for the Uncompensated Open Loop and for the Compensator Alone

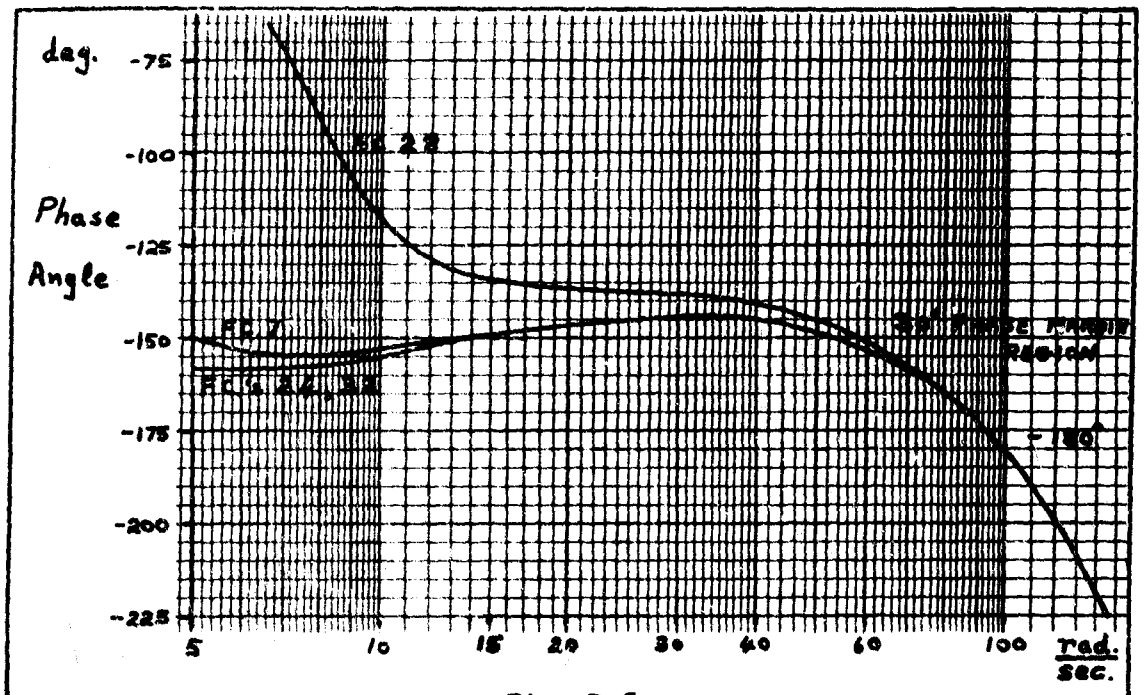

Fig. D.5

Phase Angle - Frequency Curves for the Compensated Open Loop

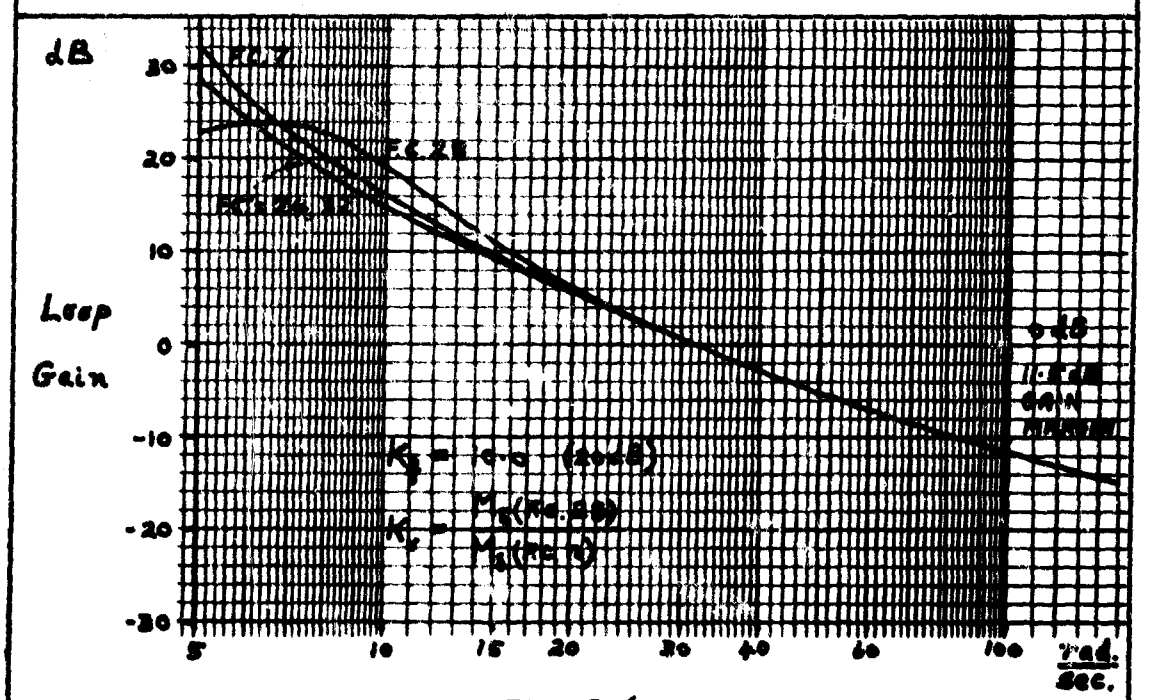

Fig. D.6

Gain - Frequency Curves for the Compensated Open Loop With K_v at its Design Value

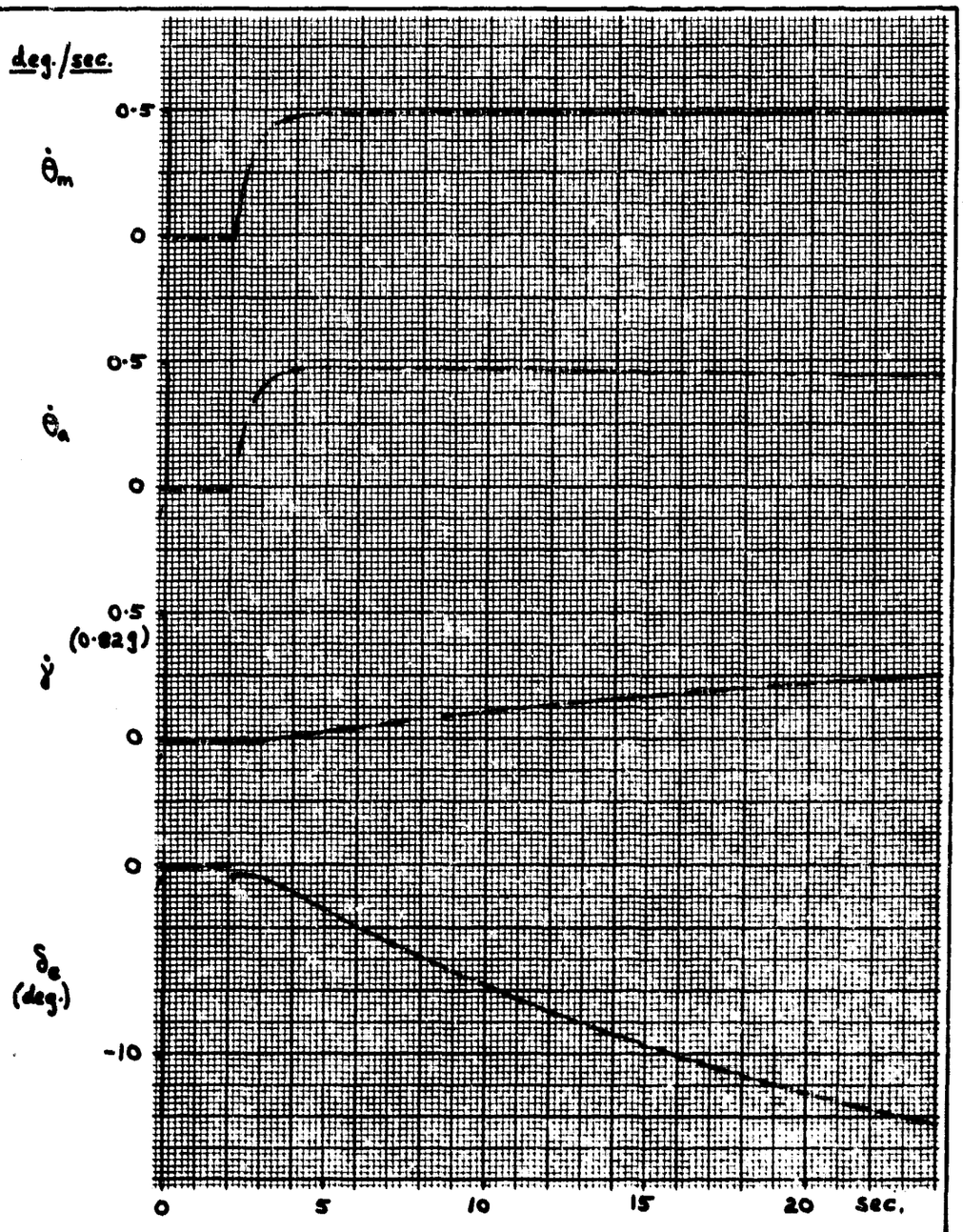

Fig. D.7

Flight Condition 24 - Aircraft Response to a Step Command Input Showing That the Pitch Rate Response Droops with the Non-Integrating Servo (K_f = 10.0, K_v = 30.4)

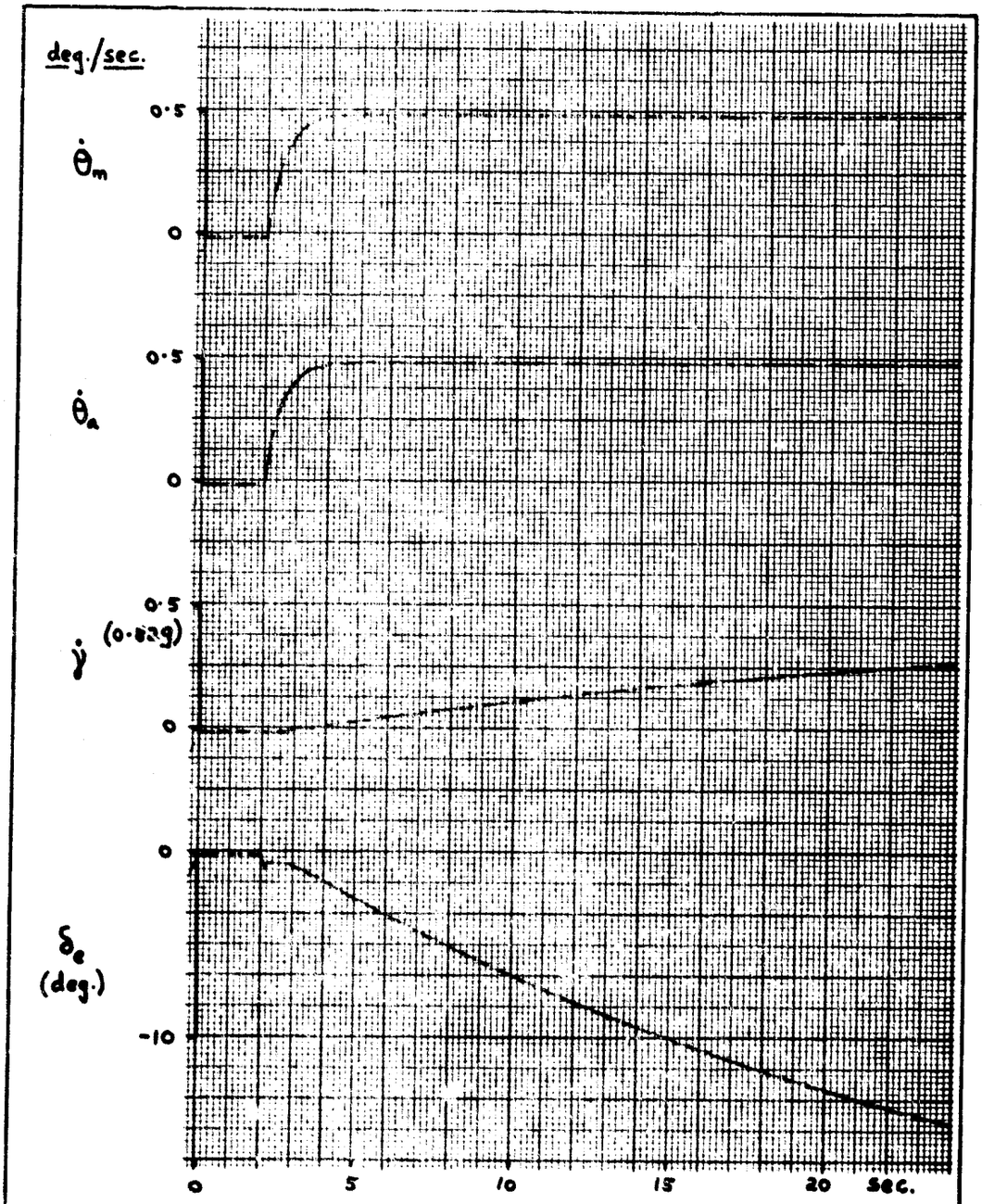

Fig. D.8

Flight Condition 24 - Aircraft Response to a Step Command Input Showing That the Pitch Rate Response Remains Steady with the Integrating Servo (K_f = 10.0, K_v = 30.4)

Appendix E

Approximation of the Aircraft Pitch Rate Transfer Function by Finite Difference Equations

Derivative Approximations

When a function $y(t)$ is tabulated at equal intervals (τ_s) of an independent variable t, the derivatives of the function at any of the tabulation points may be obtained by the use of finite difference formulas. These formulas all involve linear combinations of the tabulated values in the neighborhood of the point where a derivative is required to be evaluated; such a point is known as the pivotal point. In general, the independent variable is not necessarily time, nor do the points have to be tabulated at equal intervals. However, in the simulation of a physical system by means of differential equations which relate the time variation of the output to the input, the independent variable of interest is time, and it is a practical convenience to sample the system behavior at equal increments of time.

Differentiation formulas may be generated by starting with a Taylor series expansion for the (usually unknown) function in the region of a pivotal point. Then, through the use of the differentiation operator D and the forward, central, backward, and averager operators Δ, δ, ∇, and μ, respectively, the necessary weighting factors for the tabulated values can be found. Details of the derivation of formulas for the weighting factors are contained in Ref. 19, Ch. II, from which Table IV was compiled.

Construction of Difference Equations

As an example in the use of Table IV, a difference equation will be constructed for the aircraft pitch rate transfer function, equation (C.4). Re-writing equation (C.4) in differential operator notation, and with Y_i and E_i representing $\dot{\theta}_a$ and δ_e, respectively, at the pivotal point i,

$$(D^2 + 2\zeta_a w_a D + w_a^2) Y_i = M_\delta (D + 1/T_a) E_i \qquad (E.1)$$

Table IV

Weighting of Sample Point Values for Derivative Approximations at the ith. Point

Order of Approximation and Type	Scaled Derivative	Sample Points i-3	i-2	i-1	i	i+1	i+2
1st. Forward	$\tau_s D$				-1	1	
	$\tau_s^2 D^2$				1	-2	1
1st. Central	$2\tau_s D$			-1	0	1	
	$\tau_s^2 D^2$			1	-2	1	
1st. Backward	$\tau_s D$			-1	1		
	$\tau_s^2 D^2$		1	-2	1		
2nd. Backward	$2\tau_s D$		1	-4	3		
	$\tau_s^2 D^2$	-1	4	-5	2		

To approximate equation (E.1) by means of central differences, it is first multiplied on the left hand side (LHS) and the right hand side (RHS) by τ_s^2. Then, from Table IV,

$$\tau_s^2 D^2 Y_i = (Y_{i-1} - 2Y_i + Y_{i+1})$$

$$\tau_s^2 2\lambda_a w_a DY_i = \lambda_a w_a \tau_s (-Y_{i-1} + Y_{i+1})$$

and,
$$\tau_s^2 w_a^2 Y_i = w_a^2 \tau_s^2 Y_i$$

Therefore, by adding the above equations, and collecting like terms,

$$\text{LHS} = (1 - \lambda_a w_a \tau_s) Y_{i-1} + (w_a^2 \tau_s^2 - 2) Y_i + (1 + \lambda_a w_a \tau_s) Y_{i+1}$$

Similarly,

$$\text{RHS} = \frac{\tau_s M_a}{2} (E_{i+1} - E_{i-1}) + \frac{\tau_s^2 M_a}{m_a} E_i$$

Thus, equating LHS and RHS, and solving for Y_{i+1},

1st. Order Central Differences

$$Y_{i+1} = \frac{1}{1+\zeta_a w_a \tau_s}\left[(2 - w_a^2\tau_s^2)Y_i - (1 - \zeta_a w_a \tau_s)Y_{i-1} + \frac{\tau_s M_\delta}{2}(E_{i+1} - E_{i-1}) + \frac{\tau_s^2 M_\delta}{T_a} E_i\right] \quad (E.2)$$

In a similar way, by using alternative approximations for the derivatives from Table IV, the following equations may be obtained:

1st. Order Forward Differences

$$Y_{i+1} = (2\zeta_a w_a \tau_s - w_a^2\tau_s^2 - 1)Y_{i-1} + (2 - 2\zeta_a w_a \tau_s)Y_i + \tau_s M_\delta (E_i - E_{i-1}) + \frac{\tau_s^2 M_\delta}{T_a} E_{i-1} \quad (E.3)$$

1st. Order Backward Differences

$$Y_{i+1} = \frac{1}{1 + 2\zeta_a w_a \tau_s + w_a^2\tau_s^2}\left[(2 + 2\zeta_a w_a \tau_s)Y_i - Y_{i-1} + \tau_s M_\delta (E_{i+1} - E_i) + \frac{\tau_s^2 M_\delta}{T_a} E_{i+1}\right] \quad (E.4)$$

2nd. Order Backward Differences

$$Y_{i+1} = \frac{1}{4 + 6\zeta_a w_a \tau_s + 2w_a^2\tau_s^2}\left[(10 + 8\zeta_a w_a \tau_s)Y_i + 2Y_{i-2} - (8 + 2\zeta_a w_a \tau_s)Y_{i-1} - 4M_\delta \tau_s E_i + M_\delta \tau_s E_{i-1} + (3\tau_s M_\delta + \frac{2\tau_s^2 M_\delta}{T_a}) E_{i+1}\right] \quad (E.5)$$

An additional equation may be obtained by using a 1st. order backward difference approximation for the second derivative, in conjunction with 2nd. order backward differences for the first derivative. This mixed order backward difference approximation was used by Stein (Ref. 21:66).

Mixed Order Backward Differences

$$Y_{i+1} = \frac{1}{2 + 6\zeta_a w_a \tau_s + 2 w_a^2 \tau_s^2} \left[(4 + 8\zeta_a w_a \tau_s) Y_i - 4 M_\delta \tau_s E_i \right.$$

$$- (2 + 2\zeta_a w_a \tau_s) Y_{i-1} + M_\delta \tau_s E_{i-1}$$

$$\left. + (3 M_\delta \tau_s + \frac{2 \tau_s^2 M_\delta}{T_a}) E_{i+1} \right] \qquad (E.6)$$

Iteration of Difference Equations

The forcing function in equations (E.2) through (E.6) is represented by the sampled values E_n ($n = \ldots -1, 0, 1, \ldots$) at integral multiples of τ_s. At these sampling times, as each new value of E_n becomes available, an iteration may be made to find the computed value of Y_n. Thus, when the subscript i is set to zero in the above equations, expressions for the computed values of Y_1 are obtained. If the equations are iterated for zero initial conditions all the E_n and Y_n for $n \leq 0$ are zero, so that Y_1 can immediately be calculated. However, for non-zero initial conditions two or three values (depending on which equation is used) of E_n and Y_n for $n \leq 0$ are required to be known before the iteration can be started. In the closed loop simulation program for the complete control system (Appendix A) it was therefore necessary to use temporarily stored values of elevator deflection angle and aircraft pitch rate (from the rate gyro) in order to start the difference equations.

Accuracy of Difference Equations

To test which of the difference equation approximations to the aircraft transfer function was the most accurate a computer program was written for the AFIT IBM 1620 machine. In this program the aircraft pitch rate, calculated by one of the difference equations (E.2) - (E.6), was compared with an analytically calculated aircraft response. A listing of the program statements is given at the end of this Appendix, and an outline of the computations made is shown

in Fig. E.1.

Since this testing was done with no closed loop control system around the aircraft, it was necessary to assume an arbitrary elevator motion. Equation (E.7) in Table V was chosen to define the elevator deflection as the response of a 2nd. order transfer function (damping factor ζ_e, natural frequency w_e) to a step input of amplitude S. An analytical function for the aircraft response, equation (E.8), to this elevator motion was obtained with the aid of Laplace transform tables (Ref. 13:87). Plots of equations (E.7) and (E.8) are contained in Fig. E.2, together with the values of parameters which were used to generate them. It may be noted that the values chosen for the aircraft parameters were representative of a typical Flight Condition, so that they lie towards the centers of the ranges of variation shown in Figs. 2, 3, and 4. Also, by comparing the elevator motion for the first 0.5 sec. in Fig. E.2 with that in Fig. D.8, it is seen that the input function used to test the difference equations was a realistic approximation to elevator motion which could occur in the closed loop system. Hence, the results of testing the accuracy of the difference equations under open loop conditions were expected to be equally valid for the closed loop.

Figures E.3 and E.4 show the normalized r.m.s. errors of the difference equations as a function of time. The apparently large initial errors are due to the fact that the normalization was made with respect to the aircraft pitch rate (as indicated in Fig. E.1), which was zero at time zero. From these two Figures it is seen that 1st. order central differences give more accurate results than any of the other 1st. order approximations, and are even more accurate than 2nd. order backward differences. The curve for 1st. order backward differences followed that for 1st. order forward differences in Fig. E.3, and was therefore not plotted.

A particular feature in Figs. E.3 and E.4 is that the errors for all but the central differences start to increase when the first derivative of the aircraft pitch rate (Fig. E.2) changes sign. This

is an indication that the approximation for the second derivative by central differences (Table IV) is the most accurate, a result which may be derived theoretically (Ref. 19:86). For τ_s = 0.01 sec. the normalised r.m.s. error of the central difference equation was found to be 0.01 per cent after 2.0 sec. (i.e. after 200 iterations); the actual error at this time was 0.0008 deg./sec., when the analytical value of pitch rate (P_{200}) was -1.9850 deg./sec., so that the terminal error was 0.04 per cent.

Table V

Analytical Expressions for Elevator Deflection and Aircraft Pitch Rate Used for Testing the Accuracy of Difference Equation Solutions

Elevator Deflection

$$\delta_e(t) = S\left[1 + A_3 e^{-B_3 t}\sin(C_3 t - D_3)\right] \qquad (E.7)$$

where,

$$A_3 = \frac{1}{\sqrt{1-\zeta_e^2}}$$

$$B_3 = \zeta_e \omega_e$$

$$C_3 = \omega_e\sqrt{1-\zeta_e^2}$$

$$D_3 = \tan^{-1}\frac{\sqrt{1-\zeta_e^2}}{-\zeta_e}$$

Aircraft Pitch Rate

$$\dot{\theta}_a(t) = \frac{S M_\delta}{T_a \omega_a^2}\left[1 + A_1 e^{-B_1 t}\sin(C_1 t - D_1) + A_2 e^{-B_2 t}\sin(C_2 t - D_2)\right] \qquad (E.8)$$

where,

$$A_1 = \frac{\omega_e^2\left[1 - 2\zeta_a\omega_a T_a + \omega_a^2 T_a^2\right]^{1/2}}{\sqrt{1-\zeta_a^2}\left[(\omega_e^2 - 2\zeta_a\omega_a\zeta_e\omega_e + 2\zeta_a^2\omega_a^2 - \omega_a^2)^2 + 4\omega_a^2(1-\zeta_a^2)(\zeta_a\omega_a - \zeta_e\omega_e)^2\right]^{1/2}}$$

$$B_1 = \zeta_a\omega_a$$

$$C_1 = \omega_a\sqrt{1-\zeta_a^2}$$

$$D_1 = \tan^{-1}\frac{\sqrt{1-\zeta_a^2}}{-\zeta_a} - \tan^{-1}\frac{2\omega_a(\zeta_a\omega_a - \zeta_e\omega_e)\sqrt{1-\zeta_a^2}}{\omega_e^2 - 2\zeta_a\omega_a\zeta_e\omega_e + 2\zeta_a^2\omega_a^2 - \omega_a^2}$$

$$-\tan^{-1}\frac{\omega_a T_a\sqrt{1-\zeta_a^2}}{1-\zeta_a\omega_a T_a}$$

The constants A_2, B_2, C_2, and D_2 are obtained by interchanging the subscripts a and e in the expressions for A_1, B_1, C_1, and D_1.

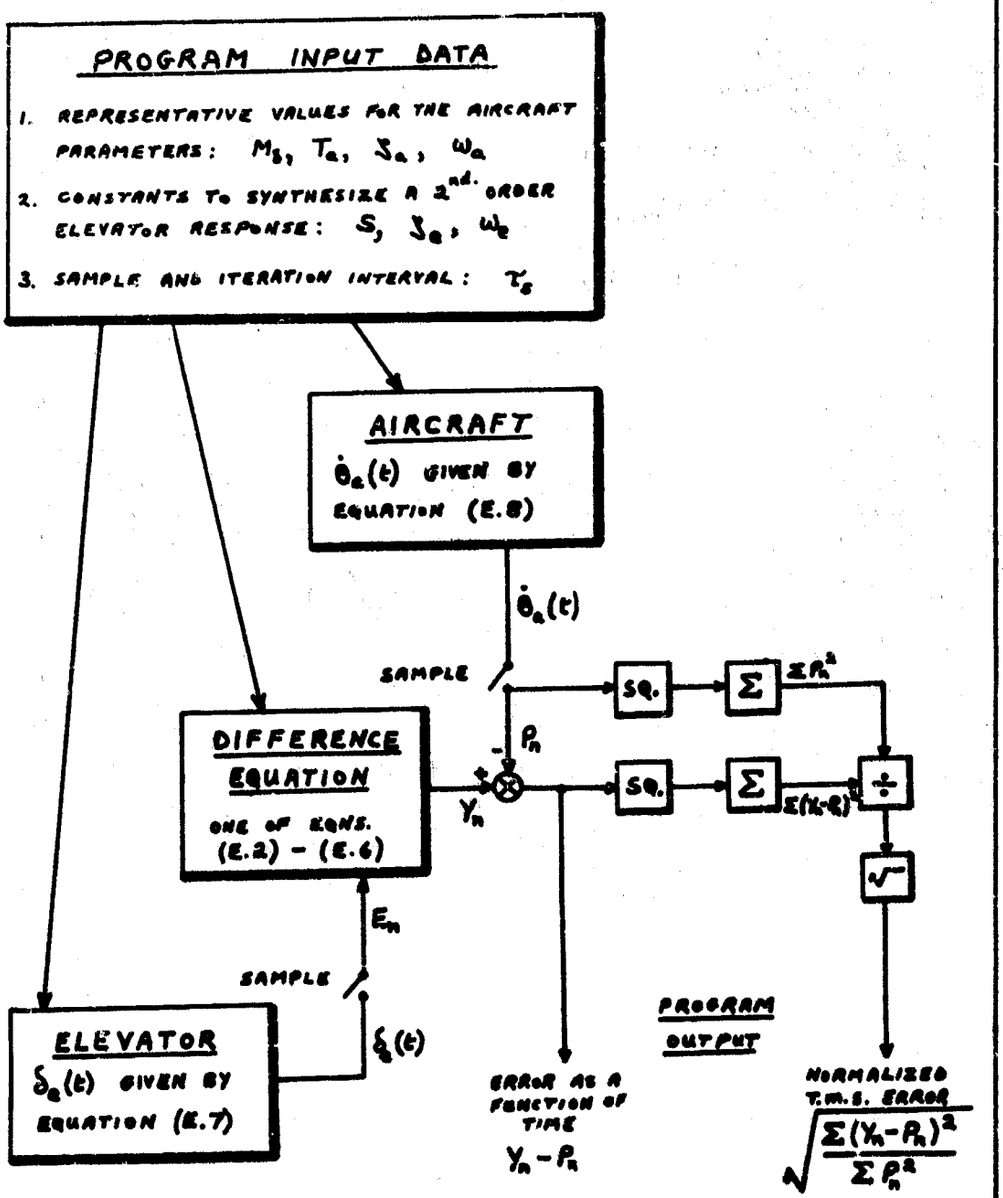

Fig. E.1

Calculations Made in the Program Used to Test the Accuracy of Difference Equation Approximations to the Aircraft Transfer Function

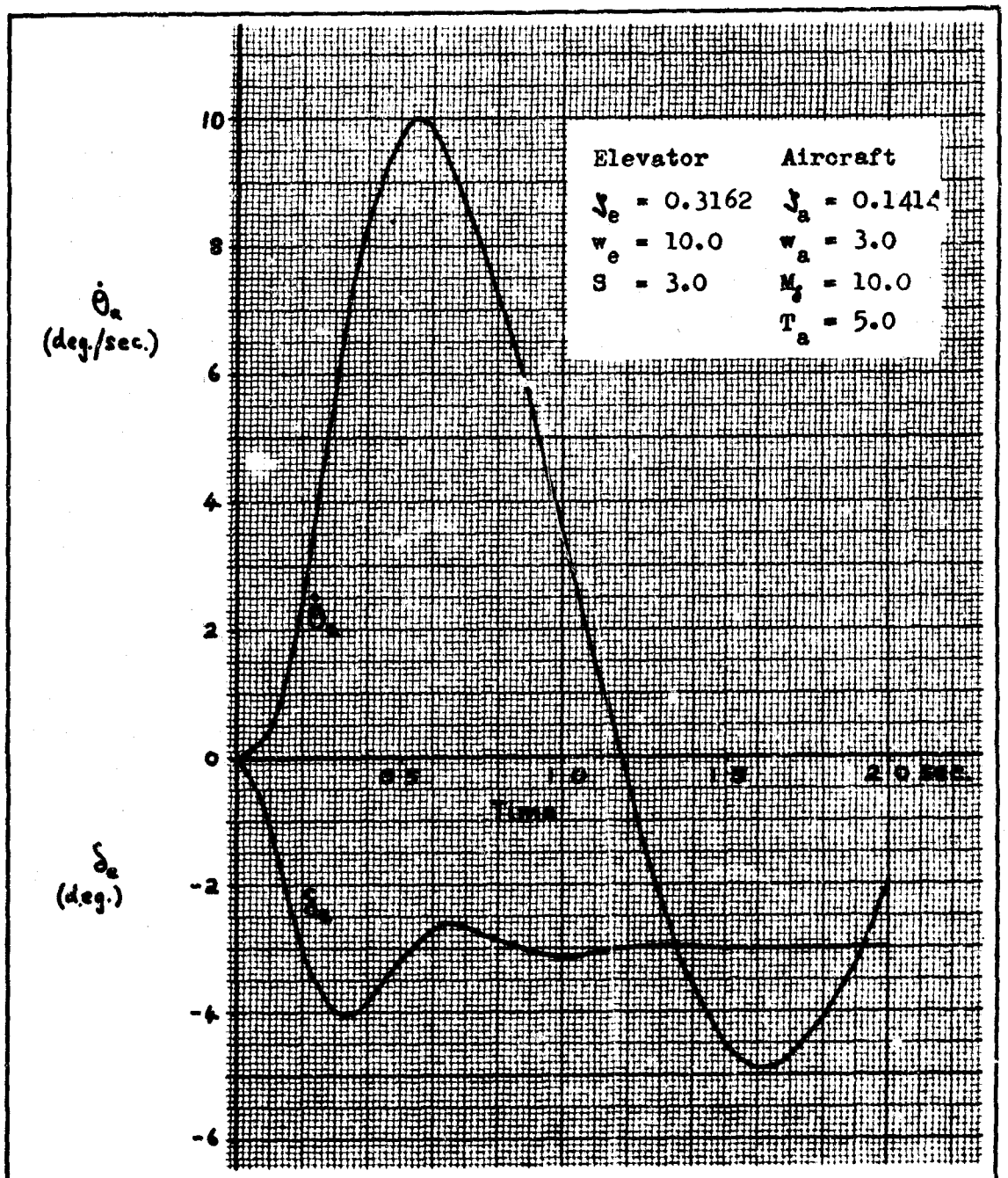

Fig. E.2

Elevator Deflection and Analytically Calculated Aircraft Response for Representative Values of Aircraft Parameters

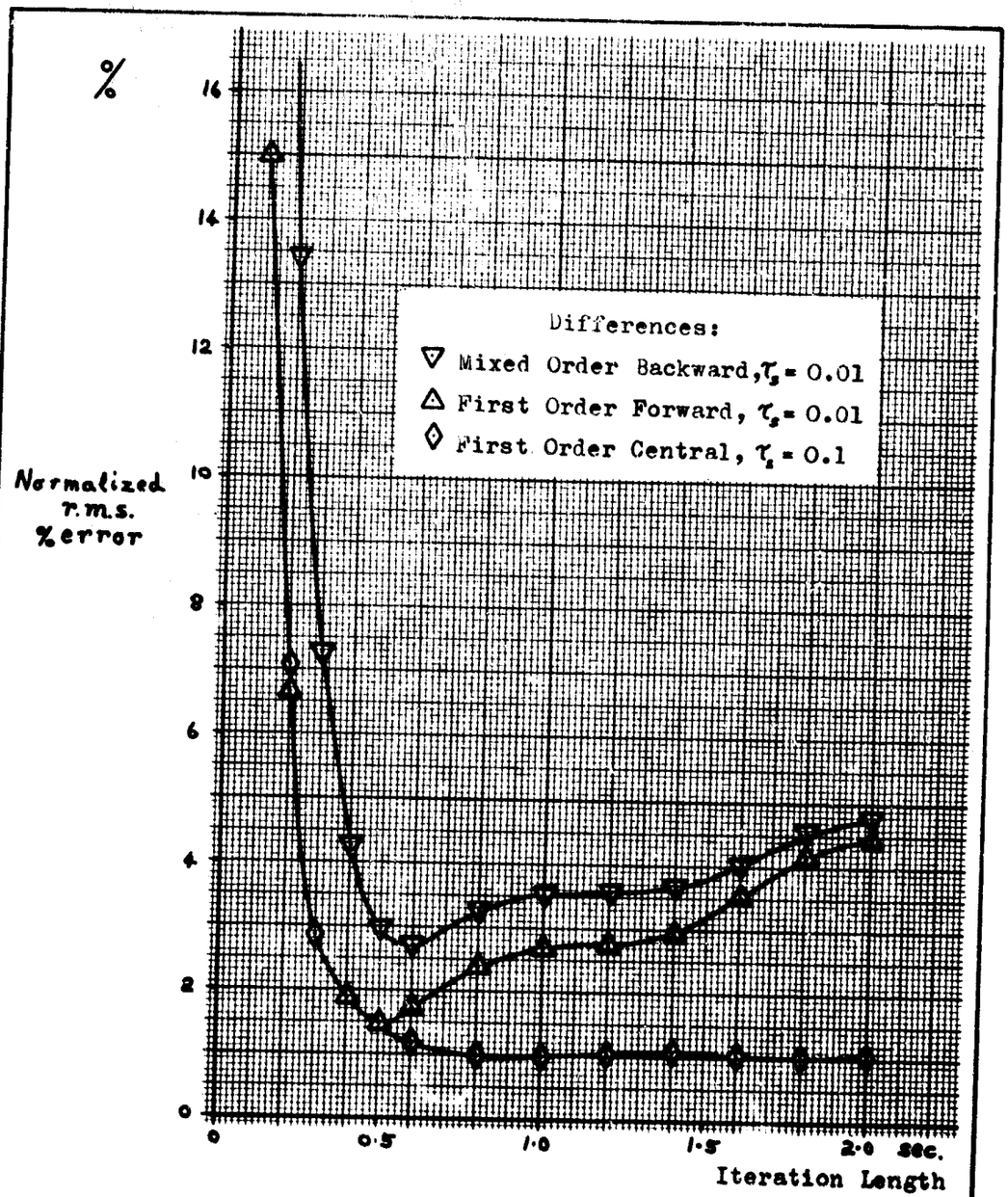

Fig. E.3

Relative Accuracy of Various Difference Equation Approximations Showing that Central Differences are the Most Accurate Even When the Iteration Length is Longest

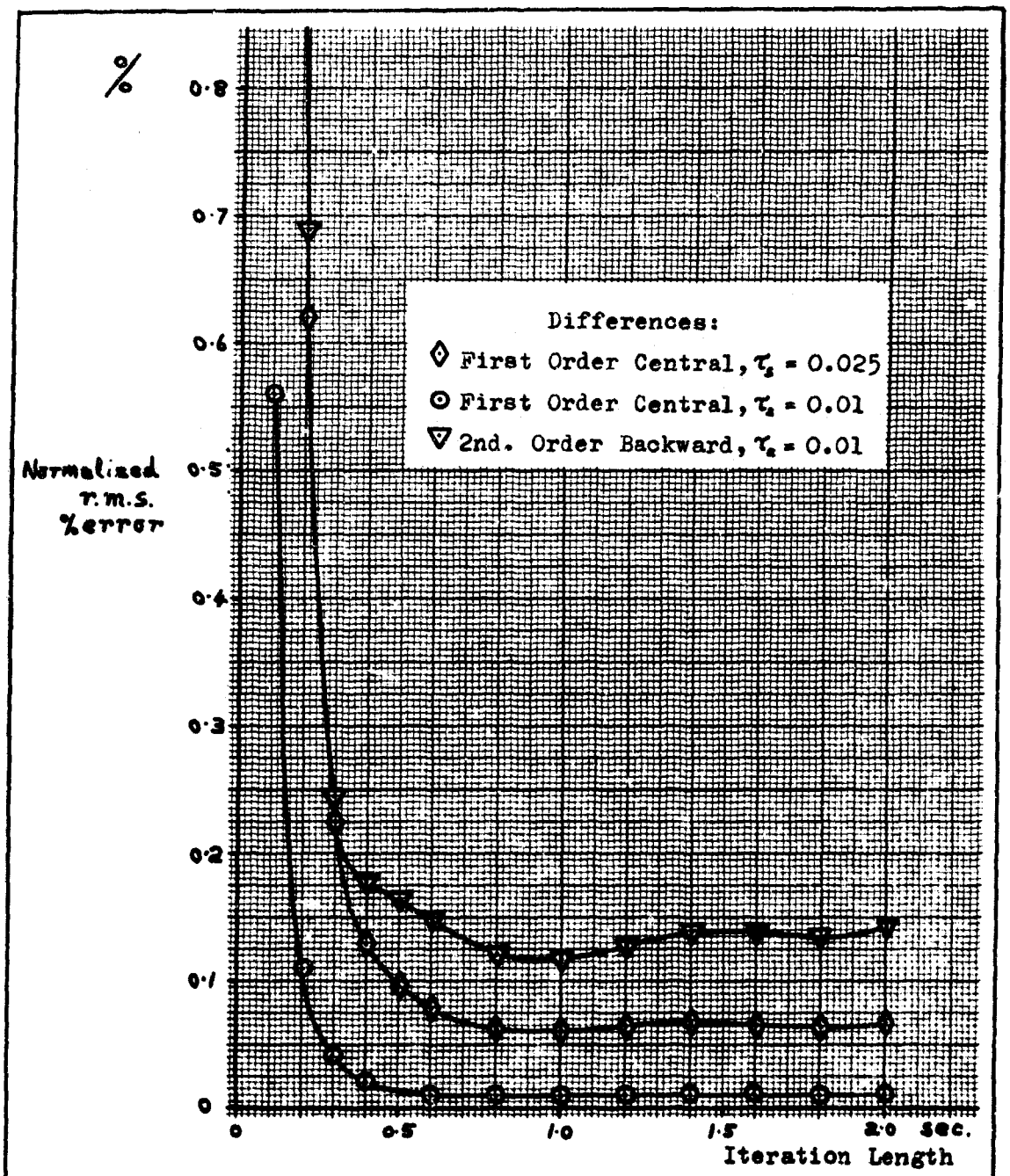

Fig. E.4

Accuracy of 1st. Order Central Differences Compared With 2nd. Order Backward Differences Showing that the Central Differences are More Accurate

```
C  C  ACCURACY OF DIFFERENCE EQUATION APPROXIMATIONS
C
C
      DIMENSION SIGH(2)
      READ, ELDEG, WEL, ZETEL
      READ, H
C     REPRESENTATIVE AIRCRAFT CONSTANTS
      DELTM=10.0
      WAC=3.0
      ZETAC=0.1414
      TAC=5.0
C     CONSTANTS FOR THE ACTUAL PITCH EQUATION. A1-D2.(8)
      S=(ELDEG*DELTM)/(TAC*WAC*WAC)
      W1=WAC
      W2=WEL
      Z1=ZETAC
      Z2=ZETEL
      CALL SIZE
      GO TO 13
      SUBROUTINE SIZE
      F1=W1*Z1
      F2=W2*Z2
      HNUM=W2*W2*SQRT(1.0-2.0*TAC*F1+TAC*TAC*W1*W1)
      RT=SQRT(1.0-Z1*Z1)
      C=W1*RT
      D=W2*W2-2.0*F1*F2+2.0*F1*F1-W1*W1
      DEN=RT*SQRT(D*D+4.0*C*C*(F1-F2)*(F1-F2))
      A = HNUM/DEN
      RETURN
 13   A1=A
      B1=F1
      C1=C
      I=1
 11   TOP=RT
      BOT=-Z1
      CALL ANGLE
      GO TO 14
      SUBROUTINE ANGLE
      IF(BOT)4,3,5
 4    IF(TOP)9,3,7
 9    P=3.1415926+ATAN(ABS(TOP/BOT))
      GO TO 2
 7    P=3.1415926-ATAN(ABS(TOP/BOT))
      GO TO 2
 5    IF(TOP)8,3,6
 8    P=6.2831853-ATAN(ABS(TOP/BOT))
      GO TO 2
 6    P=ATAN(ABS(TOP/BOT))
      GO TO 2
 3    PUNCH 50
 50   FORMAT(11HANGLE ERROR)
 2    RETURN
```

```
 14   P1=P
      TOP=TAC*C
      BOT=1.0-TAC*F1
      CALL ANGLE
      P2=P
      TOP=2.0*C*(F1-F2)
      BOT=D
      CALL ANGLE
      SIGH(I)=P1-P2-P
      I=I+1
      IF(I-3)10,12,12
 10   W1=WEL
      W2=WAC
      Z1=ZETEL
      Z2=ZETAC
      CALL SIZE
      A2=A
      B2=F1
      C2=C
      GO TO 11
 12   D1=SIGH(1)
      D2=SIGH(2)
C
C     CONSTANTS FOR ELEVATOR DEFLECTION EQUATION. A3-D3.(4)
      A3=1.0/RT
      B3=F1
      C3=C
      D3=P1
C
C     SHORT-PERIOD CONSTANTS
      ZWAY=ZETAC*WAC
      RTAY=1.0/TAC
      WAY=WAC
C
C     COEFFICIENTS FOR CENTRAL DIFFERENCE EQUATION
      CY=1.0/(1.0+H*ZWAY)
      CYE31=H*DMY*0.5*CY
      CYE2=H*H*DMY*CY*RTAY
      CY2=CY*(2.0-H*H*WAY*WAY)
      CY1=(1.0-H*ZWAY)*CY
C
C     INITIAL CONDITIONS
      PUNCH 36
 36   FORMAT(33H TIME   ELEV.  AC.P.R.  COMP.P.R.,
     C       18H  ERROR  RMSY P.C.,//)
      AC3=0.0
      AC2=0.0
      E3=0.0
      E2=0.0
      Y3=0.0
      Y2=0.0
      SMSQA=0.0
      SMSQY=0.0
```

```
C       ITERATION OF THE DIFFERENCE EQUATION
        T=0.0
        L=0
 61     L=L+1
 90     T=T+H
        AC1=AC2
        AC2=AC3
        APT1=A1*EXP(-B1*T)*SIN(C1*T-D1)
        APT2=A2*EXP(-B2*T)*SIN(C2*T-D2)
        AC3=S*(1.0+APT1+APT2)
        E1=E2
        E2=E3
        E3=ELDEG*(1.0+A3*EXP(-B3*T)*SIN(C3*T-D3))
        Y1=Y2
        Y2=Y3
        Y3=CYE31*(E3-E1)+CYE2*E2+CY2*Y2-CY1*Y1
        SMSQA=SMSQA+AC3*AC3
        SMSQY=SMSQY+(Y3-AC3)*(Y3-AC3)
        CNT=L
        TEST=ABS(T-0.1*CNT)
        IF(TEST-0.00001)32,32,90
 32     RMSYP=100.0*SQRT(SMSQY/SMSQA)
        ERR=Y3-AC3
        PUNCH 34, T, E3, AC3, Y3, ERR, RMSYP
 34     FORMAT(F5.2,F7.2,F9.4,F10.4,2F9.4)
        IF(L-20)61,99,99
 99     STOP
        END
```

UNCLASSIFIED

Security Classification

DOCUMENT CONTROL DATA - R & D

(Security classification of title, body of abstract and indexing annotation must be entered when the overall report is classified)

1. ORIGINATING ACTIVITY *(Corporate author)*
Air Force Institute of Technology (AFIT-SE)
Wright-Patterson AFB, Ohio 45433

2a. REPORT SECURITY CLASSIFICATION
UNCLASSIFIED

2b. GROUP

3. REPORT TITLE
A SELF-ADAPTIVE AIRCRAFT PITCH RATE CONTROL SYSTEM EMPLOYING DIFFERENCE EQUATIONS FOR PARAMETER IDENTIFICATION

4. DESCRIPTIVE NOTES *(Type of report and inclusive dates)*
AFIT Thesis

5. AUTHOR(S) *(First name, middle initial, last name)*
Ian S. Parry, Flight Lieutenant RAF

6. REPORT DATE	7a. TOTAL NO. OF PAGES	7b. NO. OF REFS
June 1967	103	22

8a. CONTRACT OR GRANT NO. N/A	9a. ORIGINATOR'S REPORT NUMBER(S)
b. PROJECT NO. N/A	AFIT Thesis GA/EE/67-2
c.	9b. OTHER REPORT NO(S) *(Any other numbers that may be assigned this report)* N/A
d.	

10. DISTRIBUTION STATEMENT
Distribution of this document is unlimited.

11. SUPPLEMENTARY NOTES	12. SPONSORING MILITARY ACTIVITY
	Air Force Flight Dynamics Laboratory Wright-Patterson AFB, Ohio 45433

13. ABSTRACT

In a high performance aircraft changes in Mach number, angle of attack and altitude can cause a large variation in the short-period transfer function. To provide the pilot with a consistant pitch rate control characteristic an airborne computer, with inputs of elevator deflection angle and pitch rate is used to identify and track changes in the elevator effectiveness. Simulation with an aircraft whose elevator effectiveness varied over a range of 240:1 showed that the desired loop gain was maintained within a factor of two for both pilot command inputs and for random wind gust disturbances of root-mean-square magnitude 20 ft./sec.

DD FORM 1 NOV 65 1473

UNCLASSIFIED

Security Classification

14. KEY WORDS	LINK A		LINK B		LINK C	
	ROLE	WT	ROLE	WT	ROLE	WT
Aircraft Control Systems						
Self-Adaptive						
Difference Equations						
Parameter Identification						